Characterization of Volume Change, Strength and Durability of Landfill Liner Materials with Inclusions of Industrial By-products

Şerife Öncü

Submitted to the
Institute of Graduate Studies and Research
in partial fulfillment of the requirements for the degree of

Doctor of Philosophy
in
Civil Engineering

Eastern Mediterranean University
December 2016
Gazimağusa, North Cyprus

Approval of the Institute of Graduate Studies and Research

Prof. Dr. Mustafa Tümer
Director

I certify that this thesis satisfies the requirements as a thesis for the degree of Doctor of Philosophy in Civil Engineering.

Assoc. Prof. Dr. Serhan Şensoy
Chair, Department of Civil Engineering

We certify that we have read this thesis and that in our opinion it is fully adequate in scope and quality as a thesis for the degree of Doctor of Philosophy in Civil Engineering.

Assoc. Prof. Dr. Huriye Bilsel
Supervisor

Examining Committee

1. Prof. Dr. Suat Akbulut
2. Prof. Dr. Ayfer Erken
3. Prof. Dr. Zalihe Sezai
4. Assoc. Prof. Dr. Huriye Bilsel
5. Asst. Prof. Dr. Eriş Uygar

ABSTRACT

Mixture of expansive soil and sand can be efficiently used in semi-arid climates, with improved hydro-mechanical properties, as a landfill barrier material or road-base. The soil mixture can further be enhanced with industrial waste by-products, also creating an area for waste recycling. In this study, sand and expansive soil were selected from abundantly found local resources. The testing program consisted of determination of an optimum mixture of sand-expansive soil-additive, which would not experience formation of macropores due to swell-shrink behavior with the climatic effects and would possess low hydraulic conductivity, as well as improved strength. The additives were selected from the by-products of the materials used in the local construction industry, and included polymeric fiber (PF) and marble waste. The first stage of this study focused on the volume change and strength properties of sand stabilized expansive soil reinforced with polymeric fiber. Zeolite was also used as an alternative material to sand, mixing it in 1:1 ratio with the expansive soil forming a stable structure with improved properties. PF inclusions of 1%, 2% and 3% by dry mass indicated that hydro-mechanical properties were improved with an optimum amount of 2%.

The second phase of this study assesses the suitability of expansive soil mixed with zeolite, readily obtained from natural reserves in Turkey, to be proposed as a landfill liner in a semi-arid climate. The choice of zeolite is due to its already well understood high adsorption capacity for heavy metals as well as its pozzolanicity. The volume change, strength, and hydraulic conductivity characteristics were studied with the effect of durability through aging. The results illustrated that expansive soil-zeolite mixture when used in 1:1 ratio attained improved strength characteristics with time

over a curing period of 90 days. Therefore, it was concluded that a locally available expansive soil mixed with zeolite could be a good alternative to sand-Na-bentonite.

In the third stage of the experimental program, marble waste, abundantly found as a by-product of construction industry, was evaluated as a secondary material to be utilized as potential stabilizer to improve the volume change and strength characteristics of sand-amended expansive soil. Marble waste obtained from two different sources with different gradations, denoted as marble powder (MP) and marble dust (MD) was also assessed for possible recycling by inclusion in stabilized soil mixtures. Volume change and strength tests were conducted on expansive soil-sand mixtures with 5%, 10% and 20% waste marble inclusions over curing periods of 7, 28 and 90 days. The results indicated that 10% MP and 5% MD were the optimum amounts giving the best results. However, the soil mixtures displayed brittle behavior after marble addition, hence utilization of this waste is recommended for soils exposed to lower flexural loads only. Linear correlations of swell potential with flexural strength were obtained which could be potential empirical approaches to predict flexural strength based on swell-shrinkage behavior or vice versa for the soils studied.

Keywords: Polymeric fiber, marble powder, zeolite, volume change, flexural strength, unconfined compressive strength.

ÖZ

Yarı kurak iklimlerde şişen zeminlerin iklimsel nedenlerle şişme-büzülmesinden kaynaklanan binalardaki yapısal zararı ve çatlakların oluşmasını önlemek için iyileştirilmesi gerekmektedir. Şişen zeminlerin kum ile iyileştirilmesi, bu karışımın katı atık şiltesi veya yol tabanı olarak kullanılmasında etkili bir yöntemdir. Ayrıca bu karışım endüstride kullanılan atık malzemelerin de eklenmesiyle hem güçlendirilebilir hem de geri dönüşüm için bir fırsat yaratılabilir. Bu çalışmada, yerel kaynaklardan uniform kum ve şişen silt seçilmiştir. Deneysel programın amacı uygun kum, silt ve ek bir malzemenin oranlarının seçimidir. Sıkıştırılarak hazırlanan malzemenin katı atık depolama şiltesi olarak kullanılması, dolayısıyla iklimsel nedenlerle şişme-büzülmenin yaratacağı çatlakların oluşmaması ve hidrolik iletkenliğin düşük olması amaçlanmıştır. Ek malzeme olarak inşaat sektöründe kullanılan malzemelerin atıkları olan PVC boru kırpıntıları (fiber polimer) ve mermer tozu seçilmiştir. Çalışmanın birinci aşamasında kum-şişen zemin ve ek malzeme olarak fiber polimer karışımının mukavemeti ve hacimsel değişimi irdelenmiştir. Bununla birlikte kuma alternatif malzeme olarak zeolit kullanılmıştır. Kum ve zeolit, şişen zemin ile 1:1 oranında karıştırılmıştır. Kuru ağırlığın %1, %2 ve %3 oranında katılan fiber polimer oranlarından %2 katkının serbest basınç ve eğilme dayanımlarını artırdığı ve hacimsel değişimi iyileştirdiği gözlemlenmiştir.

Araştırmanın ikinci aşamasında ise kum yerine zeolit kullanılmış ve yarı kurak bir iklimde katı atık depolama şiltesi olabilecek bir malzeme yaratılmıştır. Zeolit ağır metal filtrasyon kapasitesinden dolayı ve iyi bir pozzolan olması nedeniyle seçilmiştir. Hacim değişimleri, mukavemet ve hidrolik iletkenlik özellikleri çalışılmış ve zamana

bağlı olarak dayanıklılık çalışmaları da irdelenmiştir. Sonuçlar, bu malzemelerin 1:1 oranında kullanılırsa etkili olacağını göstermiştir. Çatlaklar nedeniyle tercihli akış kanallarının oluşması hidrolik iletkenliğin artmasına neden olur ancak bu malzeme karışımında böyle bir durum gözlemlenmemiştir. Ayrıca mukavemet zaman içerisinde artış göstermiş ve bu artışın da çalışılan süre içinde sürdürülebilir olduğu sonucuna varılmıştır. Dolayısıyla, şişen zeminin zeolit ile karışımının kum-bentonit karışımına, özellikle gelişmekte olan ve nüfus artışı görülen bölgelerde, iyi bir alternatif olduğu sonucuna varılmıştır.

Deneysel çalışmanın üçüncü aşamasında ek atık malzeme olarak inşaat sektöründe çok fazla kullanılan mermer tozu seçilmiştir. Katı atık alanlarına veya doğaya atılan bu malzemenin geri dönüşümü, fazla birikimini ve tuttuğu büyük hacmi önleyecektir. Atık mermer tozu, iki değişik kaynaktan elde edilmiş ve dane boyutuna göre iki şekilde (MP ve MD) isimlendirilmiştir. Atık mermer tozu %5, %10 ve %20 oranlarında farklı kür süreleriyle (7, 28 ve 90 gün) birlikte kullanılarak, hacimsel değişim, mukavemet ve çimentolaşma özellikleri araştırılmıştır. Deney sonuçlarına göre %10 MP ve %5 MD katkının optimum miktarlar olduğu ve karışımın özelliklerinin iyileştiği sonucuna varılmıştır. Bununla birlikte, mermer tozu katkısının daha kırılgan bir malzemenin oluşmasına neden olduğu ve eğilme dayanımının biraz azaldığı da gözlemlenmiştir. Dolayısıyla bu malzemenin eğilmeye neden olabilecek yüksek yükler altında değil de hafif trafik altındaki yollarda kullanımının daha uygun olacağı kanaatine varılmıştır.

Anahtar kelimeler: Fiber polimer, zeolit, mermer tozu, hacimsel değişim, eğilme dayanımı, serbest basınç dayanımı.

ACKNOWLEDGMENT

First of all, I would like sincerely thank to my supervisor Assoc. Prof. Dr. Huriye Bilsel for her precious knowledge, experience, valuable academic guidance and support throughout this research. My supervisor has an innovative vision which motivates me to continuously progress on my research topic. She will always be a special person in my life.

I would like to thank to laboratory engineer Mr. Ogün Kılıç for his help, ideas and suggestions for the tests and modification of equipments. Special thanks to laboratory technician Mr. Orkan Lord for his help at different stages of my laboratory works and experiments.

I am deeply indepted to my husband, Hasan Sarper, for being in my life, help and encouragement. Most importantly, without his love, motivation, patience and understanding, none of the achievements in this work would have been possible.

I would like to express my deepest thanks to my parents, Atakan Öncü and Mehmet E. Öncü, for their endless love, invaluable kindness, patience and support during my life and especially in this period. I am very grateful to my second family Gülin Sarper, Cafer Sarper and Müge Sarper for their love, support and encouragement.

Finally, I would also like to acknowledge my friends who have supported, motivated and trusted me during this study.

TABLE OF CONTENTS

LIST OF TABLES

LIST OF FIGURES

LIST OF ABBREVIATIONS AND SYMBOLS

AEV	Air-entry value
ASTM	American Society for Testing and Materials
CAH	Calcium aluminate hydrates
CASH	Calcium alumino silicate hydrates
C_c	Compression index
CEC	Cation exchange capacity
C_r	Rebound index
C_u	Coefficient of uniformity
CSH	Calcium silicate hydrates
c_v	Coefficient of consolidation
D_{10}	Effective grain size
D_{50}	Median grain size
DDL	Diffuse double layer
e	Void ratio
E_{50}	Secant modulus
G_s	Specific gravity
I_{ss}	Shrink-swell index
k_{sat}	Saturated hydraulic conductivity
LL	Liquid limit
LOP	Limit of proportionality
MD	Marble dust
MH	Silt with high plasticity
MP	Marble powder

m_v	Coefficient of volume compressibility
PF	Polymeric fiber
PI	Plasticity index
PL	Plastic limit
PVC	Polyvinyl chloride
R^2	Fit error
$R^D_{T,150}$	Flexural strength ratio
S	Degree of saturation
SEM	Scanning electron microscope
SP	Poorly graded uniform sand
SWCC	Soil-water characteristic curve
T^D_{150}	Toughness
u_a	Pore air pressure
u_w	Pore water pressure
u_a-u_w	Matric suction
UCS	Unconfined compressive strength
USCS	Unified soil classification system
w	Gravimetric water content
XRD	X-ray diffraction
XRF	X-ray fluorescence
$\Delta H/H_0$	Axial strain
$\Delta V/V_0$	Volumetric strain
$\Delta D/D_0$	Diameteral strain
Δw	Change in water content
γ_w	Unit weight of water

θ	Volumetric water content
Θ_r	Residual volumetric water content
Θ_s	Saturated volumetric water content
π	Osmotic suction
p_s'	Swell pressure
ψ	Suction

Chapter 1

INTRODUCTION

Increasing population leads to growth in resource consumption, waste disposal becoming one of the most serious prevailing environmental problems in developed and developing countries all over the world (Arasan and Yetimoğlu, 2008). Wastes which include municipal industrial, mining, nuclear and packaging by-products accumulating in landfill areas generate contamination imposing detrimental health and environmental problems. Landfill barriers, liners and covers are widely used in the waste containment facilities to prevent ingress of precipitation as well as seepage of leachate to the environment and underground water. Many of these landfills are of a composite type which might also include industrial waste as a secondary material (Olofsson et al., 2006), choice of materials depending on the available sources and suitability to the local climatic conditions.

1.1 Landfills

The design of waste containment facilities, which are the cover and liner layers, require an extensive experimental investigation to be able to choose the best solution using the abundantly existing local sources, usually sand and smectitic clay, and further to investigate alternative solutions and improvements of these methods for more enhanced and also feasible solution. Leachate is the most dangerous component of the solid waste management process. In a small landfill, the amount of leachate generated may not create a significant problem. As the size of landfill and variety of solid waste disposal increases, and under conditions of surface water penetrating through the

cover, large amounts of leachate will be generated and this will create environmental problems such as leaching of nutrients and heavy metals into the soil which leads to soil and ground water contamination (Sunil et al., 2008). To prevent or control this threat the choice of materials in a composite system must ensure the performance requirements. A serious solution is needed to take appropriate remedial measures by avoiding contamination of the underlying soils and groundwater aquifers from the leachate generated from the landfills (Kumar and Alappat, 2005).

Different methods are used for this purpose in geotechnical engineering. These methods are compacted clay liners and covers, geosynthetic clay liners, composite covers and sand-bentonite mixtures. Nearly all waste containment systems include a liner and a final cover, called barriers. The first engineered covers consisted of compacted clay barriers and the investigations showed that these covers are prone to failure as a result of desiccation cracking, frost action, differential settlement or a combination of these mechanisms. Therefore, compacted clay covers are not particularly effective and are not recommended for use in waste containment (Benson, 1999). Geosynthetic clay liners (GCLs) are factory-made clay liners that consist of a layer of bentonite sandwiched between two geotextiles that are held together by needle punching, stitching or adhesives (Meer and Benson, 2007). Short periods of flooding and prolonged periods of draughts in semi-arid areas impose swelling-shrinking on compacted clay, which result in formation of macropores, creating preferential flow paths during the subsequent wet season. Liners are used as sealing systems and therefore must possess mechanical stability, resistance to temperature elevations and chemical attack.

In recent studies, sand-bentonite mixtures are commonly used as barrier materials in different percentages of sand and bentonite. Experimental investigations are needed to choose the best percentage of sand and bentonite amounts in order to obtain reliable results. The most important parameter required in the design of barriers is the saturated hydraulic conductivity, and according to regulations the compacted soils used in landfill liner applications should possess saturated hydraulic conductivity less than 10^{-7} cm/s (EPA, 2000).

Climatic and environmental changes affect soil suction and the structure of the liners. Bentonite, which is montmorillonitic clay, has low permeability and high plasticity, which experiences tremendous cracking upon desiccation which increases during drying-wetting cycles. The sand component of a compacted bentonite-sand mixture contributes to the strength whereas the bentonite component fills the pore space between the sand grains in order to reduce the hydraulic conductivity (Akgün et al. 2006).

Bentonite-embedded zeolite (BEZ) was proposed as an alternative to bentonite-embedded sand (BES). Based on the studies, it was reported that BEZ can also satisfy lower hydraulic conductivity values when compared to BES and geosynthetic clay liners. In addition, tests showed that the shrinkage behavior of BEZ is satisfactory for landfill liner applications (Kaya et al, 2006). BEZ liners are superior to BES liners because of the high adsorption capacity of zeolite. Therefore, it would appear to be more advantageous to use BEZ instead of BES in certain hydraulic barrier system applications, such as hydraulic landfill liners and covers (Kaya and Durukan, 2004). Rapid progress of industrialization yields waste by-products, such as fly ash, blast

furnace slag, cement kiln dust, silica fume, limestone dust, marble powder, which can be utilized together with construction materials to enhance the material properties. These waste materials are also used as secondary additions to sand-bentonite barrier compositions for enhancement and recycling purposes.

1.2 Unsaturated Soils

The soils on which the wastes from the mine and the municipality are deposited and the compacted soils to be designed as liners and covers are all unsaturated soils, which will be exposed to solute transport and drying/wetting cycles respectively. Therefore, the need for unsaturated soils' concepts and techniques are very significant in characterization of the landfill sites and in designing of compacted soil barriers. Unsaturated soils either exit naturally, the soil stratum from the ground surface to the water table (vadose zone), or can be formed artificially by compaction. All compacted soil structures are initially unsaturated, constituted of solids, water and air phases. Therefore, engineering behavior of soils which remain unsaturated over long periods of dryness, and can be exposed to water ingress and structural changes during wet seasons, such as expansive, compacted, collapsible or residual soils are more realistically evaluated in unsaturated soil conditions, instead of saturated as is the case in classical soil mechanics (Fredlund, 2000). Soil suction is the most important parameter in unsaturated state which is defined as the total energy or stress that holds the soil water in the pores consists of matric suction and osmotic suction (Fredlund and Rahardjo, 1993). Matric suction is the difference between pore air pressure (u_a) and pore water pressure (u_w) which is represented by (u_a-u_w). Osmotic suction is induced by the concentration of salts in the pore water. Filter paper method, pressure plate, chilled mirror, vapour equilibrium, tensiometers and thermocouple psychrometers are the most widely used techniques for the measurement of suction.

Soil-water characteristic curve (SWCC), which is also known as water retention curve (WRC), is a relationship between soil suction and the amount of water in the soil. It is an important tool used for the estimation of engineering properties of hydraulic conductivity, shear strength and volume change in the unsaturated state. Unsaturated soil properties are very important in the design of geo-environmental systems, such as covers and landfill liners in semi-arid climates.

1.3 Aims and Scope of the Study

The primary aim of this study is to determine the hydro-mechanical properties of compacted sand–expansive soil mixtures to be used as barrier layers in waste containment systems in a semi-arid climate. As a result of this research work, an isolating material will be discovered as a solution for the waste management in N. Cyprus, which might also be used for the abandoned copper mine wastes as well as municipal wastes on the island. These are the two important environmental geotechnics issues existing locally which need immediate attention. Municipal solid wastes and copper mine wastes create important environmental problems in N. Cyprus. Abandoned copper mine waste is one of the most important environmental issues in the Eastern Mediterranean region. To prevent or mitigate the threat to ground water and the neighbouring environment, cost effective materials must be considered which are locally existing soil types as well as some industrial waste which can be considered for additional improvement of the selected soil mixtures.

The study focusses on the assessment of various materials in different combinations as possible landfill liner materials to be utilized in a semi-arid area, where climatic changes impose a significant impact on the engineering behavior of soil structures. The study was undertaken in three phases, basically using abundantly found soil

sources on the island, high plasticity silt prevailing in the vicinity of landfill areas and beach sand covering the coasts of Cyprus all around.

The waste products selected in this study are from the construction industry, waste marble and polyvinyl chloride (PVC) pipe cuttings, which impose a growing threat by accumulating in the environment, as well as massively growing in size in the dumped landfills. The marble is a product of the island obtained from quarries and processed in plants, producing the waste by-product in the form of powder or lumps, whereas PVC is a synthetic polymer processed in pipe factories and cut and shaped while flake-like cuttings are produced throughout this process. Zeolite which was to replace the sand in the mixtures was an imported material from a boron mine in Turkey, mainly selected to compare its effectiveness against sand. Zeolite has pollutant adsorption capacity and heavy metal removal properties therefore, it has been selected to study for its filtering capability which can be considered mainly for the copper mine site. Therefore, the two-fold aim of this study was to select the best proportions of an expansive soil-sand, and a secondary additive to enhance the hydro-mechanical properties of compacted soil mixture, as well as to create a recycling option for the undesired waste.

The thesis is divided into six chapters. Chapters 2 to 5 are constituted of studies on different material combinations, including background information, material properties, methods of testing, experimental results with discussions and conclusions. Chapter 2 introduces a synthetic waste (polymeric fiber), a by-product of PVC pipe production factory, gathered in the form of fine flakes to be used in the selected composite liner material mixtures of expansive soil-sand and expansive soil-zeolite.

The effectiveness of this reinforcing material was experimentally studied by determination of volume change and strength characteristics. Volume change determination included the swell-shrinkage and consolidation behavior, whereas strength was investigated through unconfined compression and flexural strength tests. Hydraulic properties of expansive soil-sand mixtures were also characterized by determining saturated hydraulic conductivity as well as establishing the soil-water characteristic curves.

Chapter 3 examines in more detail the effect of zeolite addition to expansive soil, evaluating its pozzolanic character in different curing times (0, 7, 28 and 90 days). Zeolite, which is not readily available in the local vicinity, nevertheless was considered worthwhile to do further study on, based on its filtering capability. For special cases, such as the toxic copper mine waste, this material could be a good choice where intense care is sought for environmental protection. Pozzolanic improvement was assessed by studying volume change and strength characteristics.

Chapter 4 evaluates the utilization of waste marble as a secondary additive to improve engineering properties of expansive soil-sand mixture. This is another ample waste which is the by-product of construction industry and its use in soil mitigation is an opportunity for recycling purpose. Two different waste marble, in the form of powder (MP) and dust (MD), were added to expansive soil-sand mixture in three different percentages (5%, 10% and 20%) for the investigation of all necessary engineering properties complying to landfill barrier and pavement design requirements. All of the laboratory tests included in the previous chapters were repeated on the expansive soil-zeolite mixtures for the same curing time periods (0, 7, 28 and 90 days).

Chapter 5 contains the durability analysis of expansive soil-sand and expansive soil-zeolite mixtures. Cyclic swell-shrink tests and temperature variations (25 °C, 40°C and 60°C) were applied on 28-day cured samples of expansive soil-sand and expansive soil-zeolite mixtures in order to evaluate their resistance to climatic and environmental changes.

Chapter 6 summarizes the overall conclusions of this study, and includes recommendations for future work.

Chapter 2

POLYMERIC FIBER REINFORCEMENT

2.1 Introduction

Disposal of wastes produced from various industries cause environmental contamination in the areas they are disposed since some of them are not biodegradable. Therefore, their utilization in soil stabilization is becoming popular, mainly due to technical, economical and ecological reasons, as well as the prospect of enhancing some engineering properties. To improve the ductility of stabilized soils, mainly as road base subjected to traffic loads, or landfill barriers, there is an increased usage of plastic waste materials as a secondary additive. These include polypropylene (PP) plastic sacks, polyethylene terephthalate (PRT) plastic bottles, polyvinyl chloride (PVC) pipe scrap and rubber waste which are abundantly produced every day and are regularly dispensed in disposal sites. There is a growing interest in the utilization of such materials for applications in geotechnical construction as a reinforcing material in soil mitigation. Thus a reuse alternative can also be created for these waste materials as well as improving properties of compacted soils, mainly tensile strength and failure strain before macro cracking occurs (Hannawi et al. 2013; Muntohar et al. 2013). Ziegler et al. (1998) utilized two types of short polypropylene fibers (screen and fibrillated fiber) as a reinforcement material for reducing the desiccation cracks of clay and for finding the influence of fibers on the tensile strength. They specified that the screen fibers are equally or more efficient than fibrillated fibers for the improvement of desiccation cracks and tensile strength.

The effect of polypropylene fiber, as a secondary additive to fly ash amended soil was studied by Yılmaz and Sevencan (2010) and was observed to increase unconfined compressive strength. Consoli et al. (2010) substantiated these findings by deducing that fiber inclusion improved unconfined compressive strength in cemented soils.

Studying the effect of fiber inclusion and lime treatment on engineering behavior of fly ash-soil mixtures, Kumar et al. (2007) concluded that the effect of fibers on maximum dry density and optimum moisture content of fly ash-soil-lime-fiber mixtures is insignificant. However, fiber addition to fly ash-soil-lime mixture improved unconfined compressive strength and split tensile strength by 74 and 100% respectively. The observed increase in the ratio of split tensile strength to unconfined compressive strength indicated that polyester fibers are more efficient when soil was subjected to tension rather than to compression. Jiang et al. (2010) showed that when short discrete polypropylene fibers are used in soil reinforcement, strength properties were improved up to an optimal content of 0.3% by weight of fiber inclusion, which when exceeded caused an adverse effect. Hence inclusion of polypropylene fiber could effectively improve strength and stability of soil. Onyejekwe and Ghataora (2014) studied the behavior of randomly oriented discrete synthetic fiber addition on flexural strength of soils treated with polymers and observed that the moisture-density relationship of soils was not influenced significantly. However, there has been a substantial improvement in tensile strength properties and toughness, which are the requirements for road base to prevent sudden failure after peak due to traffic load (Jamsawang et al., 2014). The chemically stabilized material with improved strength and compressibility exhibit brittle behavior under compression and flexural loading. Therefore, fibers when used as a secondary additive enhance the ductility of the

compacted soil, which is much more advantageous over chemically stabilized soils. Further advantages of using discrete fibers is the easiness of mixing with soil similar to other additives, such as cement and lime, and that they do not cause potential planes of weakness parallel to reinforcement (Tang et al., 2007). The latter is not a desirable property mainly in road base constructions and landfill liners subjected to flexural loads. Therefore, the improved mechanical properties like strength and ductility when fibers are added to compacted soil mixtures enhance the structural integrity of road bases and landfill liners (Maher and Ho, 1994). Akbulut et al. (2007) stated that strength and dynamic behavior of clayey soils improved with the utilization of scrap tire rubber, polyethylene and polypropylene fibers. In addition to synthetic fibers, organic fibrous waste materials are also increasingly used in soil mitigation, such as coir waste as reported by Jayasree et al. (2014). They have indicated that coir waste reduced swell and compression indices as well as linear shrinkage strain. It was concluded that coir waste can be effectively used as a reinforcing material for stabilization of expansive soil, at the same time providing an efficient and economic way to recycle it. Anggraini et al. (2015), based on their test results, indicated that coir fiber reinforcement increased the unconfined compressive, indirect tensile and flexural strengths of soft marine clay. Coir fiber and synthetic fiber (polypropylene) are used with fly ash in the subgrade reinforcement and their performance are compared by Chauhan et al. (2008). They stated that coir fiber is more effective in the improvement of soil strength than synthetic fiber. Similarly, Wang (1999) tested the usage of carpet waste fiber for soil reinforcement and concluded that the triaxial compressive strength and residual strength of soil increased.

Viswanadham et al. (2009) stated that heave reduced with the utilization of fiber with

expansive clays. Heave reduced with an increase of fiber content and lower aspect ratios were more effective than higher aspect ratios. They also reported that swelling reduced with increasing fiber content. In addition, swell pressure decreased by reinforcing expansive clay with fiber. Punthutaecha et al. (2006) investigated on the stabilization of sulfate-rich expansive soil by using recycled materials which were ashes and fibers. They concluded that use of polypropylene and nylon fibers in addition to waste ashes improved soil properties including swelling characteristics and shrinkage strain potential of expansive soils. Abdi et al. (2008) found that polypropylene fiber inclusion decreased the consolidation settlement. Swelling and desiccation cracks reduced by using fibers and increasing fiber contents. The reduction in volumetric shrinkage and desiccation cracks with the increasing fiber content is also determined by Harianto (2008) and Miller and Rifai (2004). Cai et al. (2006) reported that addition of lime and polypropylene fiber causes beneficial changes in swelling-shrinkage potential of clayey soil. Swell and shrinkage potential reduced with an increase in fiber content.

Limited studies have been conducted in which fibers are used as additive to enhance strength characteristics and volume change properties of sand and zeolite embedded expansive soil. A waste material from construction industry obtained from cuttings of polyvinyl chloride pipes is proposed as a secondary material for strength enhancement. The research herein focuses on the combined effect of expansive soil-sand and expansive soil-zeolite reinforced with randomly distributed PF waste material, on the strength and volume change properties. The interfacial mechanical interactions between soil particles and fiber and the influence of fiber content on unconfined compressive strength and tensile strength were investigated. A series of unconfined

compression, flexural strength tests, one-dimensional swelling, consolidation and shrinkage tests were carried out on expansive soil-sand mixture (NS) and expansive soil-zeolite mixture (NZ) with different percentages of fiber inclusion. To further study the mechanism of fiber reinforcement, scanning electron microscopy tests (SEM) were conducted, thus investigating the microstructure and the behavior of interfaces between fiber surface and soil.

2.2 Materials and Methods

2.2.1 Materials

Mixtures of expansive soil-sand and expansive soil-zeolite were used in 1:1 ratio in this study. Expansive soil was collected from Kermiya region, Nicosia, Cyprus, and zeolite was obtained from Ege Zeolit Limited, Bigadiç, Turkey. Physical properties of the two materials, including Atterberg limits (ASTM D4318-10e1), specific gravity (ASTM D854-14), linear shrinkage (BS 1377-2:90) and particle size distribution (ASTM D422-63(2007)e2) are as indicated in Table 2.1. The expansive soil is constituted of mostly silt with appreciable amount of clay, and is classified as silt with high plasticity (MH) according to the Unified Soil Classification System (ASTM D2487-11). Zeolite contains almost equal amounts of sand and silt sized particles, with a small amount of clay sized fraction. The chemical composition detected by X-ray flourescence (XRF) spectrometer is presented in Table 2.2. The sand used was taken from Famagusta coast, Silver Beach, located in the eastern part of the island. The parameters obtained from the sieve analysis (ASTM D422-63(2007) e2) effective grain size (D_{10}), median grain size (D_{50}), and coefficients of uniformity (C_u) and curvature (C_c) are 0.16, 0.19, 1.25 and 1.013 respectively. Based on these results, sand used in this study is classified according to the Unified Soil Classification System (ASTM D2487-11) as poorly graded uniform sand (SP). Particle size distributions of

expansive soil, zeolite and sand are depicted in Figure 2.1.

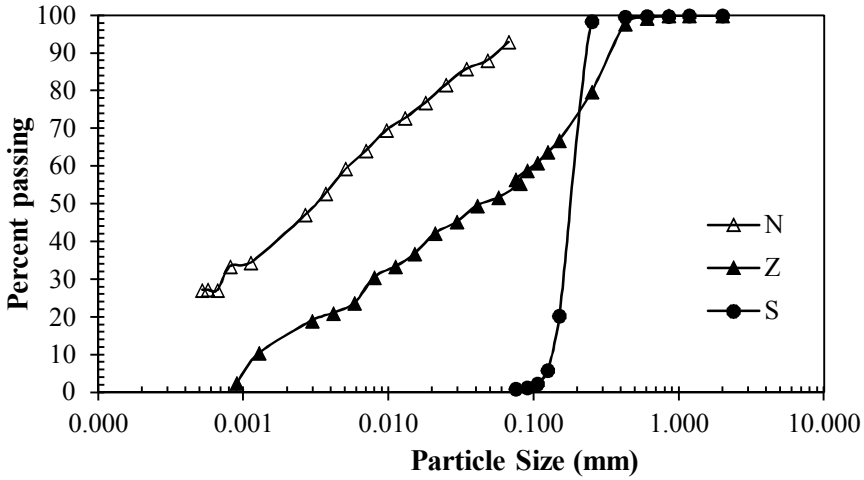

Figure 2.1. Particle size distributions of expansive soil, zeolite and sand.

Table 2.1. Physical properties of expansive soil and zeolite.

Physical properties	**Expansive soil (N)**	**Zeolite (Z)**
Liquid limit (%)	65	41
Plastic limit (%)	36	29
Plasticity index (%)	29	12
Linear shrinkage (%)	18	8
Specific Gravity	2.69	2.35
Clay size (%)	43	15
Silt size (%)	50	41
Sand size (%)	7	44

Table 2.2. Chemical properties of expansive soil and zeolite.

Chemical composition (%)	**Expansive soil (N)**	**Zeolite (Z)**
SiO_2	36.5	61.7
CO_2	17.9	7.05
CaO	16.2	4.69
Al_2O_3	11.8	12.7
Fe_2O_3	6.87	1.58
MgO	6.26	2.18
Other elements	4.47	10.1

X-ray diffraction patterns of soils used in this study shown in Figure 2.2 (a), (b) and

(c) indicate that soil contains kaolinite, illite, montmorillonite and chlorite which are clay minerals, as well as non-clay minerals of feldspar and calcite, whereas sand includes quartz and feldspar minerals and minor amounts of illite, kaolinite and chlorite. Zeolite contains clinoptilolite, quartz, montmorillonite minerals and minor amounts of illite and feldspar.

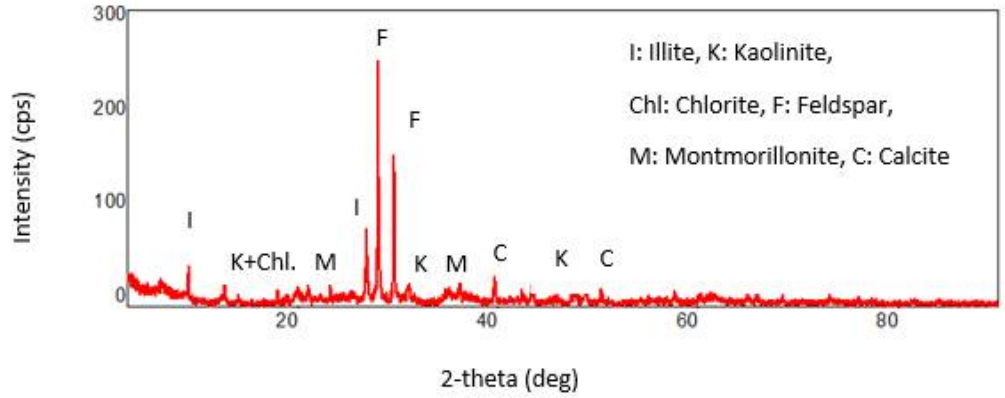

(a)

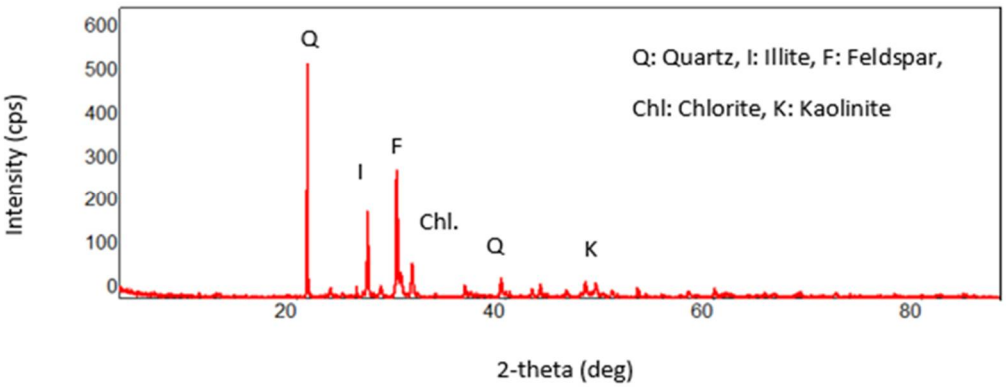

(b)

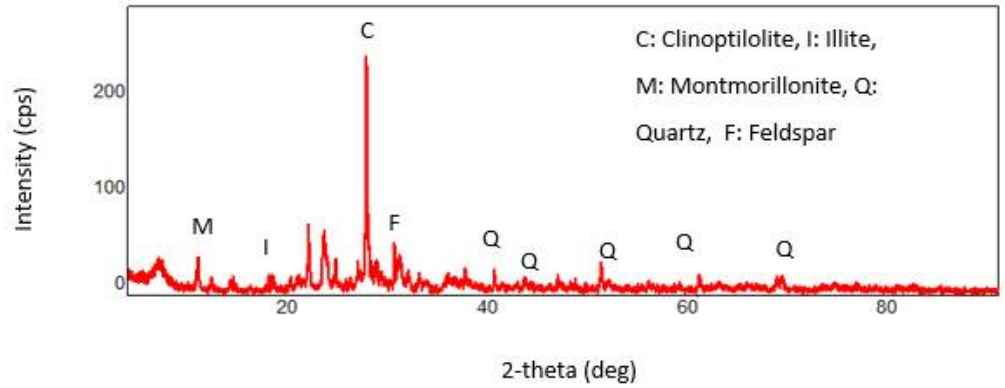

(c)

Figure 2.2. X-Ray diffraction results of (a) soil, (b) sand and (c) zeolite.

The reinforcing additive used is PVC pipe scrap, which is referred to as polymeric fiber (PF) in this study. PF is collected from a pipe manufacturing factory, which is a waste material produced in the form of varying sized thin and soft flakes during the cutting process of polyvinyl chloride pipes. PVC pipes are flexible and they are preferred for plumbing and waste water systems in the construction industry. Their usage accounts for nearly 3% of the construction materials used, thus resulting in large amounts of waste scrap. Hence immense quantities produced as products or by-products in the case of pipe industry, are dumped into landfills. Recycling process of plastic wastes is unprofitable due to difficulty in sorting of waste which would not be economic considering the low value of the material. On the other hand, utilizing it in the form of reinforcing additives in expansive soil stabilization or in landfill barriers can efficiently alleviate the accumulation of the waste in areas where landfill capacities are restricted. Photographic view and scanning electron micrograph image of the PF waste are shown in Figure 2.3. The SEM image depicts the texture of the flakes with x500 magnification. Table 2.3 includes the physical, mechanical and thermal properties of polyvinyl chloride. The aspect ratio of polymeric fibers cannot be determined due to irregular shapes and sizes.

(a)

(b)

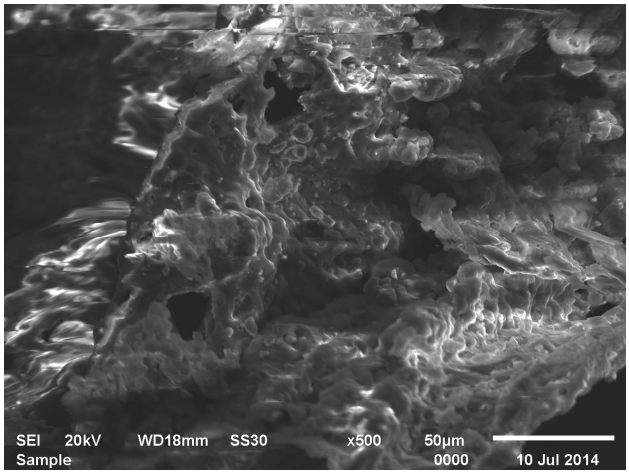

(c)

Figure 2.3. (a) and (b) PF flakes, (c) Scanning electron microscopy image of PF flakes.

Table 2.3. Properties of polyvinyl chloride (Cambridge University Engineering Department, 2003).

Properties	**Polyvinyl chloride**
Density (kg/m^3)	1300-1580
Tensile strength (MPa)	40.7-65.1
Yield stress (MPa)	35.4-52.1
Young's Modulus, E (GPa)	2.14-4.14
Melting temperature (°C)	75-105

2.2.2 Sample Preparation

The samples were prepared in eight different groups of different combinations of expansive soil, sand, zeolite and polymeric fibers. Soil groups are explained in Table 2.4.

Table 2.4. Definition of soil groups.

Soil Groups	**Definition**
NS	50% Expansive soil + 50% Sand
NS1%PF	49.5% Expansive soil + 49.5% Sand + 1% Polymeric fiber
NS2%PF	49.0% Expansive soil + 49.0% Sand + 2% Polymeric fiber
NS3%PF	48.5% Expansive soil + 48.5% Sand + 3% Polymeric fiber
NZ	50% Expansive soil + 50% Zeolite
NZ1%PF	49.5% Expansive soil + 49.5% Zeolite + 1% Polymeric fiber
NZ2%PF	49.0% Expansive soil + 49.0% Zeolite + 2% Polymeric fiber
NZ3%PF	48.5% Expansive soil + 48.5% Zeolite + 3% Polymeric fiber

The test specimens were prepared using the compaction characteristics of maximum dry density and optimum water content obtained from Standard Proctor compaction test (ASTM D698-12e2). The materials were weighed in the given proportions of dry mass and first mixed in dry state to distribute the PF evenly, as observed to be the most efficient procedure, unlike polypropylene fiber which is usually mixed in the moist state to prevent lumping. The latter method is found to be unsatisfactory for the PF flakes which resemble desiccated coconut, readily and most efficiently mixing with

the soil in the dry state, before adding the optimum water content and thoroughly mixing all the ingredients in the mixer, and kept in nylon bags for 24 hours before preparing test specimens.

2.2.3 Test Methods

Unconfined compression test (ASTM D2166-06) was carried out for all soil groups on soil specimens of 38 mm diameter and 76 mm height compacted to maximum dry density at optimum water content.

Flexural strength test was conducted in accordance to ASTM C348-14 on soil specimens statically compacted (Figure 2.4) at optimum moisture content and maximum dry density, in a special mold of 40 mm width, 40 mm depth and 160 mm height, as depicted in Figure 2.5 (a) and (b) shows the test setup and a failed soil beam under flexure.

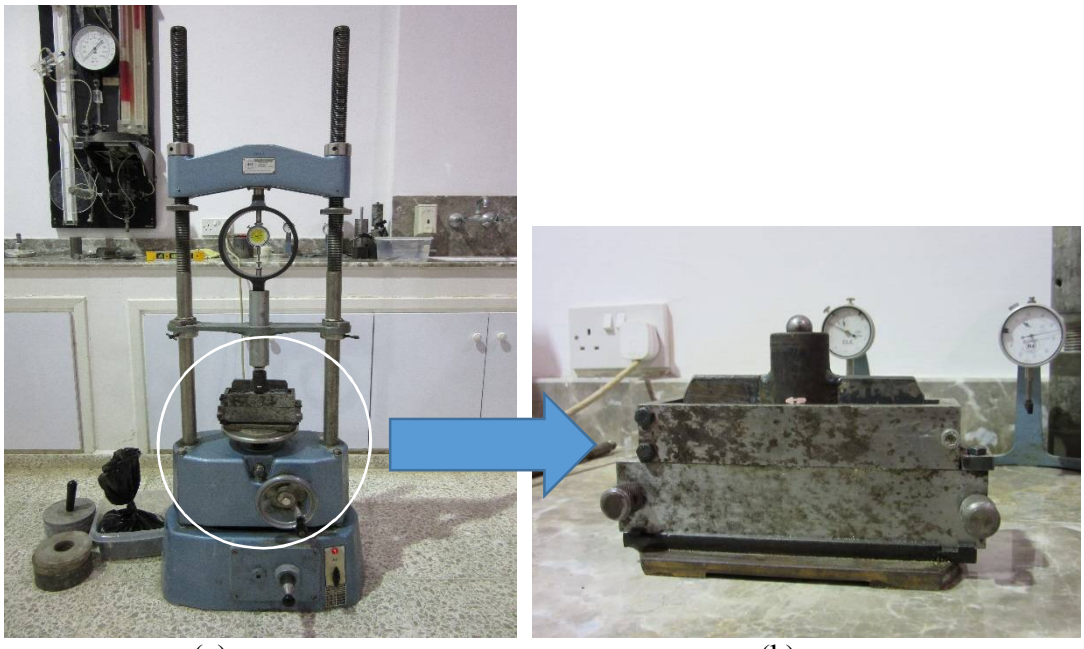

(a) (b)

Figure 2.4. (a) Preparation of flexural strength test sample with static compaction, (b) Mold of flexural test specimen.

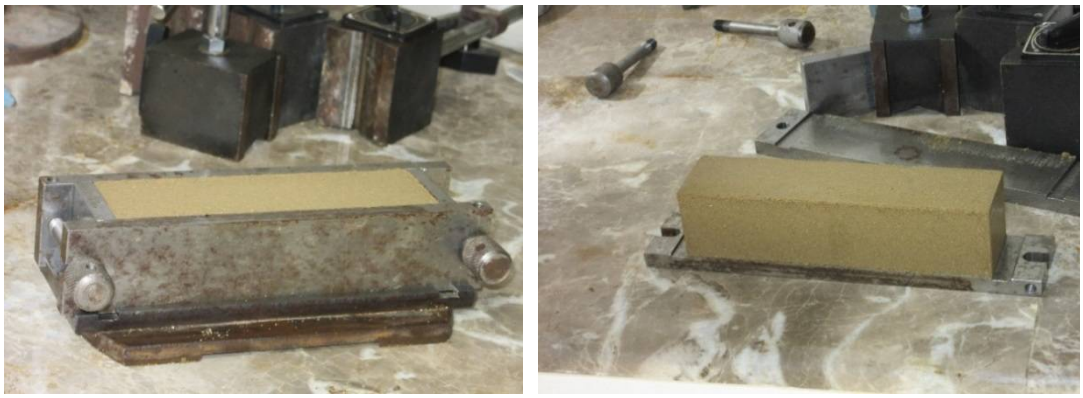

(a)

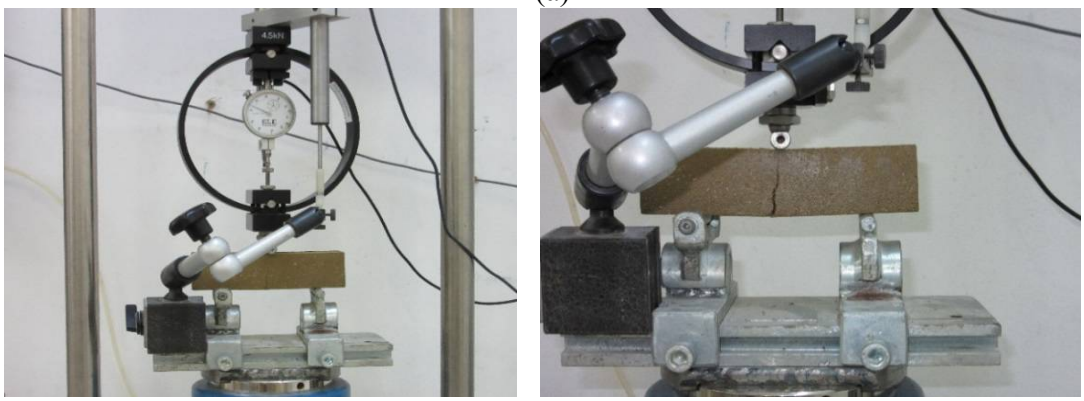

(b)

Figure 2.5. (a) Flexural strength test specimen prepared in a special mold, (b) Test setup and ruptured specimen.

One dimensional swell (ASTM D4546-14) and consolidation tests (ASTM D2435-11) were applied to the compacted specimens prepared at 75 mm diameter and 15 mm height. Swelling was conducted under 7 kPa surcharge pressure followed by consolidation test upon completion of one-dimensional swelling.

For the volumetric shrinkage test, another set of compacted soil samples were subjected to swell, and upon completion of one-dimensional swell, soil samples were drained and stored in a temperature controlled room. Height and diameter of the soil specimens were measured at different time intervals using a digital vernier caliper. This measuring period continued until there was no further change in dimensions.

Filter paper test is a simple and inexpensive method in order to acquire soil-water characteristics of soils and can be reliably used to measure suctions from 0 kPa to 1 000 000 kPa. Compacted soil samples with 50 mm diameter and 15 mm height were prepared in consolidation rings and swelling process was started by using the one-dimensional swell equipment. Dial gauge readings were taken every day until full swell was almost attained. Upon completion of swelling, the samples were air dried under 7 kPa surcharge pressure in a temperature controlled room.

Soil samples in consolidation rings were packed in moisture containers at different stages of drying, in intimate contact with three filter papers, which is essential for measurement of matric suction. The paper in contact with the soil was a sacrificial one used to protect the other two filter papers from being clogged with soil particles, and was not considered in suction determination. The intimate contact was ensured by placing bubble wrap on specimens on the filter paper discs, before tightly sealing the containers. The sealed moisture cans then were wrapped carefully with glass wool and placed in styrofoam boxes which were sealed and kept in a protected environment for equilibration period. Gloves and tweezers were used in handling the filter papers and a scale of 10^{-4} g accuracy was utilized in weighing the filter papers.

The sealed box containing the specimens were maintained for 7 days in a cabinet in the temperature controlled room until the equilibrium was achieved by water exchange between the soil and the filter paper. The filter papers were initially dry, therefore moisture movement occurred from the soil to the filter paper until equilibration of water content of both the soil and filter papers was completed. When the equilibration time was completed, boxes were opened and the samples were taken out of the

containers for the determination of water content and volume.

The top and bottom filter papers were placed into different containers in order to find their water contents. The purpose of using two filter papers was to check the reliability of the measurements. Mass of containers and filter papers were measured with a four digit sensitive balance.

2.3 Experimental Results and Discussions

The maximum dry densities of NS, NZ, NSPF and NZPF specimens obtained in standard Proctor test were 1690 kg/m^3, 1390 kg/m^3, 1670 kg/m^3 and 1375 kg/m^3 respectively, whereas optimum water contents varied from 17.5% to 18% for NS samples after PF inclusion and 24.5% to 28.5% for NZ samples after fiber addition. Therefore, it was observed that the compaction characteristics of NS remained almost the same with fiber inclusions, which is in good agreement with Kumar et al. (2006), Kumar et al. (2007), Şenol (2012), Jamsawang et al. (2014) and Onyejekwe and Ghataora (2014). NZ specimens, however showed an increment in optimum water content and a decreasing trend in maximum dry density values after polymeric fiber addition because NZ have higher fines content.

2.3.1 Unconfined Compressive Strength

Unconfined compression test applied on all soil groups yielded the stress-strain relationships as depicted in Figure 2.6. The unconfined compressive strength (peak value of compressive stress versus axial strain curve) is observed to increase slightly when PF is added to NS mixtures, while failure strain (corresponding to the peak strength) has increased by 66%. Addition of 2% PF reduced the unconfined compressive strength slightly, increasing the failure strain by almost two fold compared to NS sample. Therefore, it can be concluded that the compressive strength

has not changed significantly, whereas the samples became more ductile with the addition of fiber. Figure 2.6 (a) depicts that while the reduction of post-peak strength is sudden in NS and NS1%PF, it occurs gradually when the PF content increases. However, 3% PF causes a notable reduction both in compressive strength and failure strain, whereas post-peak strength reduction is the slowest. The variation of failure strain and fiber content is given in Figure 2.7. The unconfined compressive strength of NZ is almost the same after 1% PF addition and also a small reduction is observed in failure strain. Inclusion of 2% PF decreased the unconfined compressive strength by 45.5%, however the failure strain increased by 1.37 fold compared to NZ specimen. On the other hand, a small increment is observed in unconfined compressive strength with 3% PF compared to 2% PF while this trend is vice versa in the failure strain. Utilization of 2% PF has not provide an improvement in compressive strength but it caused the material to become more ductile, therefore 2% PF can be selected as an optimum value.

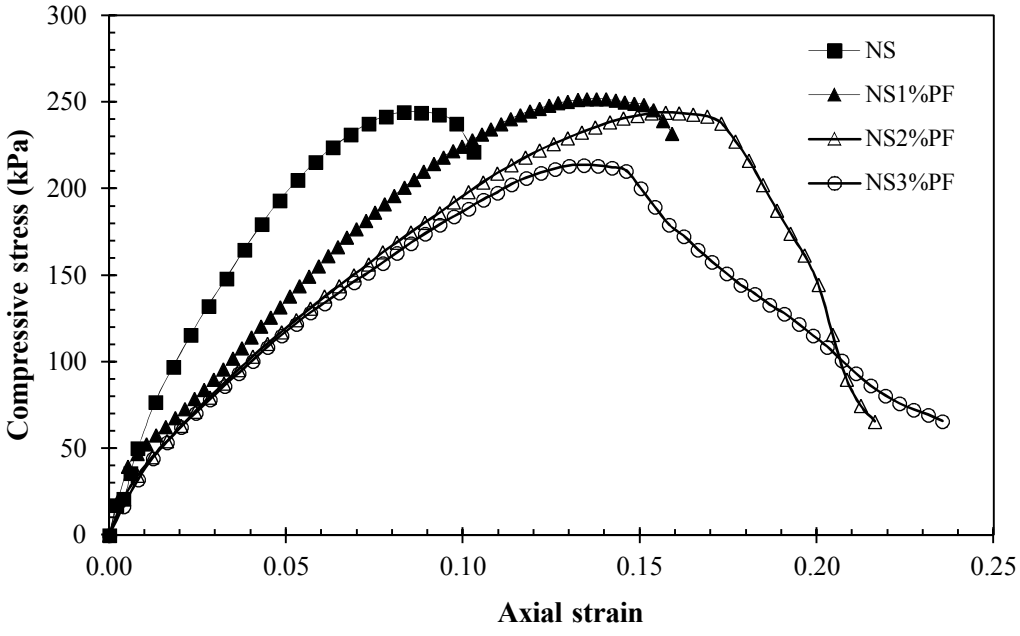

(a)

Figure 2.6. Stress-strain relationships of (a) NS group, (b) NZ group.

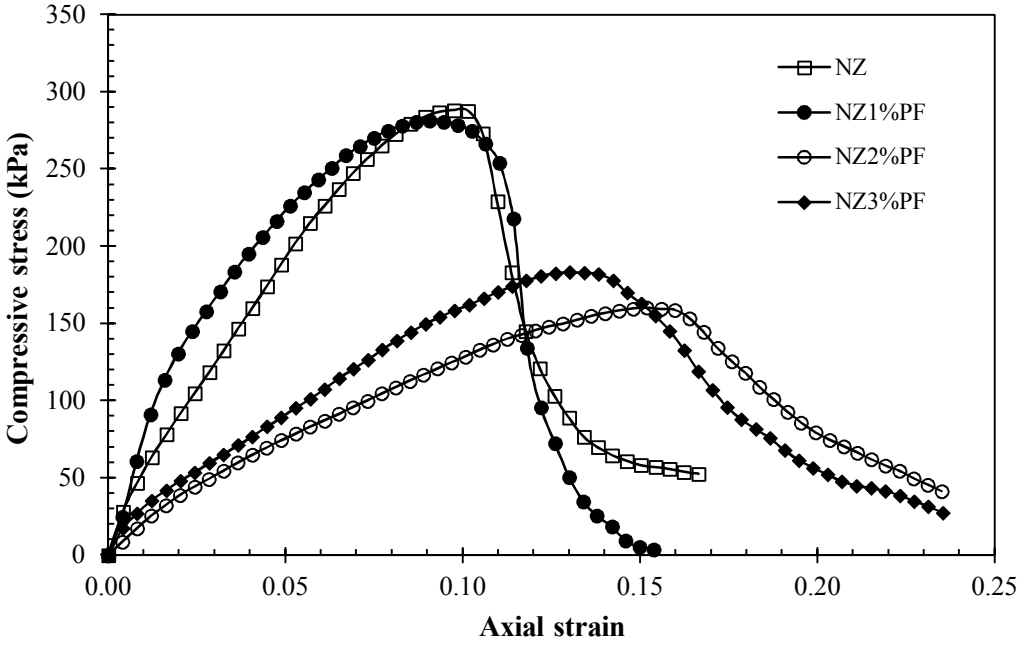

(b)

Figure 2.6. (Cont.)

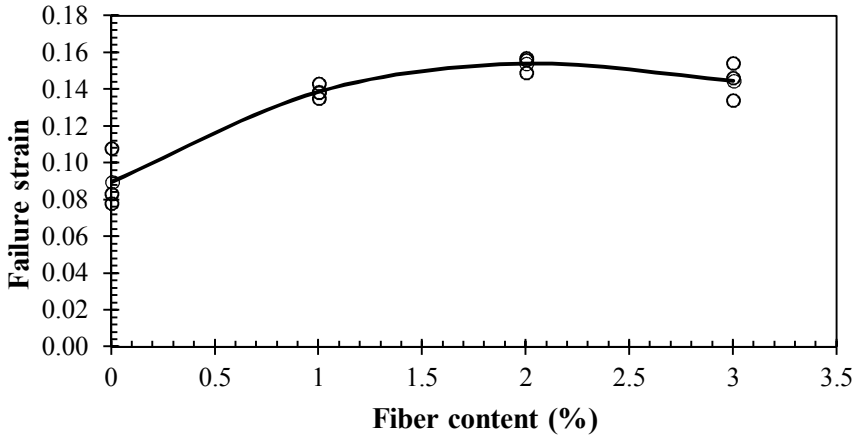

(a)

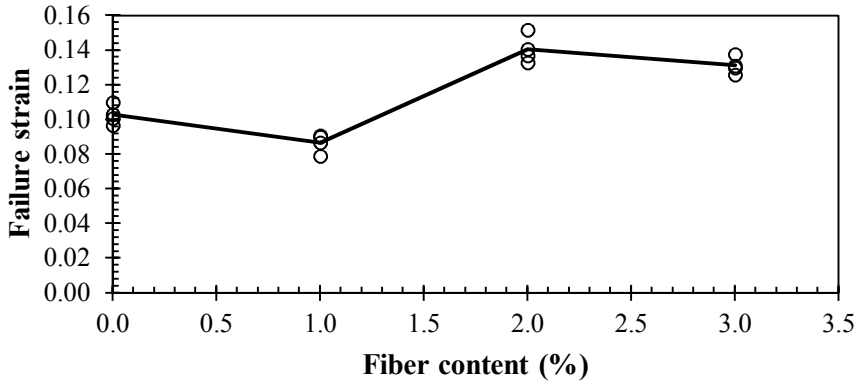

(b)

Figure 2.7. Variation of failure strain with fiber content (a) NS group and (b) NZ group.

2.3.2 Tensile Strength

Tensile strength is a prominent parameter in the projects which are subjected to heavy loads such as, highways, airfield and road pavements, landfills, embankments and land-based structures (Vaníček, 2013; Onyejekwe and Ghataora, 2014; Anggraini et al., 2015), hence behavior of stabilized soils under tension should be scrutinized. Various test methods were reported for the determination of tensile strength of soils in the literature (Tej and Singh, 2013) however, in this thesis, tensile strength is indirectly studied by flexural strength test.

2.3.2.1 Flexural Strength

Flexural strength tests were carried out for all soil groups which yielded load-deflection curves. The peak flexural load of each mixture was used in the calculation of flexural strengths by Equation 2.1. Toughness is defined as the energy absorbed during flexural loading, and is represented by the area enclosed under the load versus deflection curve up to the deflection of L/150 (Onyejekwe and Ghataora, 2014; Jamsawang et al., 2014). Increase in the deflection value is an indication of ductile behavior, hence improved toughness. Ductility and toughness are the two important parameters for pavement materials to prevent sudden failure after peak due to traffic load (Disfani et al. 2014).

$$f = \frac{1.5PL}{bd^2} \tag{2.1}$$

where, P is the flexural load, b is the width, d is the depth and L is the span length of the flexure beam.

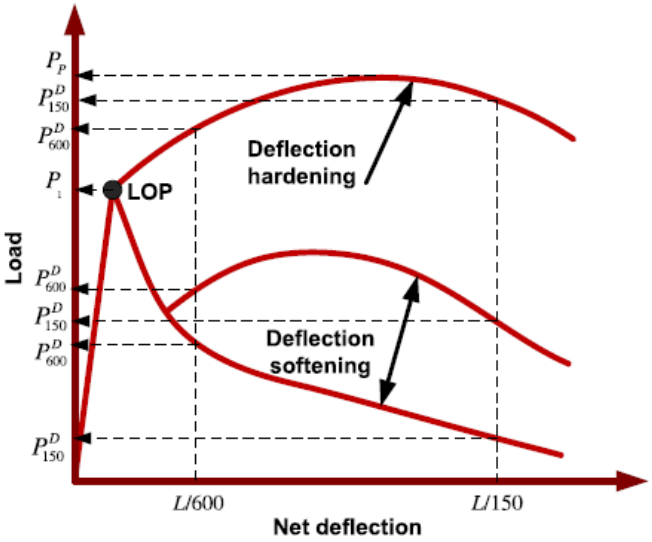

Figure 2.8. Parameter calculations obtained from load-deflection curves (ASTM C1609-10, Jamsawang et al., 2014)

Load-deflection relationships obtained from flexural strength test are presented in Figure 2.9. The flexural performance of fiber reinforced soil mixture displays either deflection-softening or deflection-hardening behavior. From Figure 2.8, the point at which the linearity of the load-deflection curve ends (P_1), the initial peak, also known as the limit of proportionality (LOP) as described in ASTM C1609-10 is determined and compared with the peak flexural load (P_f). If the two loads are almost equal, the flexural behavior is deflection-softening, conversely if P_f/P_1 is greater than 1 deflection-hardening occurs. This can further be justified by determining the equivalent flexural strength ratio given in Equation 2.2.

$$R^D_{T,150} = \frac{T^D_{150}}{P_1 \dfrac{L}{150}} \tag{2.2}$$

where, $R^D_{T,150}$ is the flexural strength ratio, T^D_{150} is toughness which is the area under the load-deflection curve from 0 to L/150 (0.6 mm) deflection. The equivalent flexural strength ratio represents the efficacy of energy absorption of the material from the beginning to the deflection of L/150 (Sukontasukkul and Jamsawang, 2012;

Jamsawang et al., 2014). If this value is less than 100%, deflection-softening, and if greater than 100% deflection-hardening behavior occurs. The latter indicates a high toughness material.

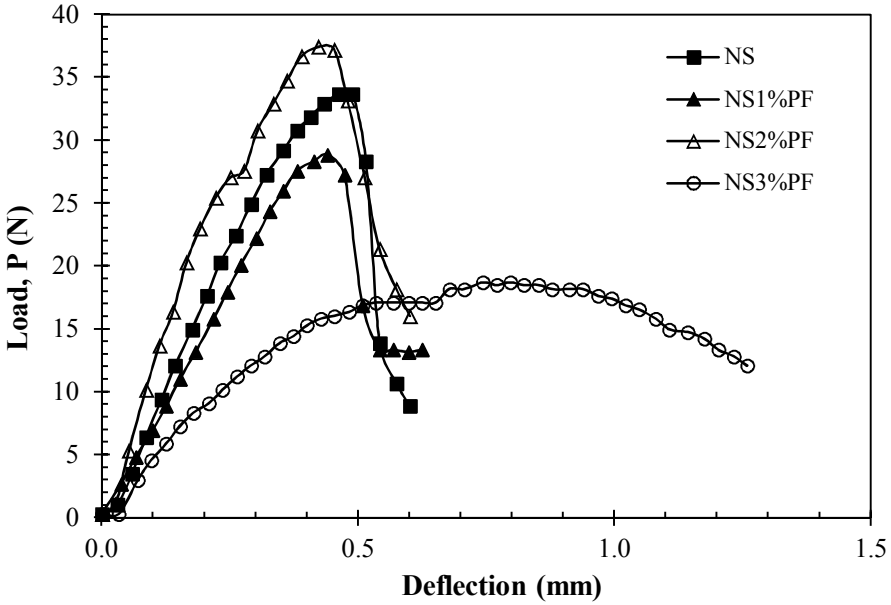

(a)

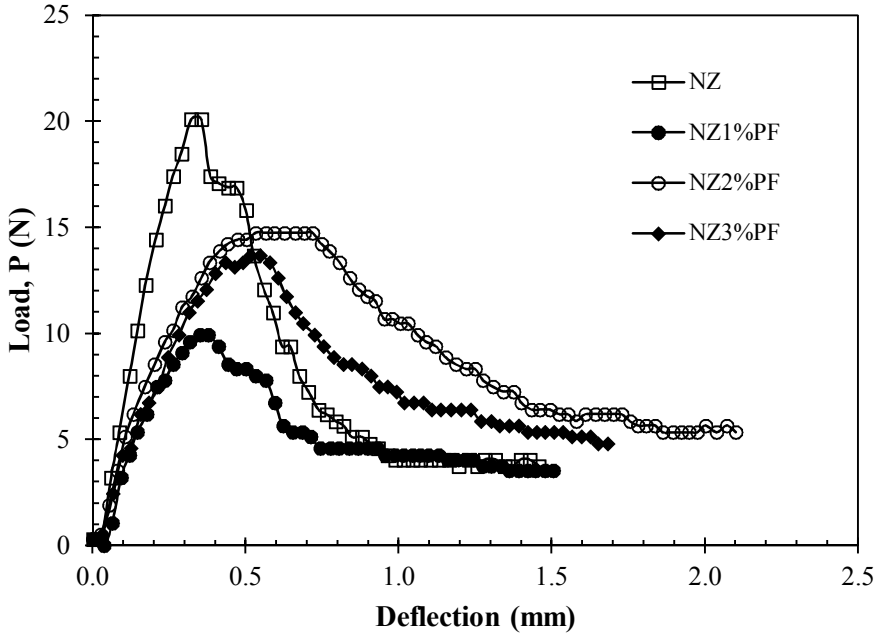

(b)

Figure 2.9. Load-deflection curves of (a) NS group, (b) NZ group.

Flexural strength versus fiber content in Figure 2.10 shows that strength reduces with

1% and 3% fiber inclusions, whereas 2% fiber inclusion gives the best result again indicating that flexural strength increases with an optimum fiber content of this amount for both NS and NZ groups.

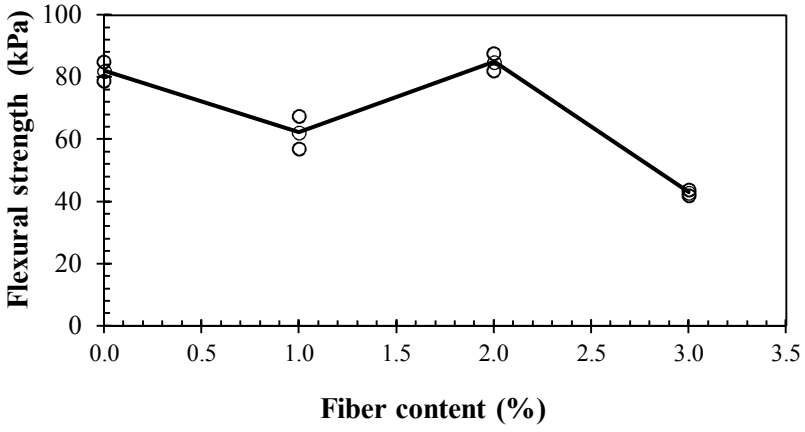

(a)

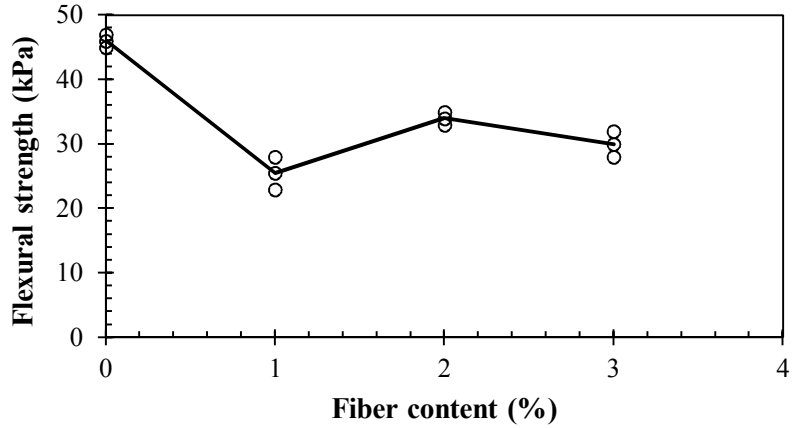

(b)

Figure 2.10. Variation of flexural strength with fiber content (a) NS group, (b) NZ group.

The results of tensile tests exhibit a significant increment in tensile strength of stabilized soil, mainly in flexure, when fibers are used compared to compressive strength. Increase in fiber content increases friction between fiber and soil particles, hence bonding is improved due to increasing interface between fiber and soil particles. The strength ratios of flexural strength to unconfined compressive strength of NSPF

and NZPF are observed on the average to be 0.30 and 0.16 respectively. The results of NSPF are in good agreement with previous research on strength characterization of stabilized soils as road base (Kumar et al., 2007; Muntohar et al., 2013).

Flexural performance in terms of first-peak strength (f), residual strength at deflection of L/150 (f_{150}^{D}), flexural toughness (area under the load–deflection curve from deflection of 0 to L/150 (T_{150}^{D}), and equivalent flexural ratio ($R_{T,150}^{D}$) are given in Table 2.5. The equivalent flexural ratio which represents the area under the load–deflection curve (or energy absorption) per strength and volume, 2% PF included NS appear to have highest equivalent flexural ratio than the other percentages of PF. This shows the effectiveness of the 2% fiber inclusion to bridge across cracks appearing under flexure, hence enhancing the energy absorption ability of stabilized soil under loading. When comparing the NS and NZ specimens, the NS appears to be performing better with PF. This can be explained by the bond between the fiber and the matrix, comes from two parts, an interfacial bond and a frictional (or anchorage) bond. When there is no chemical bond between fiber and matrix, the interfacial bonding depends strongly on the strength of the matrix, whereas the frictional bond depends mainly on the shape of the fiber. Since the shape of the polymeric fiber is crimped (curled) and with a rough surface as observed by SEM (Figure 2.2), it is able to provide frictional bond. Since the matrix strength of NS is 47% higher than the NZ based on the unconfined compressive strength, the interfacial bond is higher in PF included NS specimens. Residual strength at L/150 represents the ability of fiber reinforced soil to sustain load after the peak load. In all cases, the residual strengths decrease after the first crack, whereas 2-3% PF inclusion increases the residual strength of NS and 2% has the highest value for NZ. Therefore, 2% is observed to be effective in flexural strength

performance for both soils.

Table 2.5. Flexural performance data.

Soil group	P_1 (N)	P_f (N)	$\frac{P_f}{P_1}$	f (kPa)	f_{150}^{D} (kPa)	T_{150}^{D} (Nmm)	$R_{T,150}^{D}$ (%)
NS	21	34	1.60	78.9	20.8	11	87
NS1%PF	27	29	1.07	67.4	30.9	10	62
NS2%PF	20	37	1.87	87.7	37.6	14	117
NS3%PF	17	19	1.09	43.9	40.1	7	68
NZ	20	20	1.00	47.0	23.4	8	67
NZ1%PF	10	7.5	0.75	25.5	15.7	4	67
NZ2%PF	15	14.4	0.96	34.0	34.7	6	67
NZ3%PF	14	13.4	0.95	30.0	29.3	5	60

f: Flexural strength (kPa)

The flexural performance data depicted in Table 2.5 clearly indicates that 1% PF inclusion reduces the flexural toughness of NS and NZ while 2% PF reinforcement enhances the flexural behavior, hence providing a tougher material. The load-deformation behavior of 2% PF reinforced soil clearly indicates a flattened portion at the initial peak (P_1), where for further increment of deflection there is no load increment. This flat portion of the curve, although not so pronounced, can be attributed to the resistance of fibers in tension which contribute to further strengthening of bonds and building up of strength (Onyejekwe and Ghataora, 2014). The poor behavior of 1% PF reinforced soil can be attributed to insufficient specific surface area of the reinforcement, hence weak interlocking bonds might have formed between soil matrix and fiber, in addition to the possibility of non-uniform mixing, and formation of localized fiber-soil surfaces of weakness at the fiber-soil interface as indicated by Onyejekwe and Ghataora (2014). However, even this low amount of fiber enables a less brittle failure right after the peak value, than the specimen with no reinforcement, whereas 2% is large enough to distribute evenly in the compacted expansive soil-sand mixture, with increased contact area at the interface of soil matrix. This amount is

observed to be the optimum value improving strength and ductility, as 3% PF displays even poorer performance, which can be attributed to possible accumulation of excess fiber in the compacted specimens. Therefore, a fiber amount higher than the optimum value would cause accumulation of fibers forming lumps, hence less effective in improving strength and toughness due to reduced contact with soil particles, as also stated by Cai et al. (2006).

Flexural strength ratio of NS2%PF is higher than 100% due to the deflection limit of L/150, hence indicating a strain hardening behavior, and hence an increased toughness compared to the NS and with other percentages displaying strain softening behavior. NZ and PF added mixtures indicated a strain softening behavior, even though the flexural strength was observed to be highest with 2% PF addition. Therefore, PF inclusion was observed to be more beneficial, as far as flexural strength was concerned, when used in NS mixtures.

The use of sand in the mixture has created a stable structure with increased dry density which inhibit fiber slipping when under compressive and tensile effects (Kumar et al., 2006).

2.4 Volume Change

Strength test results demonstrated that 3% PF was not a suitable fiber content for this study. Therefore, volume change experiments were done using 1% and 2% fiber inclusion only in order to investigate the effect of fiber content on swell, shrinkage and compressibility properties.

2.4.1 Swell

Figure 2.11 (a) depicts the one-dimensional swell test results of NS, NS1%PF and

NS2%PF and the swell curves of NZ, NZ1%PF and NZ2%PF are shown in Figure 2.11 (b). Percent primary swell and primary swell time results are summarized in Table 2.6. Swell potential of NS is decreased from 0.67% to 0.26% and 0.53% after addition of 1% and 2% polymeric fiber respectively. In addition to this, swell potential of NZ showed a considerable reduction with the inclusion of polymeric fiber. NZ has a high swell potential (Snethen et al., 1977), which is 2.35%, and it decreased to medium swell of 1.25% with 1% PF and 1.06% with 2% PF reinforcement. Previous studies (Cai et al., 2006; Abdi et al., 2008; Viswanadham et al., 2009) also showed that utilization of fiber caused a reduction in swelling with increasing fiber content, which is in good agreement with the results of NZ group. However, swell potential of PF included sand mixtures are closer to the category of "low swell" (Snethen et al., 1977).

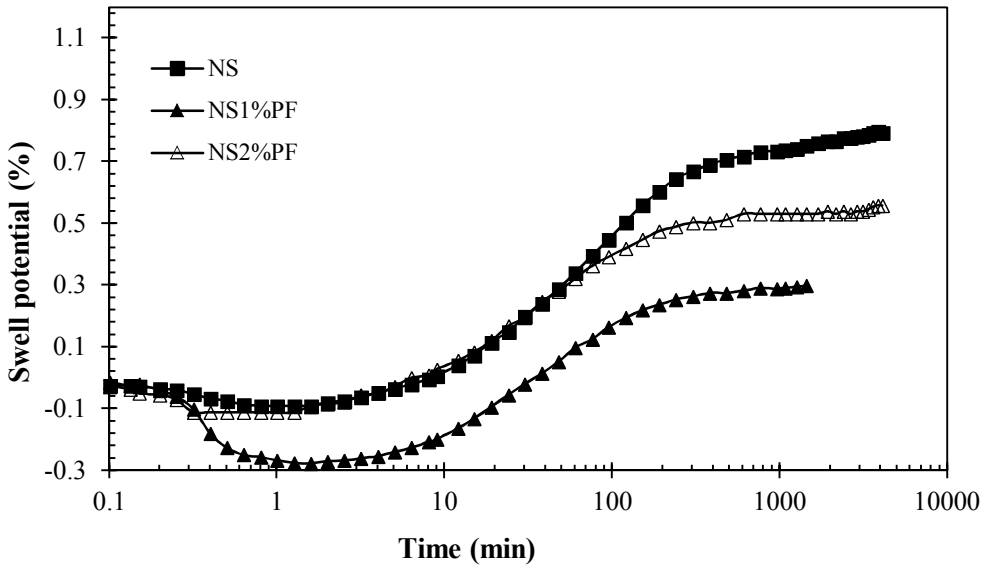

(a)

Figure 2.11. Swell curves of (a) NS group and (b) NZ group samples.

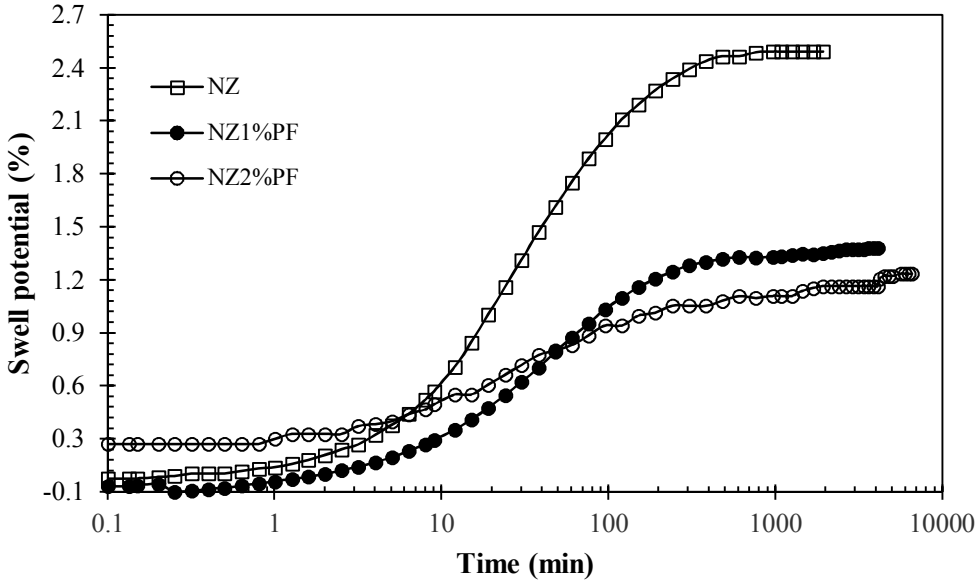

(b)
Figure 2.11. (Cont.)

Table 2.6. Percent primary swell and primary swell time results.

Soil group	Swell potential (%)	Swell time (min)
NS	0.67	204
NS1%PF	0.26	107
NS2%PF	0.53	210
NZ	2.35	110
NZ1%PF	1.25	200
NZ2%PF	1.06	320

2.4.2 Compressibility

Void ratio versus effective consolidation pressure relationships are presented in Figure 2.12. The compressibility parameters which are compression index (C_c), rebound index (C_r) and swell pressure (p_s') are summarized in Table 2.7. It can be observed that the curves are slightly flatter after reinforcement of expansive soil-sand (NS) and expansive soil-zeolite (NZ) mixtures. The compression indices of NS and NZ are reduced by 7.5 % and 6.7% respectively after 2% PF inclusion. Addition of polymeric fiber has been more efficient in reducing the compression and rebound indices than

addition of sand and zeolite alone. These findings are also supported by Jayasree et al. (2014) and Abdi et al. (2008).

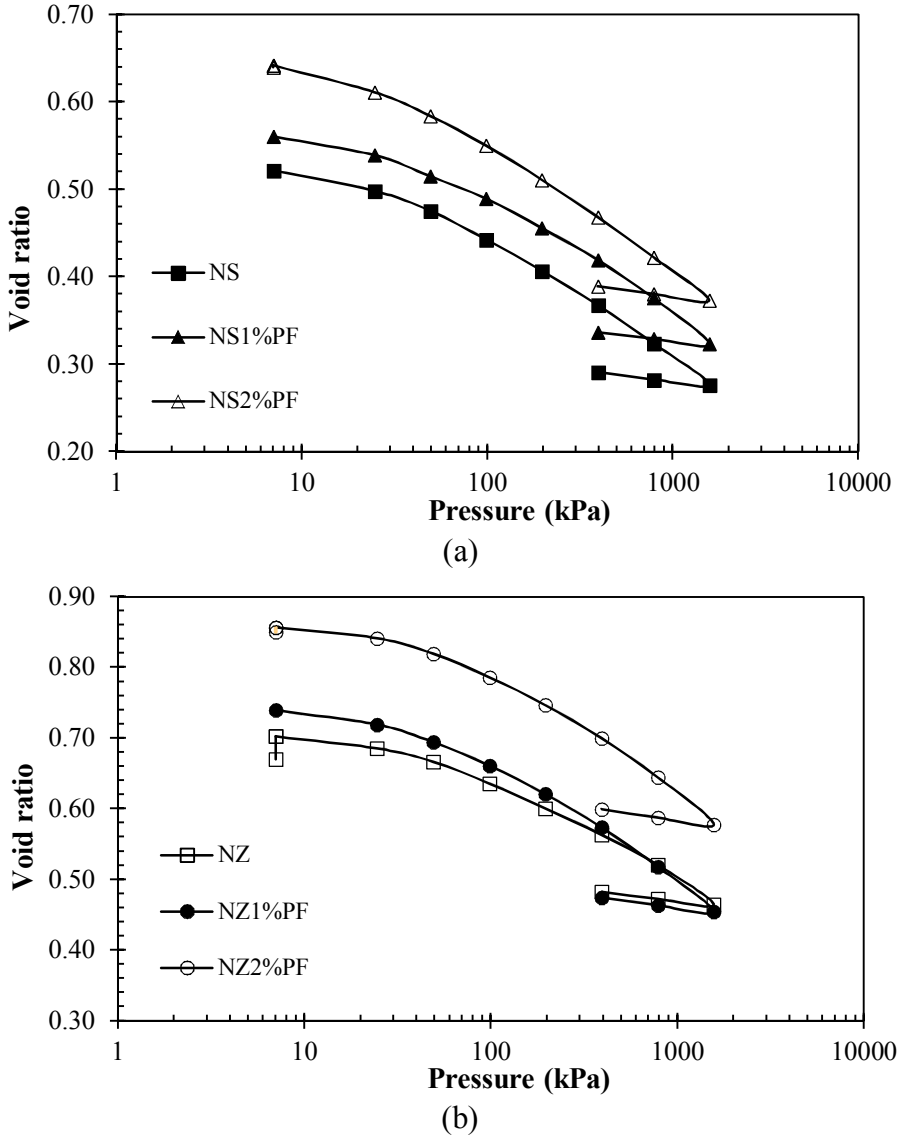

Figure 2.12. Consolidation curves of (a) NS group and (b) NZ group.

Table 2.7. Compressibility characteristics.

Soil group	C_c	C_r	p_s' (kPa)
NS	0.133	0.028	-
NS1%PF	0.126	0.027	-
NS2%PF	0.123	0.027	10
NZ	0.195	0.036	46
NZ1%PF	0.186	0.034	16
NZ2%PF	0.182	0.033	13

Compression index (C_c) and initial void ratio (e_o) values are used to obtain the ratio of $C_c/1+e_o$ which was used in the soil classification based on the compressibility (Coduto, 2001). According to this categorization, NS, NS1%PF and NS2%PF soil combinations are "slightly compressible" compared to N which is moderately compressible. NZ and NZ1%PF soil mixtures are grouped as "moderately compressible" whereas NZ2%PF is classified as slightly compressible.

Coefficient of consolidation (c_v) and coefficient of volume compressibility (m_v) values determined from consolidation test results, under different ranges of consolidation pressures were used to evaluate the saturated hydraulic conductivity (k_{sat}) using Equation 2.3 and the results are given in Table 2.8.

$$k_{sat} = c_V m_V \gamma_W \tag{2.3}$$

where, k_{sat} is the saturated hydraulic conductivity, c_V is the coefficient of consolidation, m_V is the coefficient of volume compressibility, γ_W is the unit weight of water.

Table 2.8. Saturated hydraulic conductivity results.

	k_{sat} (cm/s)			
Soil group	**98-196 (kPa)**	**196-392 (kPa)**	**392-784 (kPa)**	**784-1568 (kPa)**
NS	$4.97\text{x}10^{-8}$	$2.82\text{x}10^{-8}$	$1.60\text{x}10^{-8}$	$9.01\text{x}10^{-9}$
NS1%PF	$9.26\text{x}10^{-8}$	$5.29\text{x}10^{-8}$	$3.07\text{x}10^{-8}$	$1.95\text{x}10^{-8}$
NS2%PF	$9.78\text{x}10^{-8}$	$5.13\text{x}10^{-8}$	$2.97\text{x}10^{-8}$	$1.88\text{x}10^{-8}$
NZ	$1.44\text{x}10^{-7}$	$7.54\text{x}10^{-8}$	$4.48\text{x}10^{-8}$	$3.00\text{x}10^{-8}$
NZ1%PF	$8.73\text{x}10^{-8}$	$5.12\text{x}10^{-8}$	$3.14\text{x}10^{-8}$	$1.86\text{x}10^{-8}$
NZ2%PF	$8.31\text{x}10^{-8}$	$5.11\text{x}10^{-8}$	$3.13\text{x}10^{-8}$	$1.91\text{x}10^{-8}$

The hydraulic conductivity values presented in Table 2.8 exhibit that the effect of polymeric fiber addition has a diverse effect on the NS and NZ mixtures, increasing

the hydraulic conductivity in NSPF and reducing in NZPF mixtures. However, all values remained well below the regulatory limit. It is observed that increasing fiber content has no significant effect on the hydraulic conductivity. Addition of 1% PF and 2% PF showed almost the same influence on the hydraulic conductivity values for both NS and NZ groups.

2.4.3 Shrinkage Curves

Shrinkage test results of NS and NZ were examined as volumetric, axial and diametral shrinkage strains with respect to time and the test results are depicted in Figure 2.13 and Figure 2.14 respectively. Volumetric shrinkage strain of NS was 0.068 and it increased to 0.076 and 0.095 after addition of 1% and 2% PF respectively. Volumetric and axial shrinkage values of PF included NS samples were stabilized at approximately 7 days while showed an increasing trend in NS alone. In diametral shrinkage strain, however NS and PF included NS samples stabilized at almost the same time. In NZ group, volumetric shrinkage strain of NZ, NZ1%PF and NZ2%PF were 0.084, 0.096, 0.065 respectively. The change of volumetric shrinkage strain of NZ completed in approximately 15 days, however, PF added NZ samples stabilized in 12 days. PF reinforcement provided contact area between fiber and soil particles therefore, volumetric shrinkage strain decreased. Addition of 1% PF was not enough to maintain the interaction between soil and fiber, but 2% PF increased the soil-fiber interlocking, hence the volumetric shrinkage strain reduced. The same behavior was observed in axial and diametral shrinkage strains.

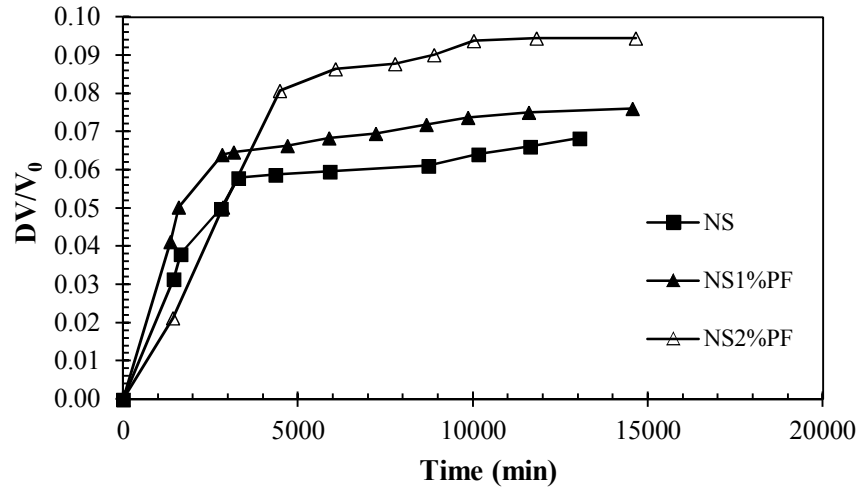

(a)

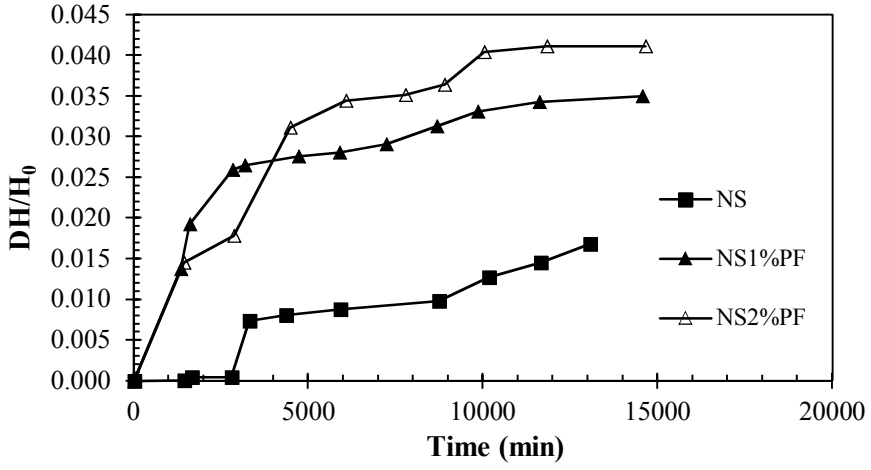

(b)

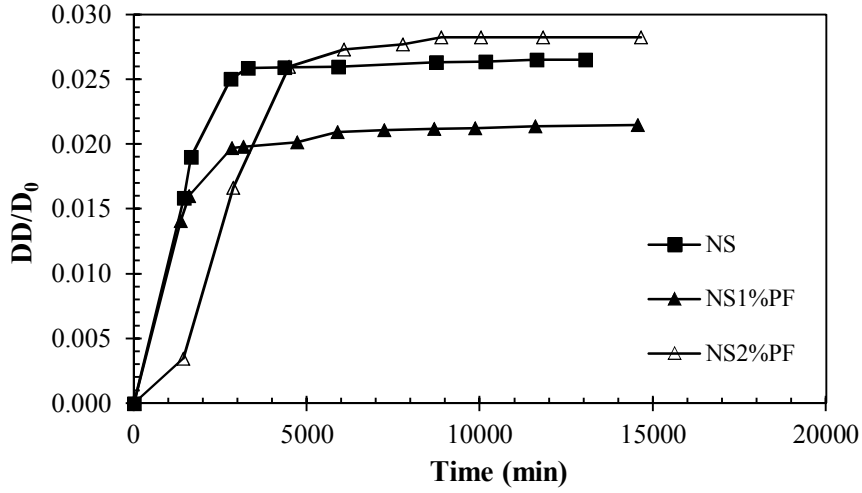

(c)

Figure 2.13. (a) Volumetric, (b) axial and (c) diametral shrinkage strains of NS group.

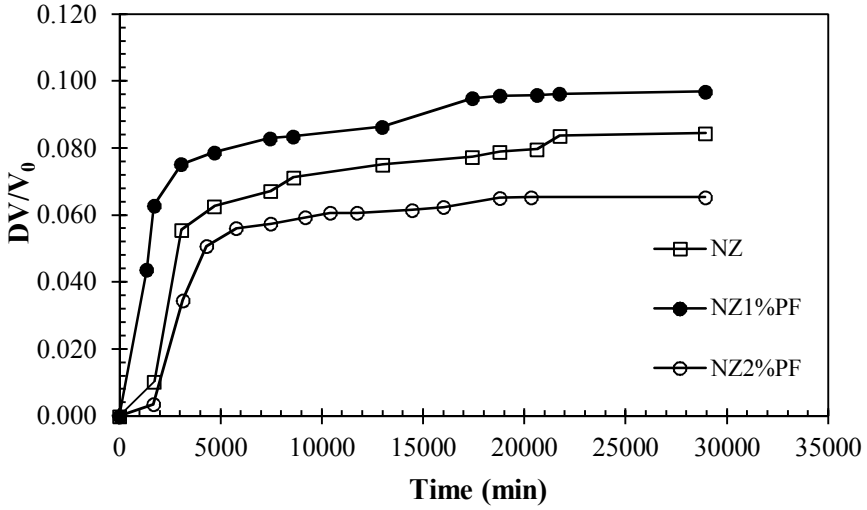

(a)

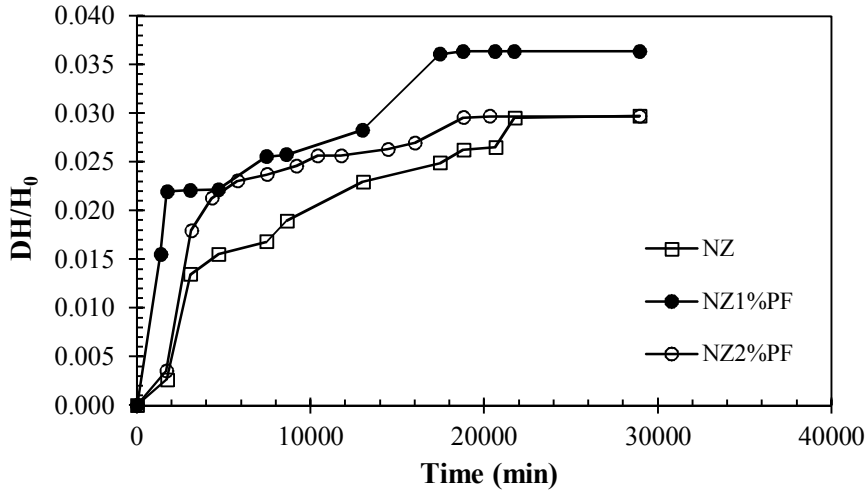

(b)

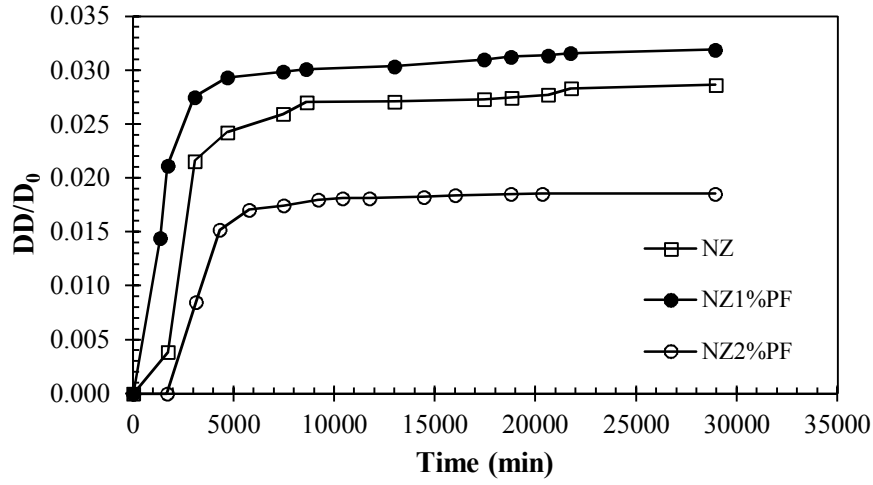

(c)

Figure 2.14. (a) Volumetric, (b) axial and (c) diametral shrinkage strains of NZ group.

Figure 2.15 shows the evaporation curves of NS and NZ mixtures along the desiccation path, obtained from the shrinkage data, from which the rate of evaporation, and different phases along the desiccation path can be observed, as well as initial and final water contents.

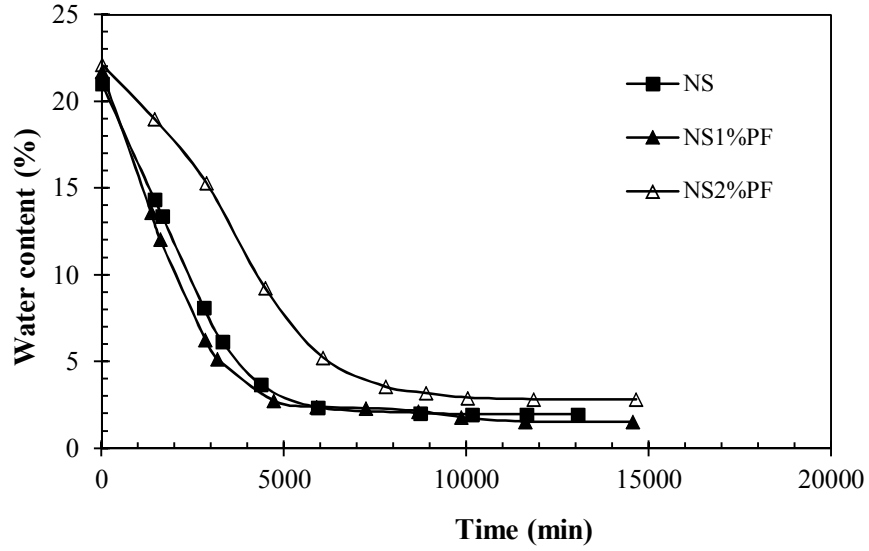

(a)

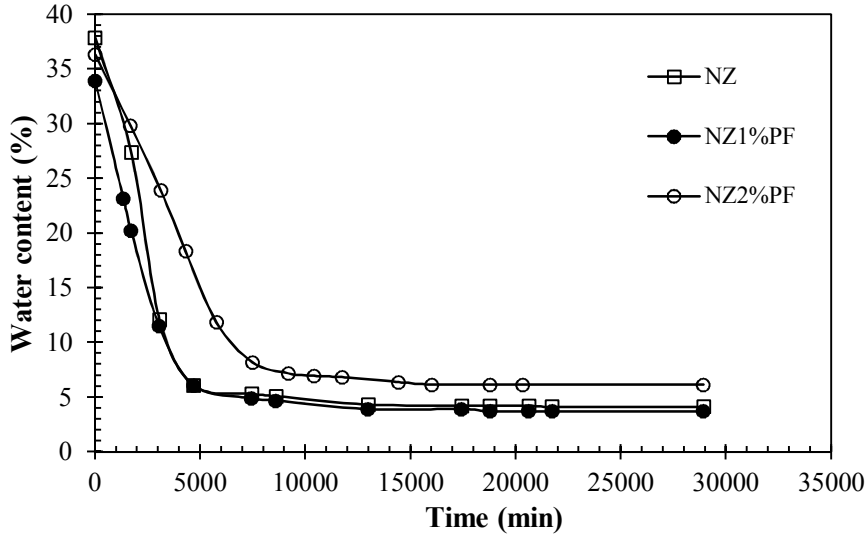

(b)

Figure 2.15. Evaporation graphs of (a) NS and (b) NZ groups.

Briaud et al. (2003) proposed a parameter called shrink-swell index, which is defined as the difference between the water content attained at the end of primary swelling

period and the water content at which shrinkage ceases ($I_{ss} = w_{sw}$-w_{sh}), and classified the shrink-swell potential based on this parameter. According to the proposed classification method, when I_{ss} < 20% shrink-swell potential is low. The I_{ss} values in Table 2.9 obtained for the values of NS, NS1%PF and NS2%PF satisfy this criterion.

Table 2.9. Evaporation results.

	Initial water content w_{sw} (%)	**Final water content w_{sh} (%)**	**Shrink-swell index I_{ss} (%)**
NS	21.0	2.2	18.8
NS1%PF	21.7	3.7	18.0
NS2%PF	22.1	2.9	19.2
NZ	37.9	4.1	33.8
NZ1%PF	34.0	3.7	30.3
NZ2%PF	36.3	6.2	30.1

Volumetric shrinkage test results, void ratio and water content data, were also fitted by the hyperbolic model (Fredlund et al., 2002) given in Equation 2.4. Shrinkage curves for all soil groups are presented in Figure 2.16 and Figure 2.17 and the fitting parameters are given in Table 2.10.

$$e(w) = a_{sh}\left[\frac{w^{c_{sh}}}{b_{sh}^{c_{sh}}} + 1\right]^{\frac{1}{c_{sh}}} \tag{2.4}$$

where, a_{sh}: fitting parameter (minimum void ratio), b_{sh}: fitting parameter (shrinkage limit), c_{sh}: fitting parameter (curvature of the hyperbola), w: gravimetric water content.

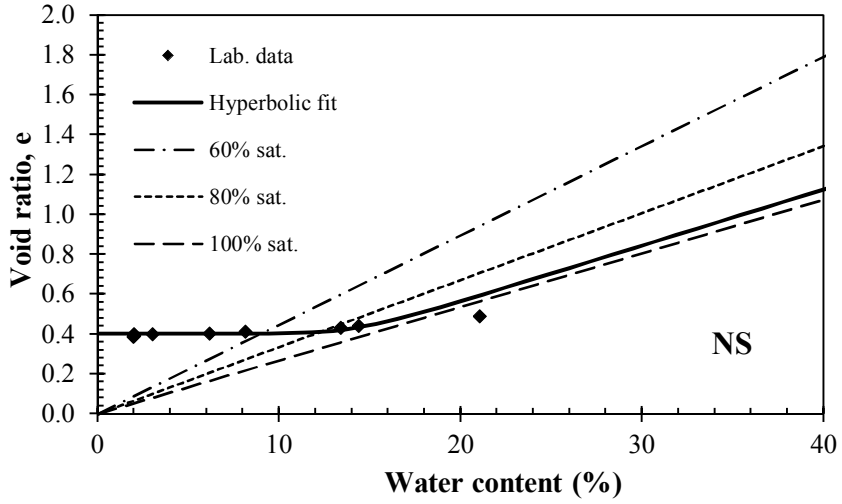

(a)

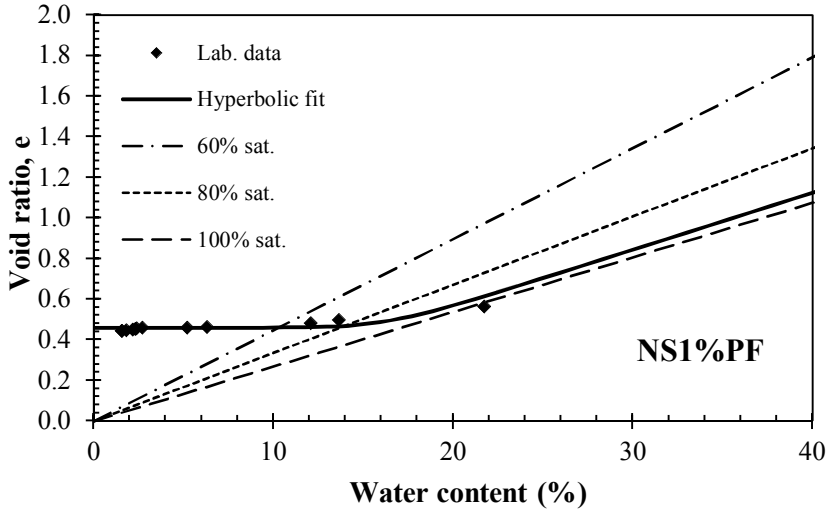

(b)

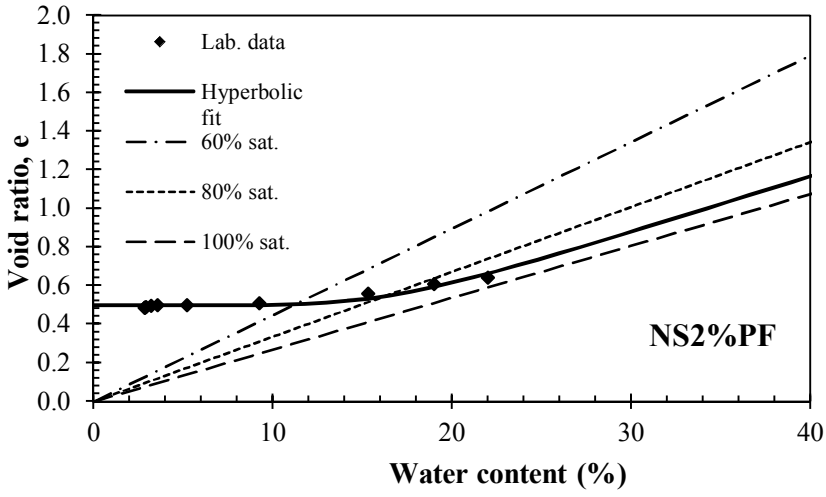

(c)

Figure 2.16. Shrinkage curves of (a) NS, (b) NS1%PF and (c) NS2%PF.

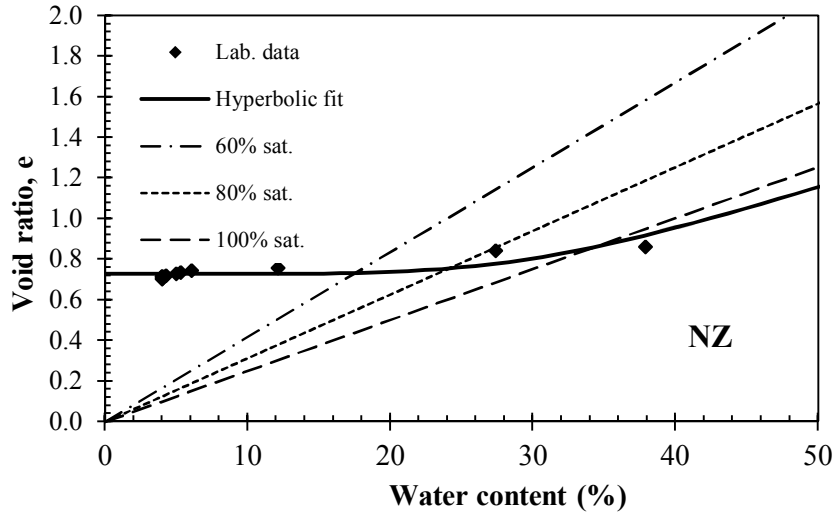

(a)

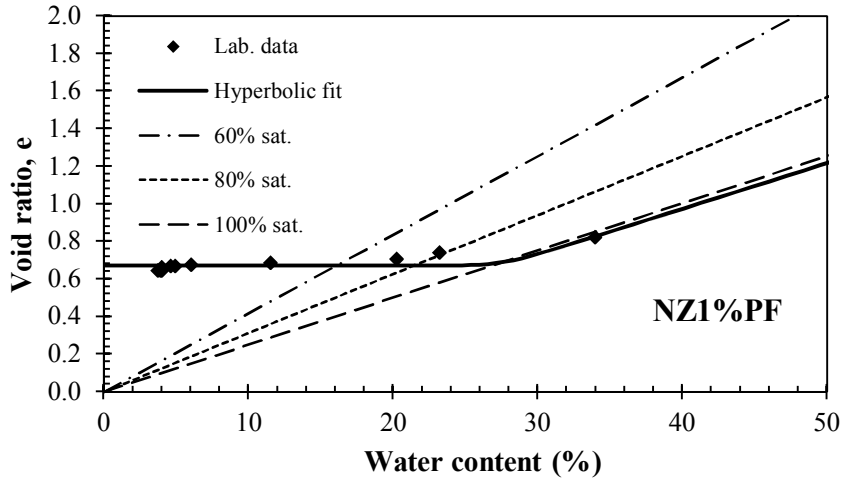

(b)

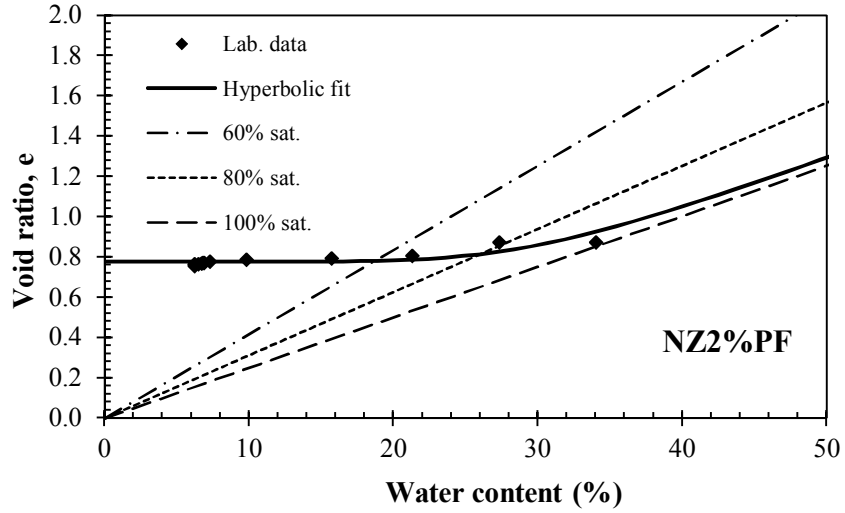

(c)

Figure 2.17. Shrinkage curves of (a) NZ, (b) NZ1%PF and (c) NZ2%PF.

Table 2.10. Hyperbolic fitting parameters of the shrinkage curves.

Material	a_{sh}	b_{sh}	c_{sh}
NS	0.401	0.14	9.47
NS1%PF	0.460	0.16	10.18
NS2%PF	0.496	0.17	6.04
NZ	0.727	0.32	5.34
NZ1%PF	0.671	0.28	5.28
NZ2%PF	0.777	0.30	6.70

Fitting parameters a_{sh} and b_{sh} represent the minimum void ratio and the shrinkage limit respectively and c_{sh} is the curvature of the hyperbola. Increment of the minimum void ratio and shrinkage limit values with fiber reinforcement explains that the volumetric shrinkage decreased with fiber inclusion. Fiber enhancement provided adhesion between soil particles and fibers, therefore the total contact area increased and caused the reduction of volumetric shrinkage strain. The soil-fiber interaction increased with the increment of fiber content and gained more resistance to shrinkage during desiccation. The test results showed that the amount of shrinkage reduced gradually with the increasing fiber content for NS group which agrees the findings of Miller and Rifai (2004), Punthutaecha et al. (2006), Cai et al. (2006) and Harianto (2008). However, from the scattered data of NZ group it can be deduced that improvement of shrinkage behavior in NS is more stable than NZ group.

2.5 Hydraulic Properties

In this section, NS group is selected for the investigation of SWCC based on the performance of its volume change behavior. Improvement on swelling-shrinking and consolidation properties were obtained with the polymeric fiber enhancement of NS and NZ. When the test results are compared, volume change properties of NS group is found to be more convenient and more advantageous than NZ group. Shrink-swell potential of NS group is low but NZ group does not satisfy this criterion. Therefore,

filter paper suction test was applied to NS, NS1%PF and NS2%PF soil specimens only.

2.5.1 Soil-Water Characteristic Curve (SWCC)

Soil suction and water content values are used in order to draw SWCC which are obtained from filter paper test. The experimental data are fitted with the models of Fredlund and Xing (1994) and van Genuchten (1980) as presented in Figures 2.18 and 2.19 respectively. Fitting parameters of each model are summarized in Table 2.11 and Table 2.12.

The mathematical equations of the selected models are given in Equation 2.5 and Equation 2.6 for the models of Fredlund and Xing (1994) and van Genuchten (1980) respectively.

Fredlund and Xing (1994) presented a three-parameter equation, which is used in the high suction range, as given in Equation 2.5. It has both drying and wetting SWCC forms and is applicable to a wide range of soils and it is applicable to all kinds of soils. This equation has two forms, wetting SWCC and drying SWCC.

$$w_w = w_s \left[1 - \frac{\ln\left(1 + \frac{\psi}{h_r}\right)}{\ln\left(1 + \frac{10^6}{h_r}\right)} \right] \left[\frac{1}{\left[\ln\left[\exp(1) + \left(\frac{\psi}{a_f} \right)^{n_f} \right] \right]^{m_f}} \right] \tag{2.5}$$

where,

w_w= gravimetric water content at any soil suction

w_s= saturated gravimetric water content obtained from the drying SWCC form

a_f= a soil parameter which is primarily a function of the air entry value of the soil in kPa

n_f= a soil parameter which is primarily a function of the rate of water extraction from the soil once the air entry value has been exceeded

m_f= a soil parameter which is primarily a function of the residual water content

h_r= suction at which residual water content occurs (kPa)

ψ= soil suction

a_f, n_f and m_f are the fitting parameters

van Genuchten (1980), given in Equation 2.6 uses three fitting parameters, namely a_{vg}, n_{vg}, and m_{vg}. The parameter a_{vg} is related to the inverse of air entry value, the n_{vg} parameter is related to the pore size distribution of the soil and the m_{vg} parameter is related to the asymmetry of the model.

$$w_w = w_{rvg} + \left(w_s - w_{rvg}\right)\left[\frac{1}{\left[1+\left(a_{vg}\psi\right)^{n_g}\right]^{m_{vg}}}\right] \tag{2.6}$$

where,

w_w= gravimetric water content at any soil suction

w_{rvg}= residual gravimetric water content

w_s= saturated gravimetric water content obtained from the Drying SWCC form.

a_{vg}= a soil parameter which is primarily a function of the air entry value of the soil in kPa

n_{vg}= a soil parameter which is primarily a function of the rate of water extraction from the soil once the air entry value has been exceeded

m_{vg}= fitting parameter

ψ= soil suction

Air-entry value is one the important parameter in the evaluation of SWCC and it represents the suction where air starts to enter the largest pores in the soil. The air entry

value (AEV) of expansive soil-sand mixture (NS) showed a reduction after 1% PF inclusion, however it continued with a significant increment with the addition of 2% PF. AEV depends on the variations in particle and pore-size distribution and soils with finer particles have lower air-entry values than coarser soils. After soil stabilization, as the porosity of sample decreases, higher values can be attained for AEV. In this study, AEV decreased with the utilization of 1% PF because of uneven distribution of PF in the soil structure or the accumulation of fibers created clusters. On the other hand, 2% PF reinforcement provided better interlocking bonds between particles. These results are similar with Lin and Cerato (2012), Aldaood et al. (2014) and Puppala et al. (2006). The general shape of SWCC's of NS, NS1%PF and NS2%PF are similar because chemical stabilization was not used.

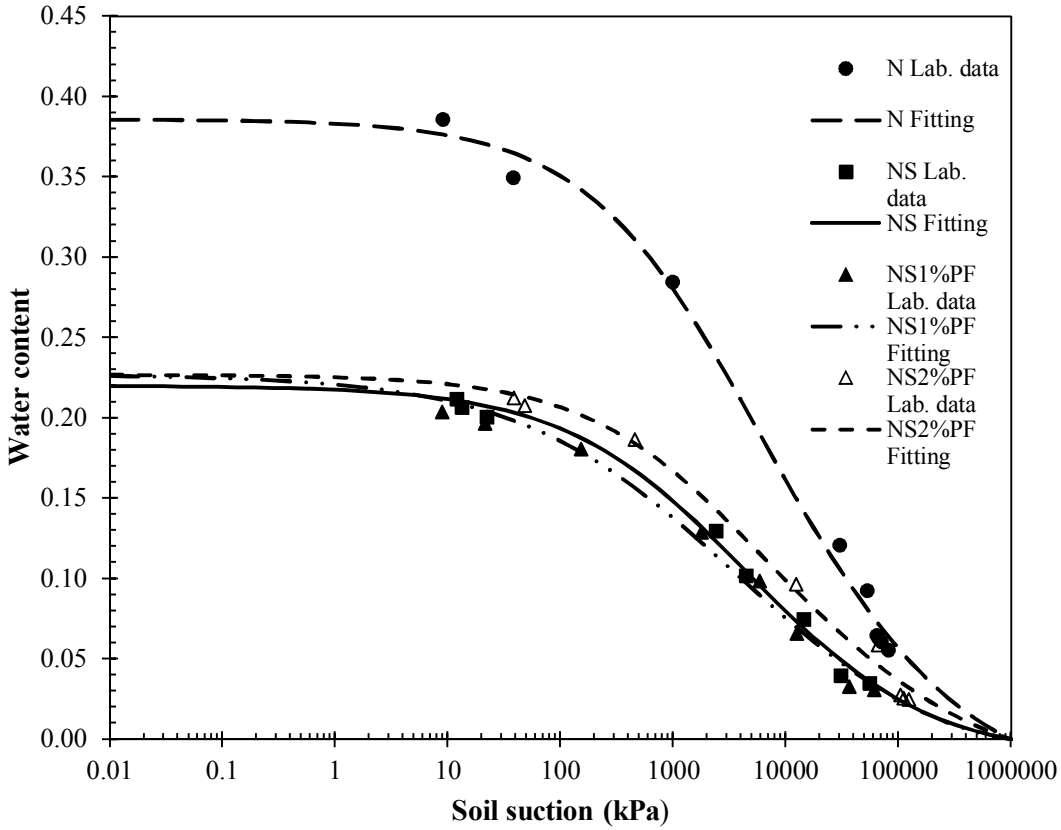

Figure 2.18. SWCC based on Fredlund and Xing model.

Table 2.11. Fitting parameters of Fredlund and Xing model.

	N	NS	NS1%PF	NS2%PF
a_f	2499.903	2499.986	2499.994	2499.165
n_f	0.578908	0.540394	0.448019	0.572385
m_f	1.76747	2.112303	2.503237	1.691402
h_r	86599.09	61388.48	65942.48	96830.99
Error (R^2)	0.99	0.99	0.99	0.9918
w_r	4.11 %	2.13 %	1.97 %	2.60 %
AEV	160.31	104.61	42.00	166.26
Max. slope	0.32	0.32	0.28	0.3171

a_f, n_f, m_f : fitting parameters, h_r : matric suction at residual water content, w_r : residual water content and AEV: air-entry value.

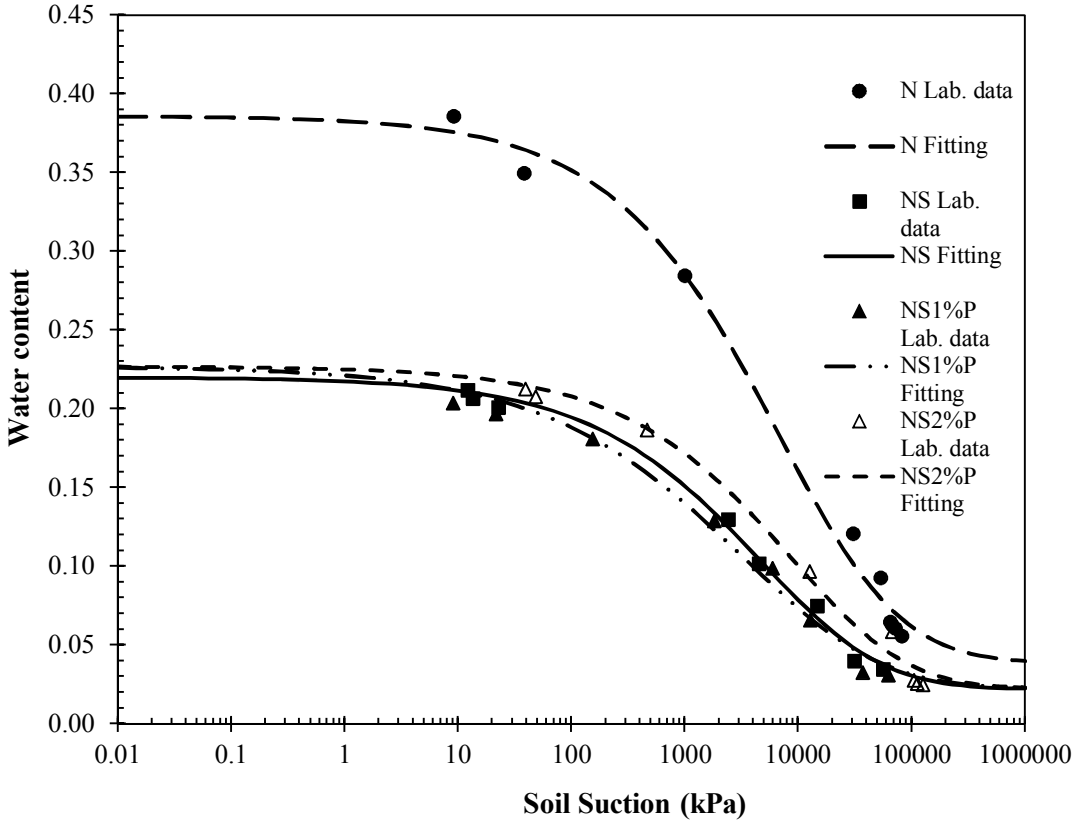

Figure 2.19. SWCC based on van Genuchten model.

Table 2.12. Fitting parameters of van Genuchten model.

	N	NS	NS1%PF	NS2%PF
a_{vg}	1.58E-05	1.23E-05	7.89E-05	4.72E-06
n_{vg}	0.532309	0.509297	0.437687	0.514428
m_{vg}	3.292737	4.227101	4.89405	5.123605
Error (R^2)	0.99	0.99	0.99	0.9897
w_r	10 %	10 %	10 %	10 %
AEV	221.40	140.81	58.00	274.26
Max. slope	0.35	0.35	0.30	0.3567

a_{vg}, n_{vg}, m_{vg} : fitting parameters, w_r : residual water content and AEV: air-entry value.

2.5 SEM Analysis

The microstructure of various samples is examined by means of scanning electron microscope (SEM) to study the matrix-fiber adhesion. Figure 2.3 (b) presents the SEM image of PF flakes which reveals the surface roughness of fibers. This is a contributing factor to adhesion at the fiber-matrix interface. Sand component of the soil sample increases fiber interface roughness and mechanical interlock, especially during compaction causing plastic deformation of fiber flakes due to abrasion. This phenomenon was also confirmed by Tang et al. (2007) and Tang et al. (2010). The SEM images of fiber reinforced compacted expansive soil-sand mixtures are depicted in Figure 2.20, which display very distinctively the binding of fiber flakes on soil matrix, therefore forming a good reinforcement in the compacted soil. The distributed discrete fibers act as a spatial network, interlocking soil grains to form a unitary coherent matrix. The interfacial forces impedes the sliding of the fibers in the matrix, hence resisting tensile stresses, developing a "bridging" effect (Tang et al., 2007). In Figure 2.20, the granular aggregates are the sand particles and the smooth matrix is the expansive soil, bridged by the fiber flakes which are clearly functioning as tensile elements when fully mobilized at the interface.

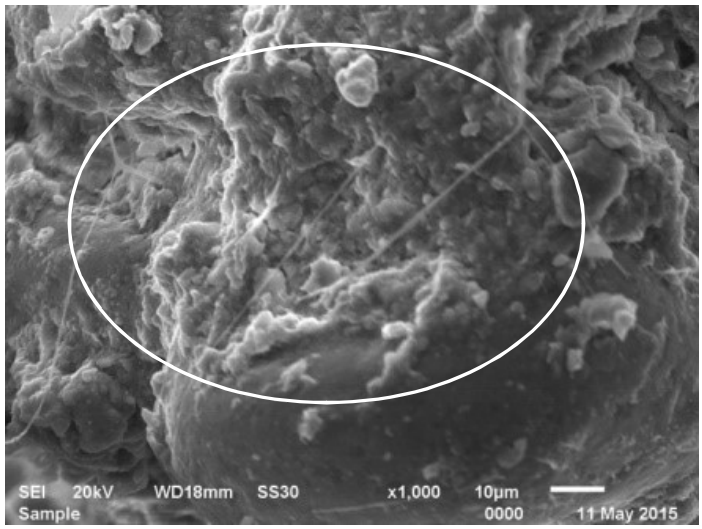

(a)

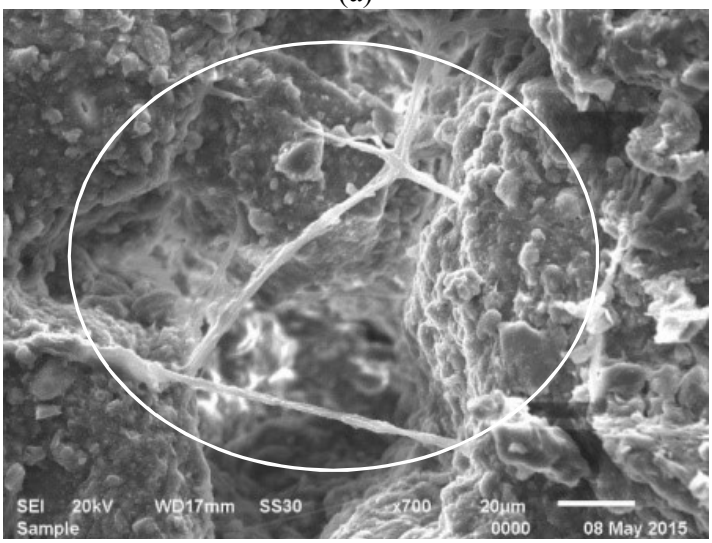

(b)

Figure 2.20. SEM images of PF-reinforced soil microstructure with magnifications of (a) x1000 and (b) x700.

2.6 Conclusions

The work presented in this study focuses on the efficiency of polymeric fiber waste obtained from pipe cuttings as a reinforcing material in stabilized soils. Expansive soil initially mitigated by sand (NS) or zeolite (NZ) achieving further enhancement by randomly oriented discrete fiber reinforcement was tested for strength and volume change properties. The results revealed that the fiber inclusion did not cause any appreciable change in the unconfined compressive strength, yet flexural strength

performance was observed to have improved in the expansive soil-sand mixture.

The volume change behavioral studies have yielded the following findings:

1. The swell potential of NS group was reduced by 20% from moderate to the borderline of low swell based on primary swell values with 2% PF inclusion, whereas NZ group displayed a reduction of 55%, yet remaining in the moderate-high swell category. Therefore, PF inclusion has proved to be more efficient in the NS specimens.

2. The shrink-swell potential based on shrinkage test results yielded low potential for NS specimens, yet NZ specimens presented high swell-shrink potential for all mixtures.

3. The compression indices of NS mixtures reduced by 7.5% with 2%PF inclusion, remaining in the slightly compressible range. The NZ compressibility, however was observed to reduce by 6.7% from moderately compressible to slightly compressible category with 2% PF inclusion.

4. Saturated hydraulic conductivity determination based on consolidation test results indicated that under pressures of at least 100 kPa all the values remained below the regulatory limit of 10^{-7} cm/s, except the NZ mixture with no PF inclusion.

5. Soil-water characteristics along the desorption cycle during desiccation process was studied with NS group alone, and based on the fitting parameters

of the models applied to the experimental data, it was concluded that the air entry suction increased considerably with 2% PF inclusion, indicating that a more impervious structure.

6. SEM images clearly depict the PF flakes acting as bridging elements in tension.

Based on these findings, further research on the pozzolanic effect of zeolite was undertaken to observe the expected improvements in mechanical properties of the NZ mixtures, the results of which are given in Chapter 3.

Chapter 3

ZEOLITE AMENDED EXPANSIVE SOIL BEHAVIOR

3.1 Introduction

Performance of landfill liners is influenced by desiccation cracks, which form preferential flow paths upon rewetting, hence increasing hydraulic conductivity. Therefore, clayey soils have disadvantage when moisture fluctuations are erratic. Recently zeolite is considered as an innovative landfill material due to its filtering properties as well as low volumetric shrinkage capacity. It was observed that bentonite-zeolite mixtures are not influenced by moisture content variations and possess very low hydraulic conductivity.

Natural zeolites are derived from acidic and volcanic tuffs, which occur in the form of rock forming minerals in many parts of the world. They are commonly found in saline alkaline lake deposits, vertical sedimentary sequences, hydrothermally altered volcanic or sedimentary rocks and deep-sea sediments (Bish and Guthrie, 1994). There are five types of naturally occurring zeolites found in abundance in the form of brittle, solid rocks, and are of commercial interest due to their favorable ion exchange properties. These are clinoptilolite, erionite, chabazite, mordenite and phillipsite. Zeolites are composed of tecto-silicates with open framework, consisting of cages and tunnels which adsorb smaller molecules, like a “molecular sieve”. Therefore, they possess high adsorption capacity and can act as a filter in the event of leachate through liner. Mainly the clinoptilolite type has a selectivity to heavy metals. Pollutant

adsorption capacity and heavy metal removal properties of zeolites are investigated by many researchers indicating the ability to absorb and trap heavy metals present in the leachate, such as Pb^{2+}, Zn^{2+}, Cd^{2+}, Ni^{2+}, Fe^{2+} and Mn^{2+} (Kayabalı, 1997; Kayabalı and Kezer, 1998; Jacobs and Förstner, 1999; Langella et al., 2000; Cincotti et al., 2001; Mier et al., 2001; Tuncan et al., 2003; Erdem et al., 2004; Ören and Kaya, 2006; Motsi et al., 2009; Misaelides, 2011).

Yükselen-Aksoy (2010) focused on the swelling potential, compressibility, hydraulic conductivity and shear strength properties of two different natural zeolites in order to use in geotechnical and geoenvironmental applications. Test results showed that compressibility and swelling potential of zeolites were not high and hydraulic conductivity was suitable for the limitation of landfill liners and therefore zeolites could be used in such applications. Ören and Özdamar (2013) analyzed the effect of zeolite particle size and compaction water content on the hydraulic conductivity behavior. They concluded that when the compaction water content increased the hydraulic conductivity of compacted zeolite reduced and compacted granular zeolites have higher hydraulic conductivities than compacted fine zeolites.

Zeolites are suitable to be used in combination with bentonite as hydraulic properties of natural zeolite can be adjusted to meet particular requirements by adjusting the grain size through crushing and sieving process (Kaya and Durukan, 2004). Kaya et al. (2006) studied the suitability of using bentonite embedded zeolite (BEZ) as alternative to bentonite embedded sand (BES) and concluded that when zeolite was used volumetric shrinkage reduced, indicating that the mixture was not susceptible to moisture fluctuations, and the hydraulic conductivity was in the order of 10^{-10} cm/s.

Galvão et al. (2008) compared compaction characteristics, volumetric shrinkage strain and hydraulic conductivity of bentonite embedded sand (BES) and bentonite embedded zeolite (BEZ) and they suggested that BEZ is a good material for a landfill liner. Kayabalı (1997) investigated the use of a bentonite-zeolite layer beneath clay liner and concluded that this would reduce the thickness of clay liner by 25%, and would also act as a chemical filter.

Pozzolanic activity of zeolites are investigated by various researchers who concluded that zeolitic tuffs are excellent pozzolans (Caputo et al., 2008; Mertens et al., 2009; Demirbaş, 2009; Uzal et al., 2010; Özen, 2013). Pozzolans are siliceous and aluminous materials, which in themselves possess little or no cementitious property, but they are able to combine with calcium hydroxide ($Ca(OH)_2$) at ordinary temperatures and in the presence of water to form new reaction compounds possessing binding character. A material is defined as natural pozzolan when the summation of silicon dioxide (SiO_2), aluminum oxide (Al_2O_3) and iron oxide (Fe_2O_3) is more than 70% (ASTM C618-15). The pozzolanic activity of zeolites is affected by various factors such as; surface area, particle-size, Si/Al ratio, cation exchange capacity (CEC), mineralogy and chemistry.

The objective of this chapter is to examine the volume change and strength characteristics of expansive soil-zeolite (clinoptilolite) mixture within curing periods of up to 90 days, in order to assess its suitability as a landfill material in a semi-arid climate.

3.2 Materials and Methods

3.2.1 Materials

The material properties of the expansive soil and zeolite used in this phase of the study are explained in detail in the previous chapter. Physical and chemical properties are listed in Table 2.1 and Table 2.2 respectively, and the X-Ray diffraction results are provided in Figure 2.2.

3.2.2 Methods

Initially, expansive soil and zeolite were dried at 50°C in the oven and pulverized to particle size finer than 425 μm. Soil specimens were prepared at optimum water content and maximum dry density determined by standard Proctor energy (ASTM D698-12e2). The samples were tested in five different categories of expansive soil and zeolite. First group is expansive soil (N) and the second group 50% expansive soil and 50% zeolite (NZ). Different curing time periods were applied to NZ specimens (0, 7, 28 and 90-days). Therefore, laboratory tests were performed on five groups which are N, NZ (0-d), NZ (7-d), NZ (28-d) and NZ (90-d).

One-dimensional swell test (ASTM D4546-14), consolidation test (ASTM D2435-11), volumetric shrinkage test, unconfined compression test (ASTM D2166-06) and flexural strength test (ASTM C348-14) were performed. All of the test methods were explained in detail in Chapter 2.

3.3 Experimental Results and Discussions

3.3.1 Physical Properties

The physical properties of liquid limit, plasticity index (ASTM D4318-10e1), linear shrinkage (BS 1377-2:90) and specific gravity (ASTM D854-14) when zeolite was added yielded reduced values of 50, 17, 13 and 2.51 respectively. Therefore, natural

soil and zeolite mixtures (NZ) can be classified as a borderline between low and high plasticity silt, since zeolite possesses low plasticity (Table 2.1).

3.3.2 Compaction Characteristics

The compaction curves obtained by standard Proctor test are depicted in Figure 3.1. Studying the dry density-water content relationships, it can be observed that there is a minimal change in the optimum moisture content, from 26% to 24.5%, and in the maximum dry density, from 1380 kg/m^3 to 1390 kg/m^3. Therefore, it can be deduced that expansive soil (N) and expansive soil-zeolite mixtures (NZ) have exhibited almost similar dry density and optimum moisture content values, the degree of saturation at the optimum value being closer to the 100% saturation line for sample N.

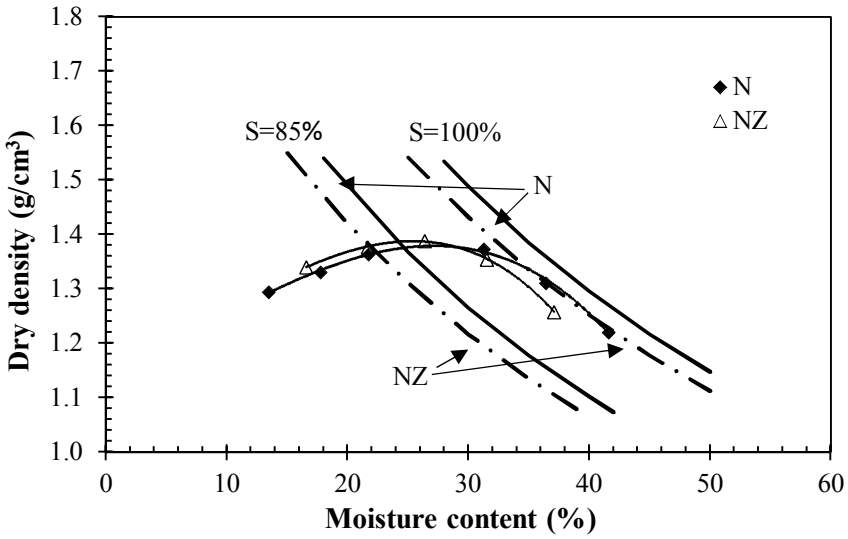

Figure 3.1. Compaction curves of N and NZ.

3.3.3 Volume Change

3.3.3.1 One-dimensional Swell

Swell versus time curves obtained from one-dimensional swell test results for five different soil groups are given in Figure 3.2. The expansive soil possesses a high swell potential of 4.95% which is reduced by 53% in NZ (0-d) mixture to 2.35%. A further

reduction of swell potential is observed with the increase of curing period. Swell potential of NZ (7-d), (28-d) and (90-d) are 1.57%, 0.38%, 0.35% respectively. Therefore, there is a marked decrease in percent swell value from 0-7 days curing to 28-days after which depicts an insignificant reduction until 90 days curing. These findings are in good agreement with Demirbaş (2009), and Yükselen-Aksoy (2010) who also reported the pozzolanic behavior of zeolite reducing swell potential. Zeolite used in this study consists of a total percentage of SiO_2, Fe_2O_3, and Al_2O_3 more than 70% as presented in Table 2.2, which is the significant requirement of pozzolanic character. As can be observed in Figure 3.2, the tendency of secondary swell which progresses after the completion of primary swell in untreated soil eliminated completely after the addition of zeolite. Therefore, it can be inferred that zeolite is very beneficial in improving swelling characteristics, especially in preventing the creep behavior of secondary swell, which takes place over a prolonged period of time. This behavior is attributed to the reaction product of calcium silicate hydrate which caused binding and cementation of soil particles enhancing the integrity of specimens against volume change.

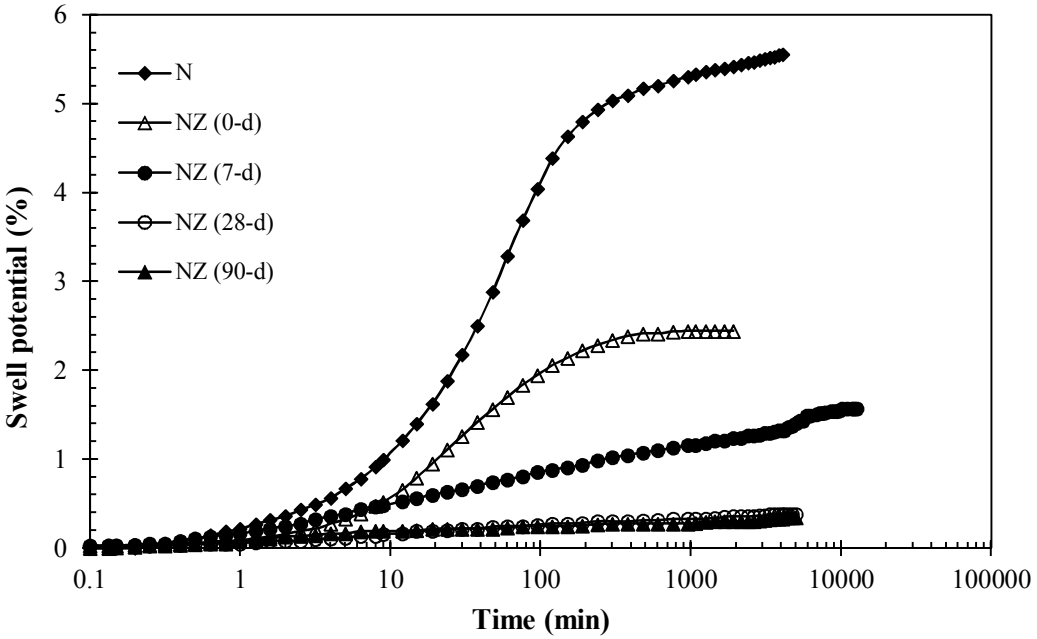

Figure 3.2. Percent swell versus time curves.

3.3.3.2 Compressibility

Figure 3.3 depicts the void ratio versus effective consolidation pressure relationships obtained from one-dimensional consolidation test results. The parameters of compression index (C_c), rebound index (C_r) and swell pressure (p_s') are summarized in Table 3.1. Generally a decreasing trend was observed in compression and rebound indices after treatment of expansive soil. NZ (0-d) has a compression index of 30% less than the original soil, which reduced further with curing reaching to 30% additional reduction from 0-day to 90-day curing period. Similarly, the rebound index reduced by 50% when zeolite is added and a further reduction of 17% is observed within 90 days curing period. Therefore, while the compressibility of N, NZ (0-d) and NZ (7-d) remained in the "moderately compressible" range, NZ (28-d) and NZ (90-d) samples were observed to be "slightly compressible" (Coduto, 2001). This improvement is explained again with the pozzolanic process causing structural changes due to rearrangement of particles with curing time.

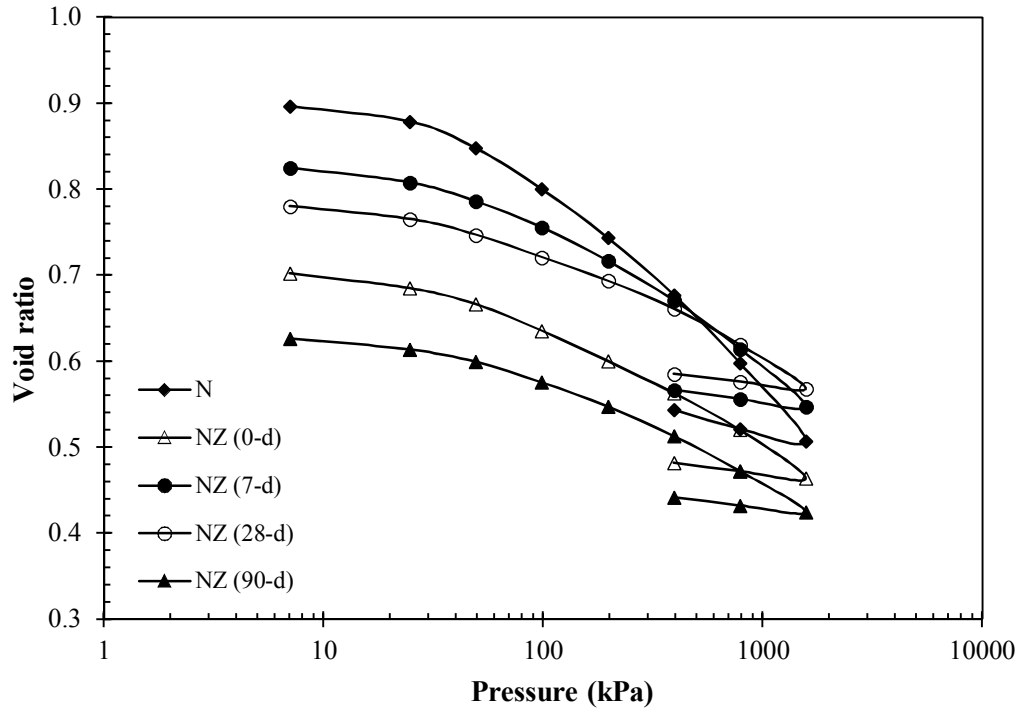

Figure 3.3. Void ratio versus logarithm of effective consolidation pressure.

Table 3.1. Compressibility characteristics of all soil groups.

Material	C_c	C_r	p_s' (kPa)
N	0.275	0.071	83
NZ (0-d)	0.195	0.036	46
NZ (7-d)	0.192	0.037	25
NZ (28-d)	0.145	0.030	-
NZ (90-d)	0.135	0.030	15

Saturated hydraulic conductivity values under three different effective consolidation pressure ranges corresponding to different curing times are illustrated as a set of curves in Figure 3.4. The hydraulic conductivity values at different curing times, under varying pressure ranges depict that expansive soil has the lowest values at all pressure ranges which increased after zeolite inclusion. Hydraulic conductivity values are highly dependent on the fines content which is significantly higher in expansive soil than the fines fraction of zeolite. The cured samples of NZ have provided hydraulic conductivity values lower than the typical regulatory limit of 1 x 10^{-7} cm/s at all curing

times, verifying similar research findings by Ören and Özdamar (2013) and Du et al. (2015). The reduction from 0-day to 90-day curing is observed to be almost 75% at all pressure ranges. The reductions in the hydraulic conductivity values can be attributed to the calcium silicate hydrate forming during pozzolanic process, binding the particles and causing the reduction of pore spaces.

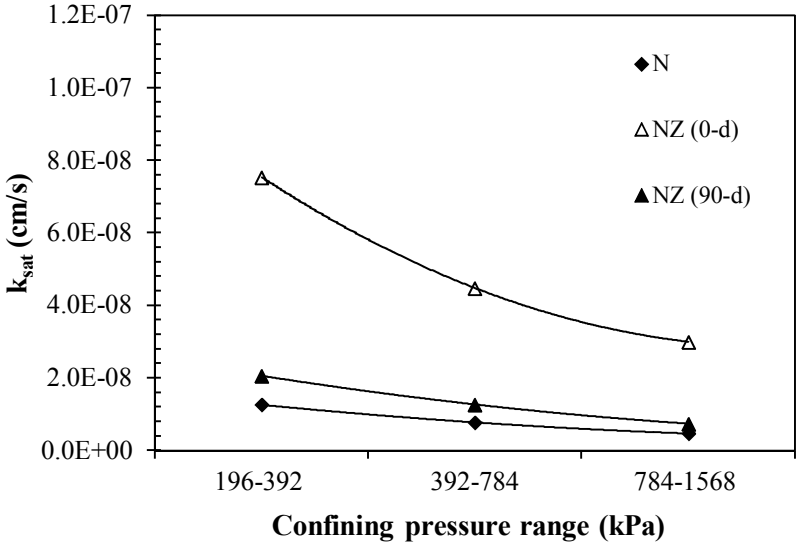

Figure 3.4. k_{sat} values under different consolidation pressure ranges and curing times.

3.3.3.3 Shrinkage

Shrinkage tests are evaluated in terms of volumetric, axial and diametral shrinkage strains with respect to time and the test results are presented in Figure 3.5. Volumetric shrinkage strain is 0.189 for the expansive soil and a decreasing trend is observed for the shrinkage strains after addition of zeolite (NZ-0d) and cured samples of NZ (7, 28 and 90-d) reducing the volumetric shrinkage strains to 0.08, 0.08, 0.075 and 0.053 respectively. The significant effect of volumetric shrinkage improvement is observed in 90-days cured sample. A similar behavior can be observed in axial and diametral shrinkage strains. Addition of zeolite decreased the axial and diametral shrinkage strains however NZ (7 and 28-d) samples showed an increment in axial shrinkage

strain values. Considerable reductions are observed in NZ (90-d) samples for both axial and diametral shrinkage strains.

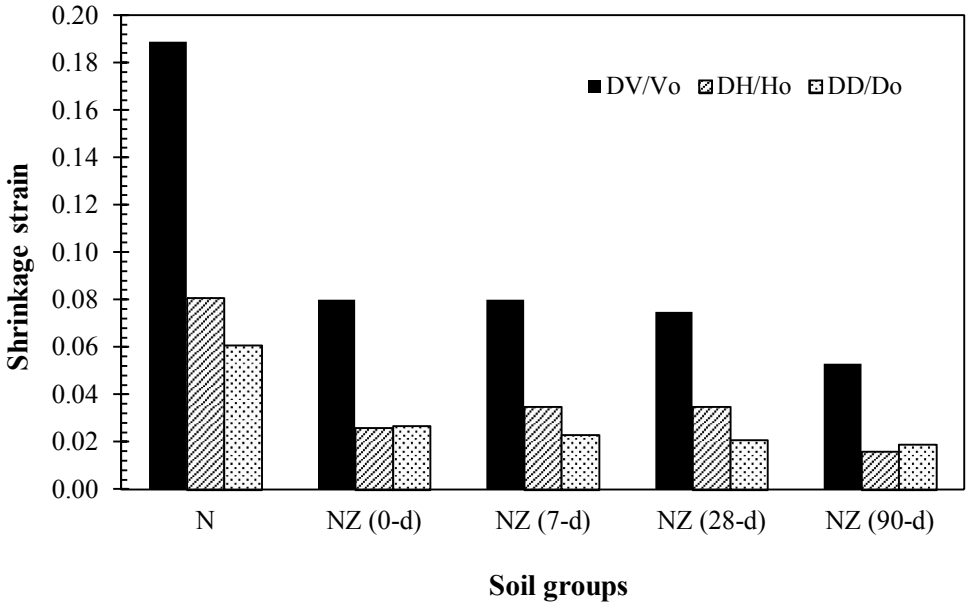

Figure 3.5. Volumetric, axial and diametral shrinkage strains.

Kleppe and Olson (1985) reported that volumetric shrinkage strain should be less than about 5% which causes relatively minor cracks and the values more than 10% leads to severe cracks. Test results in this study show that NZ (90-d) sample reached to 5.3% volumetric shrinkage strain which can be considered compatible with the aforementioned criterion.

Shrinkage curves and fitting parameters for all soil groups are shown in Figure 3.6 and Table 3.2 respectively. The highest shrinkage limit (b parameter) and the final void ratio (a parameter) represent the best result in shrinkage which is obtained after 90-day curing period. However, uncured sample NZ (0-d) also gives the same result. Shrinkage limit and final void ratio of expansive soil increased by 22% and 28% respectively after zeolite addition and 90-days aging.

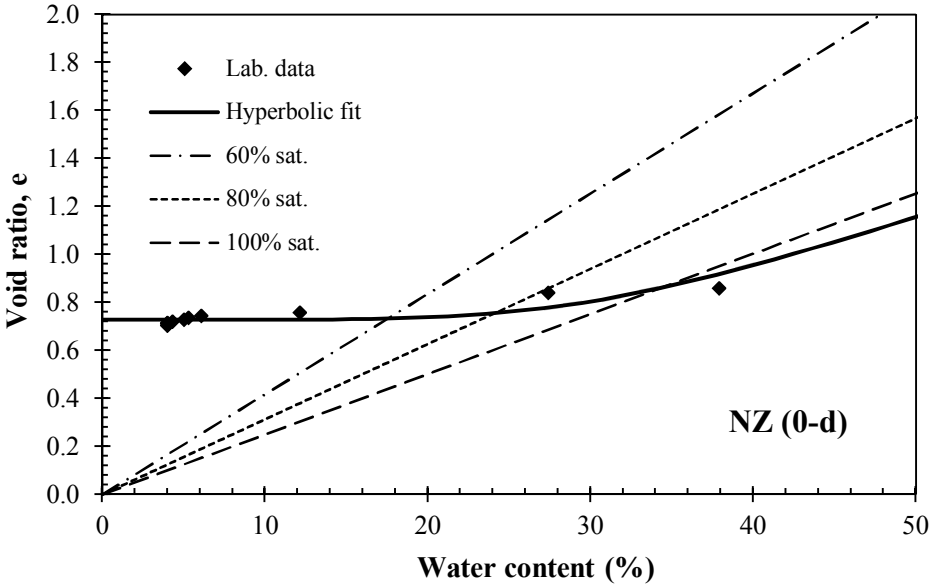

(a)

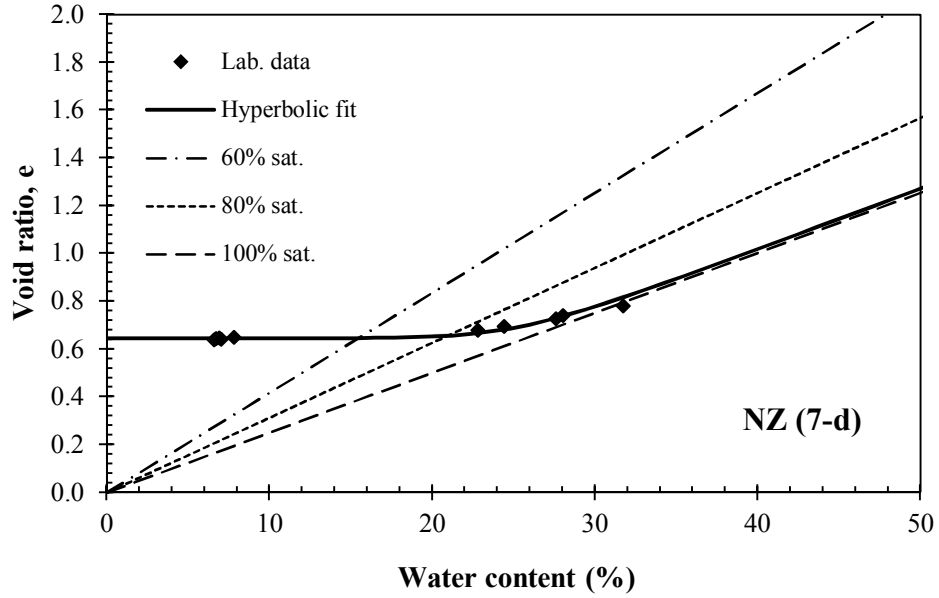

(b)

Figure 3.6. Shrinkage curves (a) NZ (0-d), (b) NZ (7-d), (c) NZ (28-d) and (d) NZ (90-d).

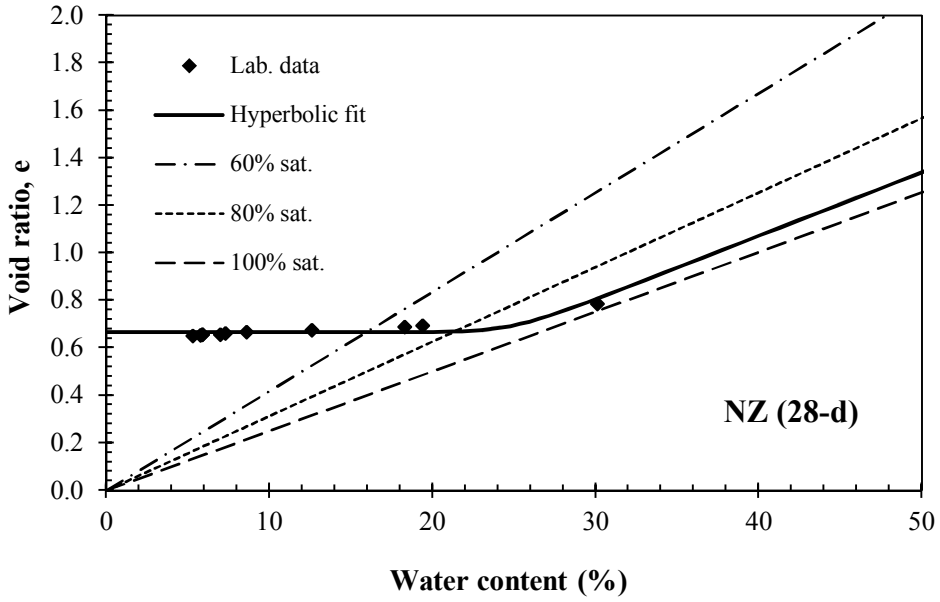

(c)

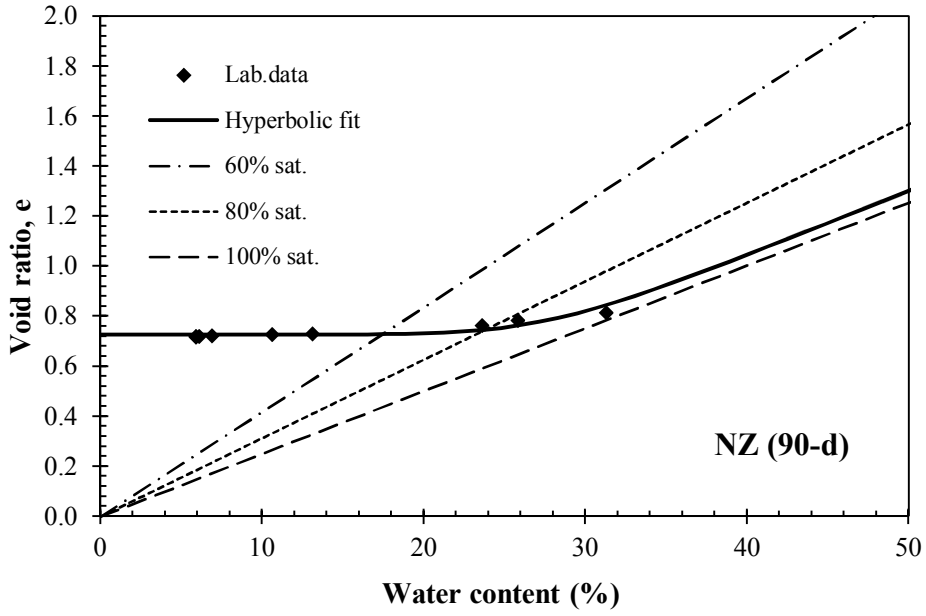

(d)

Figure 3.6. (Cont.)

Table 3.2. Hyperbolic fitting parameters of the shrinkage curves.

Fitting parameter	N	NZ (0-d)	NZ (7-d)	NZ (28-d)	NZ (90-d)
a_{sh}	0.566	0.727	0.645	0.666	0.727
b_{sh}	0.23	0.32	0.25	0.25	0.28
c_{sh}	3.64	5.34	9.55	17.71	8.55

Two different analyses were done for the interpretation of shrinkage data and both of them reveal that NZ (90-day) gives the best results.

Based on the shrinkage data, evaporation curves were plotted to observe the desiccation path of the soil samples due to aging as depicted in Figure 3.7, summarizing test parameters in Table 3.3.

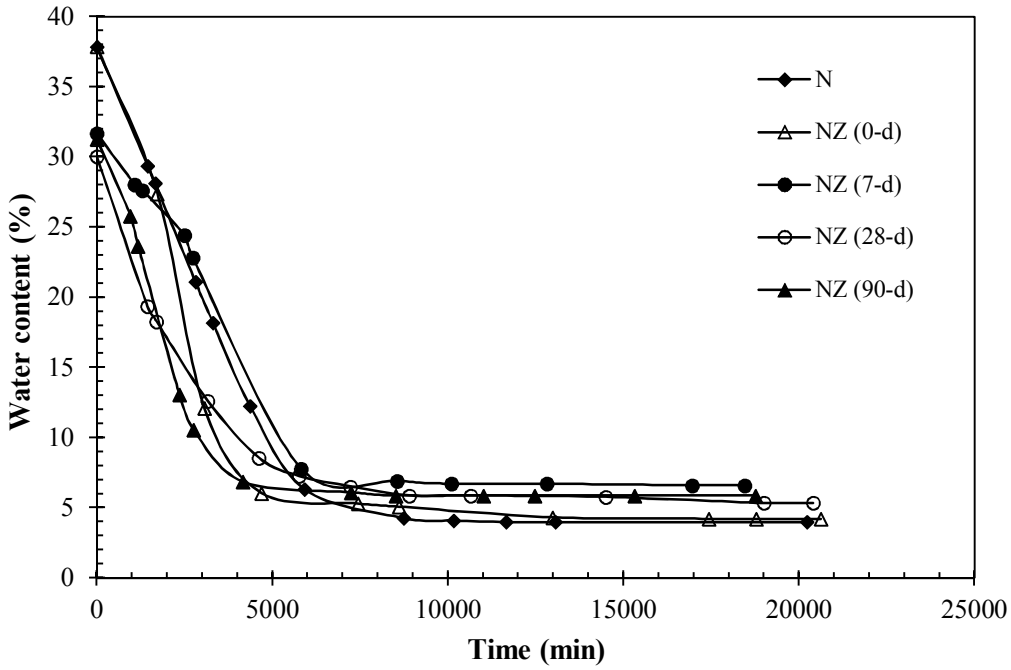

Figure 3.7. Evaporation curves.

Evaluating the evaporation curves, it can be observed that along the drying path, initially the water content of soil samples were decreased rapidly in a linear relationship, after which drying progressed nonlinearly with a reduced rate, and finally reaching a constant value. A decreasing trend is observed in rapid drying duration of N after addition of zeolite and increasing curing periods. A significant reduction in rapid drying duration of 22% and 53.5% was observed with 28-days and 90-days aging respectively.

Table 3.3. Evaporation test results.

	Initial water content (%)	Final water content (%)	Shrink-swell index (I_{ss})
N	37.8	4.0	33.8
NZ (0-d)	37.9	4.2	33.7
NZ (7-d)	31.7	6.6	25.1
NZ (28-d)	30.0	5.3	24.7
NZ (90-d)	31.3	5.9	25.4

Shrink-swell index parameter (I_{ss}) was obtained by using the initial and final water content values and the results showed that all the soil groups are within "moderate potential" shrink-swell range of 20-40% (Briaud et al., 2003).

3.3.4 Strength Properties

3.3.4.1 Unconfined Compressive Strength

Unconfined compressive strength of N is 411 kPa and decreased by 31% after zeolite inclusion (NZ) whereas failure strain increased by 1.8 fold. However, an increasing trend of unconfined compressive strength of NZ mixtures was observed with aging as presented in Figure 3.8. The biggest increment of UCS was obtained within 28-day curing period, which has increased from 290 kPa at 0-day curing to 390 kPa. Thereafter, UCS changed with a lower rate of increment reaching to 394 kPa at 90-day curing period. Hence, the strength increment is almost negligible after 28 days. Secant modulus, E_{50}, which is the slope of the straight line drawn from the origin to the point representing 50% of the peak compressive strength, can be used to characterize stiffness of the soil. The secant modulus of the specimens tested in UCS are presented in Table 3.4, which indicate that aging increased the stiffness of NZ mixtures.

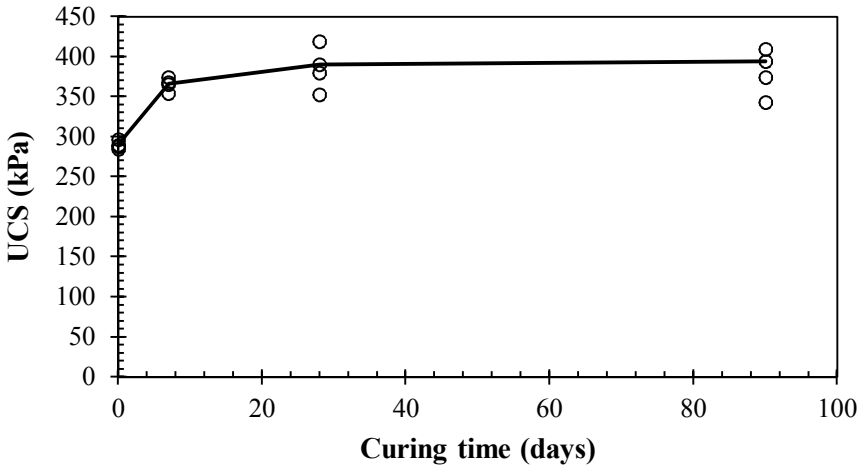

Figure 3.8. Unconfined compressive strength test results on NZ.

Table 3.4. Secant modulus (E_{50}) results.

Material	E_{50} (kPa)
NZ (0-d)	4143
NZ (7-d)	6032
NZ (28-d)	10333
NZ (90-d)	11467

3.3.4.2 Flexural Strength

Load-deflection curves are obtained from flexural strength test for all soil groups as shown in Figure 3.9 and the test results are given in Table 3.5.

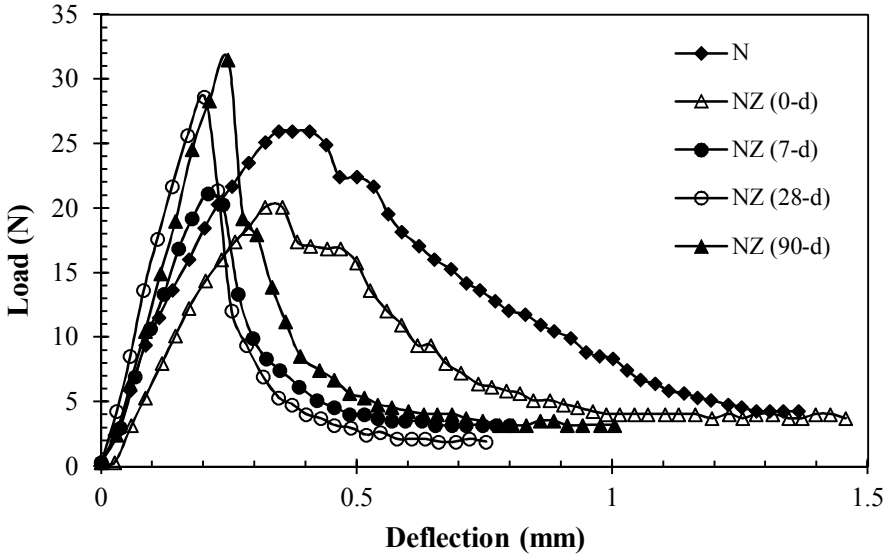

Figure 3.9. Load-deflection relationships.

Table 3.5. Flexural strength test results.

Material	Flexural strength (kN/m^2)	Deflection at failure (mm)
N	61	0.41
NZ (0-d)	47	0.35
NZ (7-d)	50	0.21
NZ (28-d)	67	0.20
NZ (90-d)	74	0.25

Initially, flexural strength of N is reduced after zeolite addition, however, it varied in an increasing trend with curing time. Flexural strength of NZ (0-d) showed an increment of 57% after 90 days curing period which is a noteworthy improvement of tensile behavior. Flexural strength of expansive soil is improved after stabilization and this complies with Muntohar (2011). This improvement of flexural strength is the end product of the pozzolanic reactions, strong cementation bonds developing in time yielded higher toughness yet reduced ductility.

Relationships between flexural strength with respect to swell and shrinkage strains, as well as compression index are displayed in Figures 3.10-3.12. In Figure 3.10, the

reduction in swell potential can be observed to be 85% from 0-day to 90-day cured specimen, which corresponds to an increment of 70% in flexural strength. In Figure 3.11, a reduction of 34% volumetric shrinkage caused 30% increment in flexural strength. The reduction in compression index is observed in Figure 3.12 to be about 75% at the end of the 90-day curing period, which resulted in approximately 30% increment in flexural strength. Therefore, swell potential, volumetric shrinkage strain and compressibility are reduced significantly with the utilization of zeolite, the rate of change of each varying in different amounts with respect to increasing flexural strength.

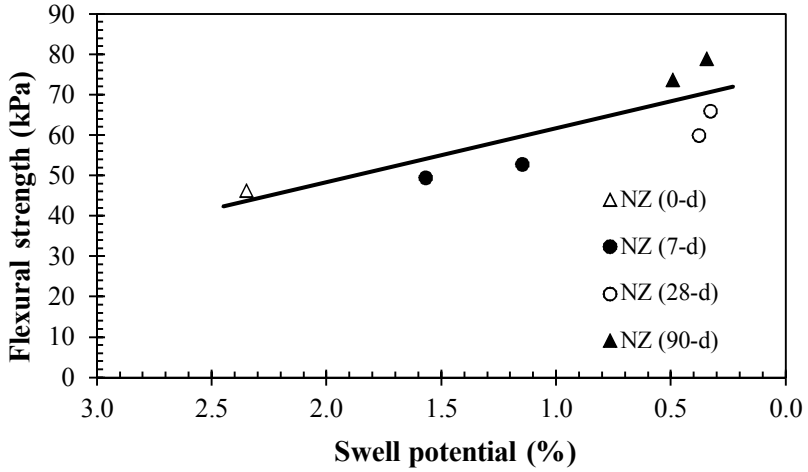

Figure 3.10. Relationship between flexural strength and swell potential.

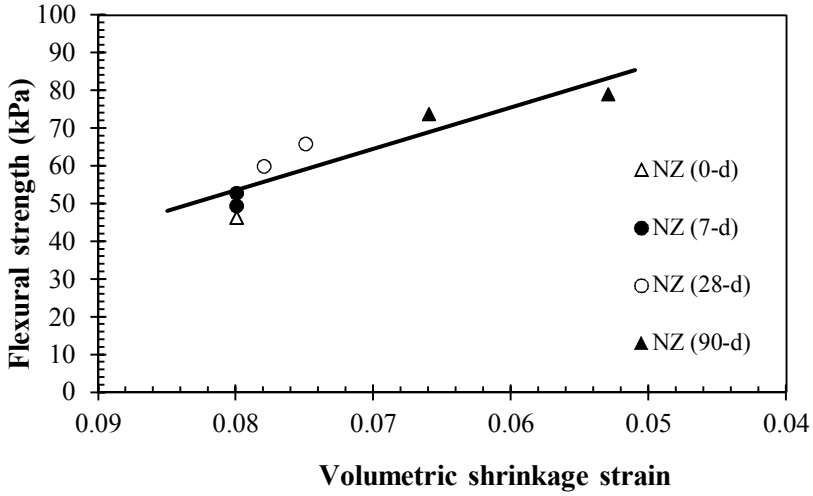

Figure 3.11. Relationship between flexural strength and volumetric shrinkage strain.

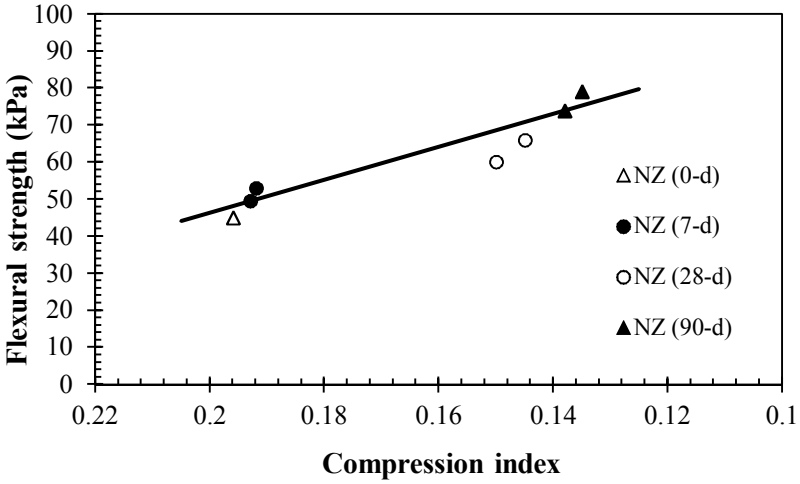

Figure 3.12. Relationship between flexural strength and compression index.

3.4 SEM Analysis

Figure 3.13 (a) shows the scanning electron microscopy (SEM) image of expansive soil-zeolite (NZ) in the as compacted state, which shows flocculated soil fabric of NZ mixture. Figure 3.13 (b) reveals the micro-structural change due to hydration process within the expansive soil-zeolite mixtures resulting in the formation of elongated tobermorite-like gels (CSH) around the soil particle edges within curing period of more than 90 days. Figure 3.13 (c) depicts the more homogeneous structure formed with

further curing over 120 days, which enhanced the CSH fiber formation combining the zeolite and soil particles together. It is this change in structure and fabric which caused the improvement in mechanical properties of mixtures in terms of reducing volume change, compressibility and increasing strength and durability in time. This hydration process proceeds continuously over long time periods, yet with a decreasing rate (Mitchell and El Jack, 1966).

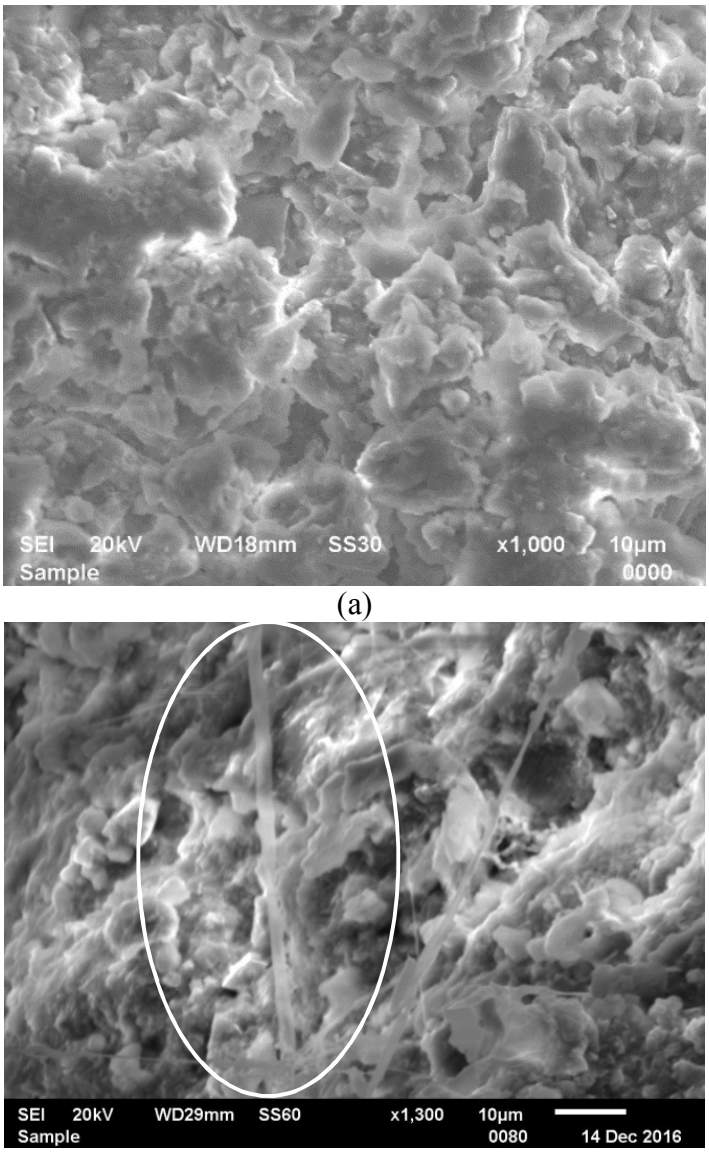

Figure 3.13. SEM micrographs of cured NZ mixtures after (a) 0 day, (b) 90 days, (c) 120 days.

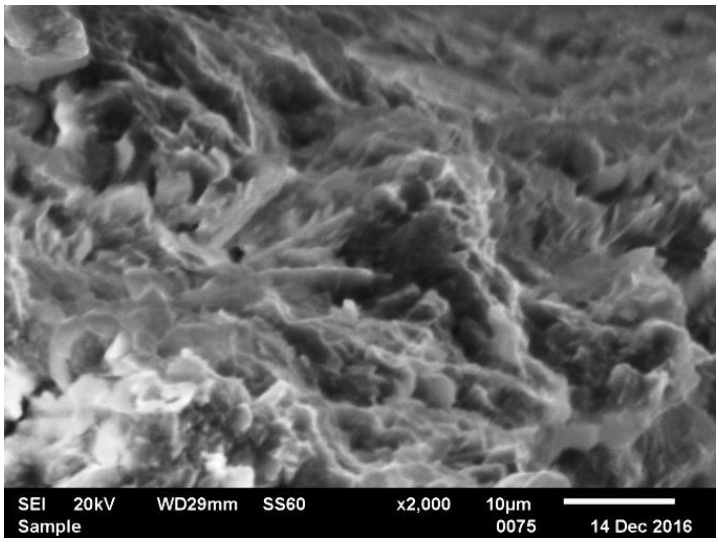

(c)

Figure 3.13. (Cont.)

3.5 Conclusions

An experimental study on the effect of curing on volume change and strength characteristics of expansive soil and zeolite mixture was perused and its suitability for geotechnical and geo-environmental applications was discussed, deriving the following conclusions:

1) Swell potential of expansive soil was reduced by 53% after addition of zeolite (NZ) and a further reduction of 85% was recorded from 0-day to 90-day curing period.

2) Desiccation behavior of zeolite added expansive soil revealed substantial reductions in volumetric, axial and diametral strains within 90 days. Average reduction in volumetric strains was observed to be 58% when zeolite added to expansive soil, which through pozzolanic effect yielded 34% more reduction within 0-day to 90-day curing periods.

3) Compressibility characteristics were improved by 30% reduction in the compression index with the addition of zeolite. A further reduction of 30% was observed throughout 90-day curing period.

4) Hydraulic conductivity values at different pressure ranges indicate that NZ mixtures have approximately 83% higher values than untreated natural soil due to increased grain size with the use of zeolite. However, these values were reduced by 80% within 90-day curing period. Nevertheless, hydraulic conductivity values of both uncured and cured NZ samples remained below 1 x 10^{-7} cm/s which is the upper limit for soil barriers.

5) The desiccation of saturated samples yielded evaporation curves, which indicated that with the addition of zeolite rapid drying duration reduced by 54% within 90-day curing period. Furthermore, the shrink-swell potential obtained from the evaporation data indicated that the cured specimens remained in the "moderate potential" range.

6) While no significant improvement in unconfined compressive strength of expansive soil-zeolite mixture was observed, flexural strength of NZ increased by a considerable amount of 57% within 90 days curing.

7) Linear relationships of flexural strength versus swell percent, compression index, and volumetric shrinkage were observed with increasing curing time, the rate of decrease of volumetric shrinkage with increasing flexural strength in time being the most significant.

The aforementioned improvements were based on the structural changes at micro level due to pozzolanic reactions, displayed by the scanning electron micrographs, which indicate the improved structure of the expansive soil-zeolite mixtures by cementation product of tobermorite.

Chapter 4

USE of WASTE MARBLE AS SECONDARY ADDITIVE

4.1 Introduction

Different materials are used to alleviate swelling-shrinking problems of soils on structures such as lime, cement, and bitumen. Addition of lime decreases the swell potential of the soil, whereas cement stabilization increases shear strength, showing higher strength gains compared to lime-treated soils (Nelson and Miller, 1992). Gueddouda et al. (2011) studied the effect of different combinations of cement, lime and salt (NaCl) on the expansive clay and concluded that the most feasible and economic alternative is using lime-salt combination as an additive for improvement of the expansive clays. Abdullah and Alsharqi (2011) however, showed that only 2% cement addition over 28-days curing period would be enough to improve the expansive soil. Sahoo and Pradhan (2010) observed that the maximum increase in strength of expansive soil was obtained with 8% lime addition and a marginal decrease in strength was observed with higher lime contents. Farooq et al. (2011) examined the effect of lime addition (0, 2, 4, 6 and 8%) and curing period (0, 7, 14 and 28 days) on unconfined compressive strength of expansive soil. They reported that the best result was obtained with the addition of 4% lime content for all curing periods. Conversely, Kiliç et al. (2015) deduced that 6% lime utilization decreased the percent swell, swell pressure and increased the unconfined compressive strength of clay over 90 days curing period. Önal (2015) studied the usage of lime as a stabilizer for the improvement of bearing capacity of the pond base soils and concluded that unconfined compressive strength

increased by adding 8% lime with the curing periods of 28, 56 and 180 days.

Recently utilization of industrial waste materials as stabilizing agents became very popular for both recycling and soil improvement purposes, including fly ash, marble dust, rice husk ash, waste tire and wood ash (Amit and Singh, 2013). Suneel et al. (2010) focused on the long-term consolidation and strength behavior of fly ash stabilized marine clay. Various fly ash percentages were used in the testing programme and an increasing trend on shear strength properties with the increment of fly ash content was observed. Fly ash inclusion reduced the plasticity characteristics, optimum water content, compression index and coefficient of consolidation while increasing the unconfined compressive strength. Phanikumar (2009) compared influence of lime and fly ash on physical properties, compaction characteristics and swell of expansive clays. Test results showed that liquid limit reduced, whereas plastic limit increased with increment of lime and fly ash contents, hence resulting in a reduced plasticity index, and consequently swell potential. Maximum dry density increased and optimum water content reduced with both lime and fly ash additions. Shrivastava et al. (2014) studied the influence of rice husk ash on the lime stabilized black cotton soil. Liquid limit, plasticity index and differential free swell index values reduced after rice husk ash addition. Gandhi (2013) compared marble dust and rice husk ash in the improvement of expansive soils and indicated that marble dust was more efficient than rice husk ash for Atterberg limits, free swell index, CBR and swelling pressure tests. Cömert et al. (2010) studied the treatment of sub-base soils with a mixture of fly ash, marble dust and waste sand addition, and concluded that the optimum ratios were 20% fly ash, 5-10% marble dust and 5% waste sand based on unconfined compression test results. Fırat et al. (2012) concluded that fly ash, marble dust and waste sand improved

swelling ratio, CBR and water conductivity, hence are effective stabilizers in road sub-bases. Tuncan et al. (2000) recommended the use of 20% lime, 10% fly ash and 5% cement utilization for stabilizing petroleum contaminated waste soil as an effective sub-base material. Gupta and Sarma (2014) utilized sand, fly ash and marble dust with different proportions for the stabilization of black cotton soil and specified that this mixture can be used as a sub-grade material for construction of flexible pavements in rural roads with low traffic volume.

Agrawal and Gupta (2011) studied the effect of different percentages of marble dust in the stabilization of expansive soil. Influence of marble dust on the physical properties of the stabilized soil are investigated and found that liquid limit, plasticity index and shrinkage index reduced after using marble dust, however, plastic limit and shrinkage limit increased. Abdulla and Majeed (2014) used marble powder with varying proportions by weight of soil and reported that liquid limit, plastic limit and plasticity index values decreased with the marble dust inclusion. Çimen et al. (2011) determined that marble content affected the maximum dry density but optimum water content did not change. Sabat and Nanda (2011) specified that optimum water content showed an increasing trend while maximum dry density decreased with the use of marble dust.

Zorluer and Usta (2003) added marble dust to a CL type of soil in five different percentages (0, 1, 3, 5 and 7%) by dry mass and observed the swell potential reducing with marble dust content addition up to 5%, which showed an increasing trend when 7% was added. They explained this behavior as high marble dust content causing a hard structure in the soil specimen. Başer and Çokça (2010) used waste limestone dust

and waste marble dust for the improvement of expansive soils. The expansive soil was prepared as a mixture of kaolinite, bentonite and the stabilizing agents, which were waste limestone dust and waste marble dust, were added to the soil in amounts of 5%, 10%, 15%, 20%, 25% and 30% by dry mass. Laboratory results showed that swell percentage reduced and rate of swell raised with the additive percentage. The influence of marble dust utilization on swelling behavior was also investigated by Agrawal and Gupta (2011), Çimen et al. (2011), Sabat and Nanda (2011), Abdulla and Majeed (2014) and reported that swell potential and swell pressure decreased with the increment of marble dust content.

Gurbuz (2015) focused on the stabilization of clayey soil by using waste marble powder in sub-bases of the road construction. Waste marble powder was added to the clayey soil with various percentages (2.5%, 5%, 10%, 15%, 20% and 25%) to peruse the unconfined compressive strength and ductility behavior. Test results showed that the peak strength and ductility increased with the increment of marble content up to 10% and then it continued a decreasing trend with the higher marble amounts. Based on these results, 10% waste marble was chosen as an effective dosage.

Akinwumi and Booth (2015) studied the effect of waste marble fines inclusion in the treatment of engineering properties of lateritic soil by using 2%, 6% and 10% marble dosages and have found that the liquid limit and plasticity index values reduced with the marble content. In compaction characteristics, the maximum dry density raised and the optimum water content reduced with the increasing of waste marble fines. Unconfined compressive strength results showed an increasing and coefficient of permeability showed a decreasing trend with the increment of marble content.

In the previous studies, waste marble was added to the expansive soil or it was used with a secondary waste material such as fly ash as a stabilizing agent. In this study, however, utilization of waste marble as a secondary material in sand-amended expansive soil is adopted, with the intention of recycling this industrial waste accumulating in the environment, as well as discovering a suitable mixture for landfill liner or sub-base stabilization of pavement and road constructions. Laboratory testing program consisted of swell-shrinkage, compressibility and flexural strength tests. In addition, evaluation of durability was examined with respect to different curing periods.

4.2 Materials and Methods

4.2.1 Materials

In this phase of the study uniform sand and expansive soil (MH) were used of which physical properties and XRD results are given in Table 2.1 and Figure 2.1 respectively.

Marble waste, which is the by-product of the expanding construction industry on the island, was added as a secondary material to expansive soil-sand mixture. The estimated annual amount of marble waste production is approximately 1500-2000 tonnes. Utilization of this material in soil stabilization can be a potential solution to increasing accumulation of waste marble products. Two different types of waste marble obtained from different marble production plants, of different gradations, denoted as marble powder (MP) and marble dust (MD), were used. In the marble production plant marble is produced and then the cutting process is done with the aid of jetted water to prevent excessive friction. The marble cuttings and dust in the form of solution is then collected in a tank as shown in Figure 4.1 (a). The waste solution is then pumped to the precipitation tank and a flocculant solution is injected to liquid

waste for the purpose of binding small particles into larger lumps (Figure 4.2 (b)). After this process, the liquid waste forming a homogeneous mud is pumped to filter press with high pressure. This filter press produces solid waste which are collected in a container as shown in Figure 4.2. In this study, MP was obtained in the form of powder, already ground, whereas MD was prepared in the laboratory by grinding the waste chunks collected from the factory.

(a)

Figure 4.1. (a) Marble cutting process, (b) Precipitation tank.

(b)
Figure 4.1. (Cont.)

Figure 4.2. Waste marble dust in solid form.

Particle size distribution analysis (ASTM D422-63e2) showed that marble powder consists of 6% clay size, 32% silt size and 62% sand size particles, whereas marble dust includes 80% silt size and 20% sand size particles (Figure 4.3).

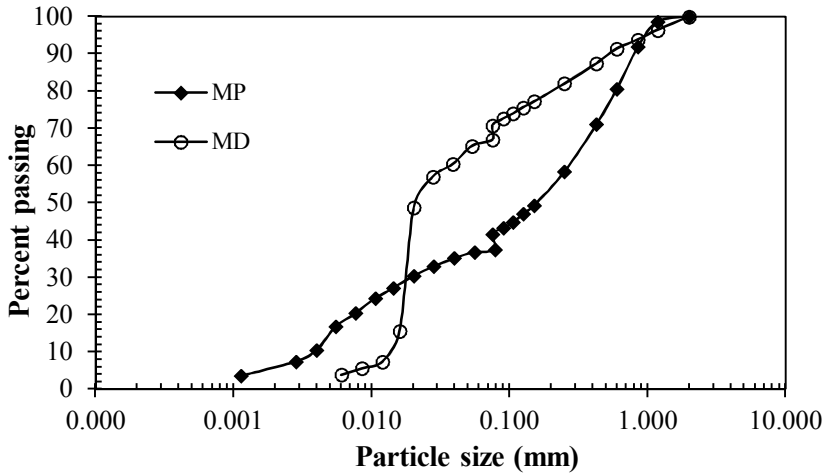

Figure 4.3. Particle size distributions of MP and MD.

Chemical compositions of expansive soil, waste marble powder and waste marble dust are obtained from X-ray fluorescence (XRF) spectrometer and the test results are presented in Table 4.1.

Table 4.1. Chemical composition of expansive soil, marble powder and marble dust.

Chemical composition (%)	**Expansive soil**	**Marble powder**	**Marble dust**
SiO_2	36.5	0.178	4.4
CO_2	17.9	42.6	35.9
CaO	16.2	55.7	54
Al_2O_3	11.8	0.0708	0.977
Fe_2O_3	6.87	0.0641	0.0891
MgO	6.26	1.22	0.778
Other elements	4.47	0.1671	3.8559

Waste marble powder and waste marble dust include 55.7% and 54% CaO (lime)

content respectively which is concurrent with the previous researchers who indicated that marble waste they have used for stabilization purpose possessed very high lime (CaO) content of up to 55 % (Zorluer and Usta, 2003; Başer, 2009; Cömert et al., 2010).

A pozzolan is defined as a finely divided siliceous or aluminous material, which in the presence of water and calcium hydroxide will form a cementing agent (Nalbantoglu and Gucbilmez, 2001; Shahjahan, 2001). The reaction between calcium from lime with silica and/or alumina in the presence of water is called pozzolanic reaction. The cementitious products are calcium silicate hydrate (CSH), calcium aluminate hydrate (CAH) and calcium alumino-silicate hydrate (CASH) (Eades and Grim, 1960; Eades et al., 1962). Lime-soil mixtures gain long-term strength due to pozzolanic reactions (Little, 1999; Bhattacharja et al., 2003; Kampala and Horpibulsuk, 2013) which provide remarkable improvement in the soil properties such as compressibility, shear strength, unconfined compressive strength and stiffness (Rajasekaran and Narasimha Rao, 2002; Khattab et al., 2007; Consoli et al., 2009; Tang et al., 2011; Wang, 2017).

X-ray diffraction (XRD) analysis was done to detect the minerals of marble powder and marble dust and the test results are presented in Figure 4.4. Quartz, calcite, kaolinite and sepiolite are the common minerals for both of marbles.

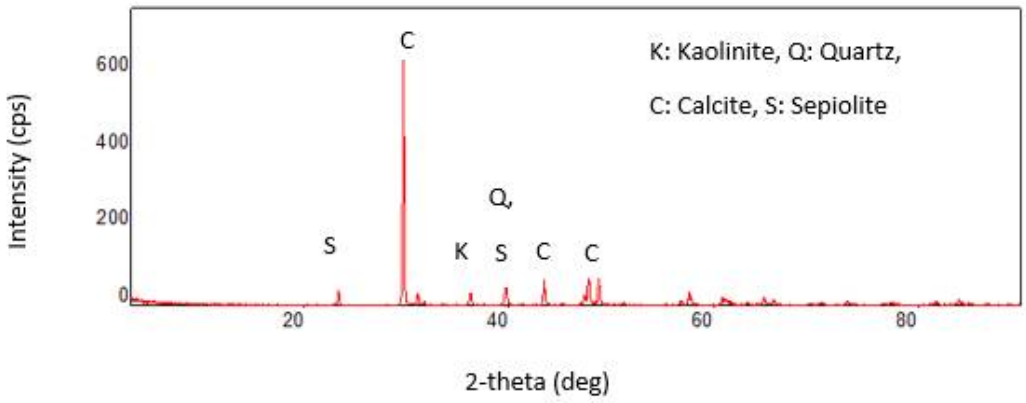

(a)

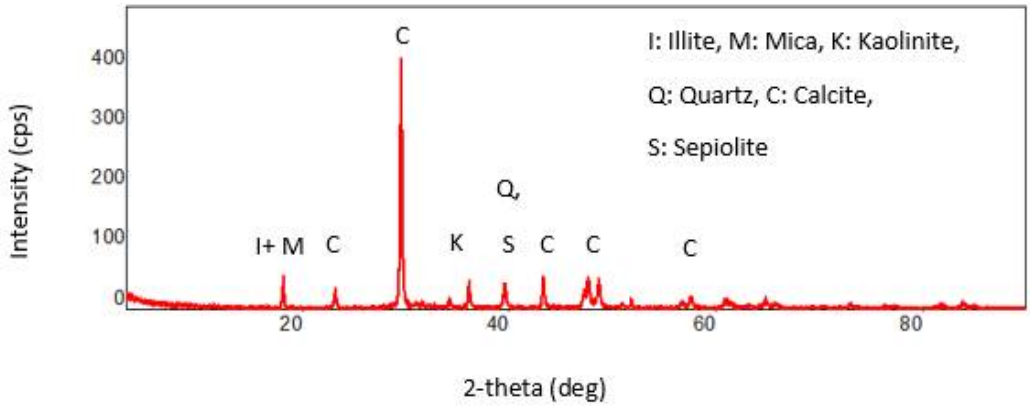

(b)

Figure 4.4. XRD results of (a) marble powder and (b) marble dust.

4.2.2 Methods

Expansive soil and waste marble were pulverized, the sand was washed with distilled water for reducing the total soluble salt concentration, and oven-dried materials were used in the sample preparation. All of the tests were carried out on compacted soil specimens which were at their optimum water content and maximum dry density. Standard Proctor compaction test (ASTM D698-12e2) was applied in order to obtain compacted soil samples. Sand was added to expansive soil in 1:1 ratio, then waste marble powder and marble dust were added to expansive soil-sand mixture in three different percentages, which are 5%, 10% and 20% by dry mass. The tests were conducted at 0, 7, 28 and 90-day curing periods. The soil samples are categorized as

expansive soil-sand (NS), expansive soil-sand-marble powder (NSMP) and expansive soil-sand-marble dust (NSMD) and the experiments were performed on 7 groups of soils. Definitions of soil groups are listed in Table 4.2.

Table 4.2. Definitions of soil groups.

Soil Groups	Definition
NS	50% Expansive soil + 50% Sand
NS5%MP	47.5% Expansive soil + 47.5% Sand + 5% Marble powder
NS10%MP	45.0% Expansive soil + 45.0% Sand + 10% Marble powder
NS20%MP	40.0% Expansive soil + 40.0% Sand + 20% Marble powder
NS5%MD	47.5% Expansive soil + 47.5% Sand + 5% Marble dust
NS10%MD	45.0% Expansive soil + 45.0% Sand + 10% Marble dust
NS20%MD	40.0% Expansive soil + 40.0% Sand + 20% Marble dust

One-dimensional swell test (ASTM D4546-14), consolidation test (ASTM D2435-11) and volumetric shrinkage test, unconfined compression test (ASTM D2166-06) and flexural strength test (ASTM C348-14) were carried out as mentioned in Section 2.2.3.

4.3 Test Results

4.3.1 Physical Properties

Consistency limits (ASTM D4318-10e1), linear shrinkage (BS 1377-2:90), and specific gravity (ASTM D854-14) test results are depicted in Table 4.3.

Table 4.3. Physical properties of soil mixtures.

	Liquid limit (%)	Plastic limit (%)	Plasticity index (%)	Linear shrinkage (%)	Specific gravity
NS	32	30	12	9	2.69
NS5%MP	30	17	13	10	2.65
NS10%MP	29	19	10	10	2.69
NS20%MP	26	15	11	9	2.68
NS5%MD	35	21	14	12	2.69
NS10%MD	37	27	10	12	2.52
NS20%MD	38	30	8	9	2.58

In the MP group, liquid limit and plasticity index decreased with the increasing waste marble content, corroborating the results of Akinwumi and Booth (2015), Abdulla and Majeed (2014) and Agrawal and Gupta (2011). On the other hand, in the MD group, liquid limit and plastic limit values increased while the plasticity index reduced with the increment of marble dust content, similar to findings of Başer (2009), Sivrikaya et al. (2014) and Gurbuz (2015). The plasticity index has been reduced by 17% in 10% MP and by 33% in 20% MD samples after 24 hours of mellowing time, which are the lowest indices attained. The difference in the behavior of MP and MD added expansive soil-sand mixtures arises from the amount of fines contained in each sample, the latter consisting of 42% more fines, therefore larger surface area in contact with the expansive soil, facilitating the pozzolanic reaction to take place. However, these values are not adequate enough to evaluate the pozzolanic strength of marble waste, but merely represent the initial state of the mixtures before being compacted for strength and volume change studies. Consequently, it can be deduced that the effect of waste marble on plasticity index of samples is insignificant when particle sizes are dominantly in the coarse range and when in non-cured state.

4.3.2 Compaction Test Results

Compaction curves are obtained for each soil group and presented in Figure 4.5. Table 4.4 includes the compaction parameters, optimum water content and maximum dry density, which reveal that maximum dry density increased while optimum water content reduced as the marble powder content increased in the MP group, which supports the findings of Akinwumi and Booth (2015). Addition of 5%, 10% and 20% MP to expansive soil-sand mixture of 1:1 ratio increased the content of coarse particles by 3%, 9%, and 10% respectively. Therefore, the water retention capacity of the mixture reduced, consequently reducing the optimum water contents. In MD added samples, the fines increased by 8-12%, hence increasing the optimum water contents of the mixtures. Likewise the maximum dry densities followed an increasing trend in MP group, while reducing in MD group.

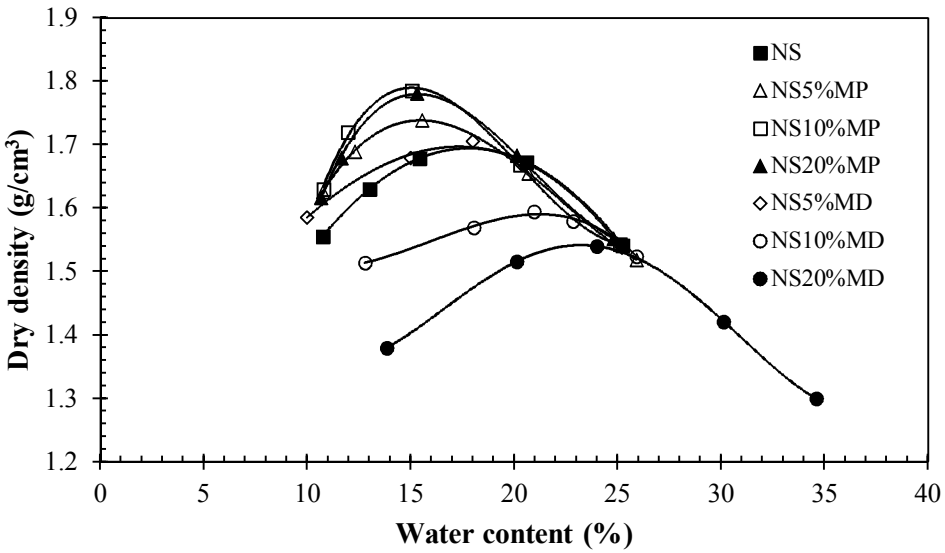

Figure 4.5. Compaction curves of NS, NSMP and NSMD soil groups.

Table 4.4. Compaction test results.

	Optimum water content (%)	Max. Dry density (kg/m^3)
NS	17.5	1690
NS5%MP	15.5	1740
NS10%MP	15.0	1790
NS20%MP	15.3	1781
NS5%MD	18.0	1705
NS10%MD	21.0	1590
NS20%MD	24.0	1540

The decrease in optimum water content occurred by the binding and aggregation of clay-sized particles of marble powder with the clay component of the soil. Hence, marble powder addition increased the silt-sized particles and the soil mixture became coarser, requiring less water to achieve higher density. Conversely, MD group showed a decreasing trend in maximum dry density with the increasing marble dust content hence higher optimum water content was achieved, similar to the findings of Sabat and Nanda (2011). The aggregation of soil with the inclusion of marble dust induced increment in pore volume, therefore the dry density reduced. The increment in optimum water content has occurred as a result of the necessity of additional water within the flocculated soil due to the pozzolanic reaction between soil and lime content of MD (Kumar et al., 2007; Jha and Sivapullaiah, 2015).

4.3.3 Volume Change Properties

4.3.3.1 Swell Results

One-dimensional swell percentage versus time graphs were obtained from one-dimensional swell tests on specimens with three marble percentages at different curing times. The swell percentages with respect to logarithm of time plots are depicted in Figure 4.6 and Figure 4.7 for marble powder and marble dust respectively. The plots reveal that the primary swell percentages are significantly reduced with curing time.

The secondary swell, which displays a progressive increase in the 0-day cured specimens, with the rate of 0.20%/min, stabilizes easily within nearly 4 days with 5% and 20% MP and 3 days with 10% MP included and 90-day cured specimens. Studying the swell percentage versus logarithm of time curves of MD treated specimens, it can clearly be seen that there is no secondary swell tendency whatsoever. This behavior is the result of aforementioned pozzolanic reactions occurring faster and more effectively in MD specimens which include higher content of fines. The major component of swell percentage, the primary swell, and the time taken for primary swell to be completed are obtained from the swell-time curves and are summarized in Table 4.5.

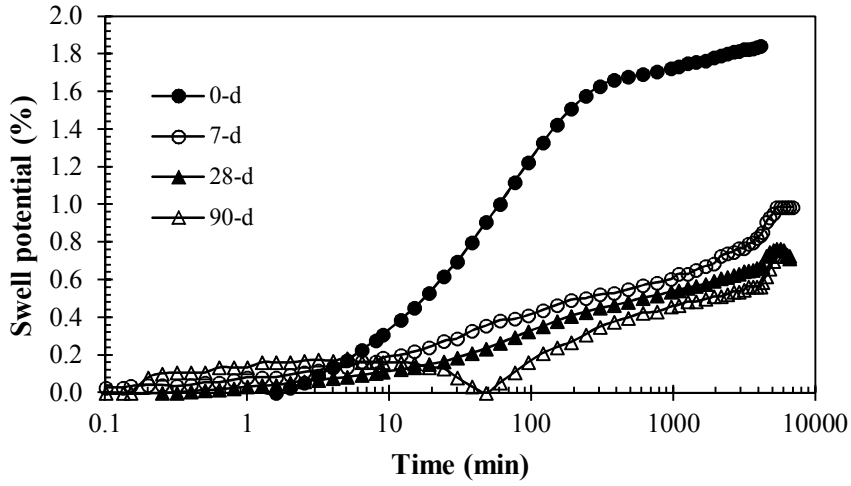

(a)

Figure 4.6. Aging effect on swell curves of (a) 5%MP, (b) 10%MP and (c) 20%MP.

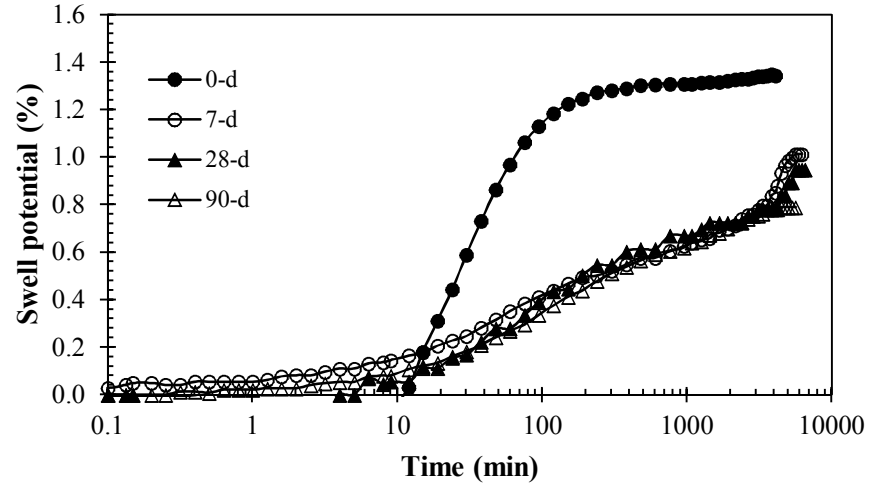

(b)

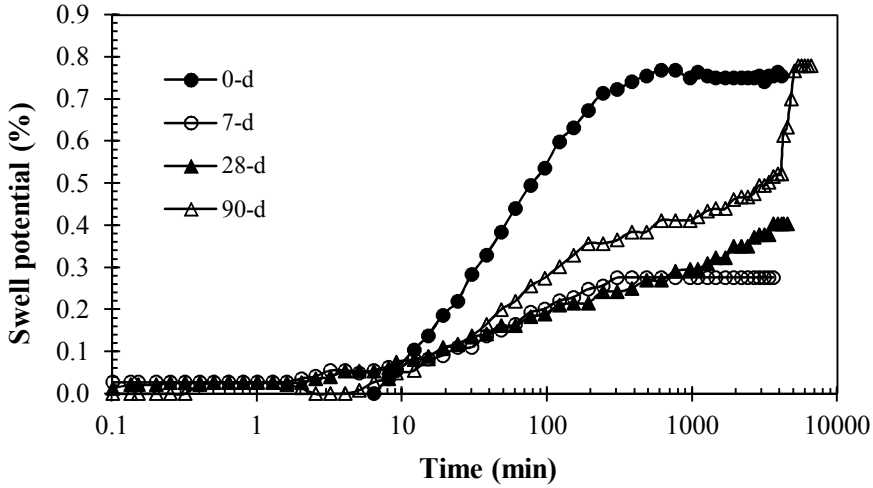

(c)

Figure 4.6. (Cont.)

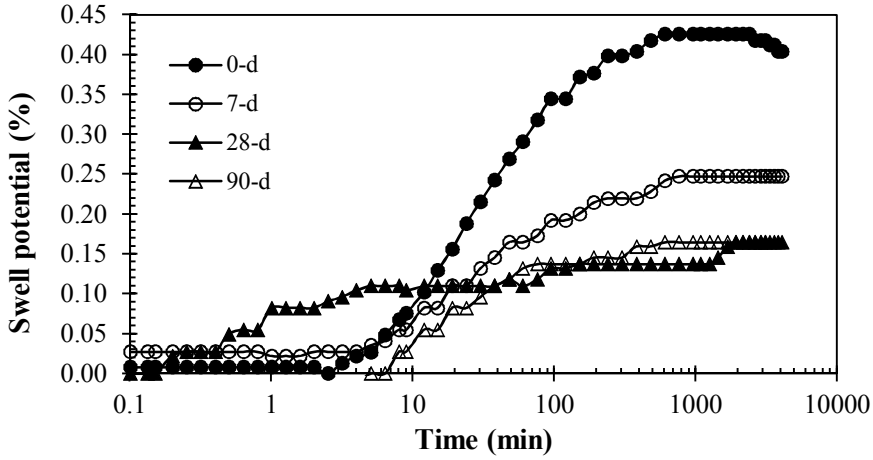

(a)

Figure 4.7. Effect of curing time on swell curves of (a) 5%MD, (b) 10%MD and (c) 20%MD.

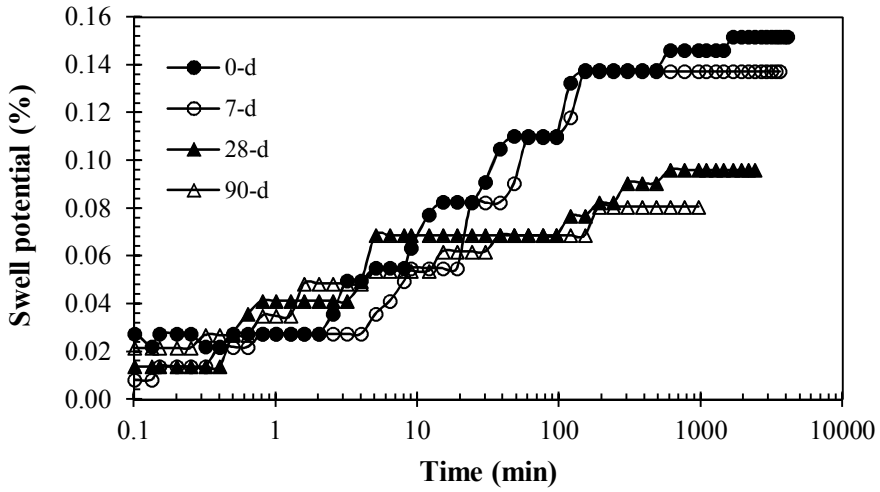

(b)

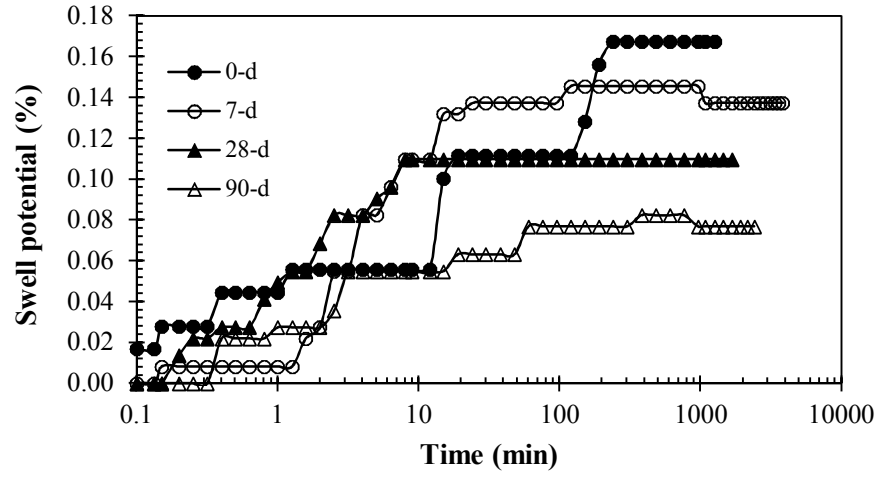

(c)

Figure 4.7. (Cont.)

Table 4.5. Primary swell results of the soil groups.

Curing time	Swell parameters	NS	MP			MD		
			5%	10%	20%	5%	10%	20%
	Primary Swell (%)	0.67	1.64	1.24	0.497	0.43	0.15	0.17
0-day	Time (min)	204	203	90	1300	200	150	250
	Primary Swell (%)	-	1.03	1.01	0.276	0.25	0.14	0.15
7-day	Time (min)	-	5500	5000	300	400	150	22
	Primary Swell (%)	-	1.00	0.94	0.40	0.16	0.10	0.11
28-day	Time (min)	-	5500	2500	3000	1800	600	8
	Primary Swell (%)	-	0.98	0.56	0.35	0.16	0.08	0.08
90-day	Time (min)	-	5000	420	180	60	190	380

20% MP has yielded the lowest primary swell percentage of 0.35% at 90-day curing period. However, the change of swell percentage with curing was not consistent, which was perceived to have occurred due to surplus of marble content. Furthermore, 20% MP specimen revealed a secondary swell tendency which has ended up in a total swell strain of 0.78. Utilization of 10% MP, however showed a gradual reduction in swell strain with curing time and no additional secondary swell component, which appeared to be the most suitable marble content for sustainable results. Therefore, it can be concluded that 5% is not adequate for cementation and 20% is an excessive amount for the treatment, therefore 10% is the optimum amount for this type and gradation of marble waste. In the MD group, which contains an appreciable amount of fines in the marble component, swelling percentage of each marble content showed a decreasing trend with aging and all of the test results are in "low swell" category (Snethen et al., 1977). The fine marble particles have been more effective in this group, and 5% waste inclusion was observed to be sufficient to provide pozzolanic reactions causing agglomeration of particles, hence formation of flocculated and stronger fabric between the soil particles (Jha and Sivapullaiah, 2015). These observations agree with past research on the efficacy of marble dust utilization in soil treatment, reducing swell potential (Zorluer and Usta, 2003; Başer and Çokça, 2010; Agrawal and Gupta 2011; Çimen et al. 2011; Sabat and Nanda, 2011; Abdulla and Majeed, 2014).

4.3.3.2 Volumetric Shrinkage Results

Volumetric shrinkage strain versus time results of cured MP and MD groups are displayed in Figure 4.8 and Figure 4.9 respectively, and the maximum volumetric shrinkage strains are listed in Table 4.6.

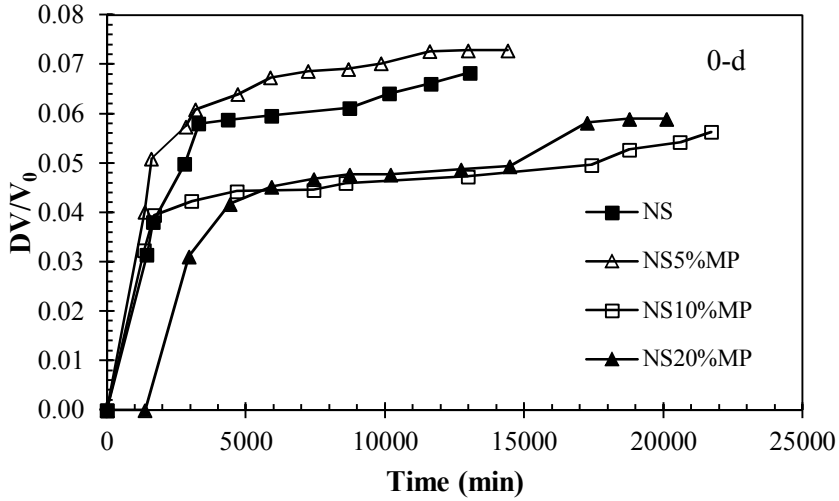

(a)

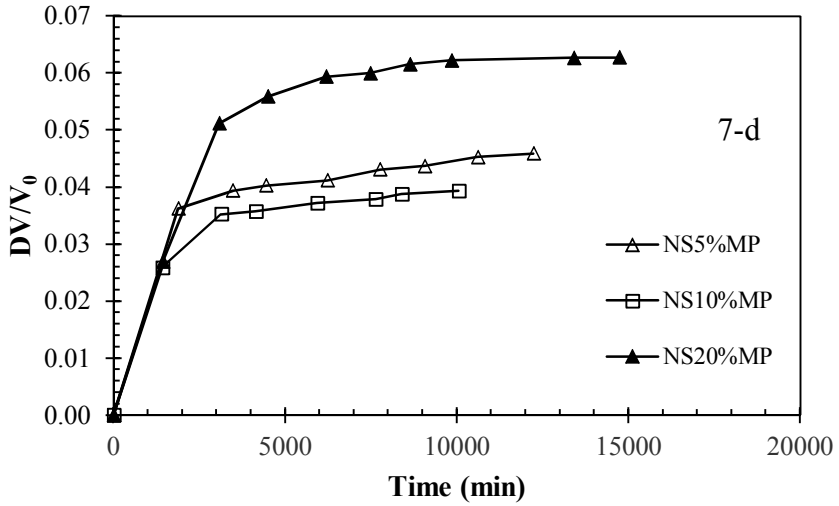

(b)

Figure 4.8. Volumetric shrinkage strain versus time of MP group for (a) 0-day, (b) 7-day, (c) 28-day and (d) 90-day curing periods.

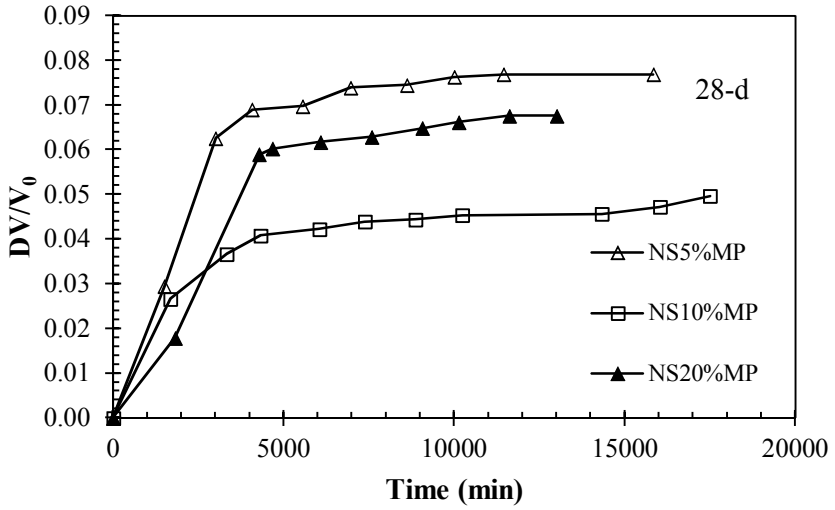

(c)

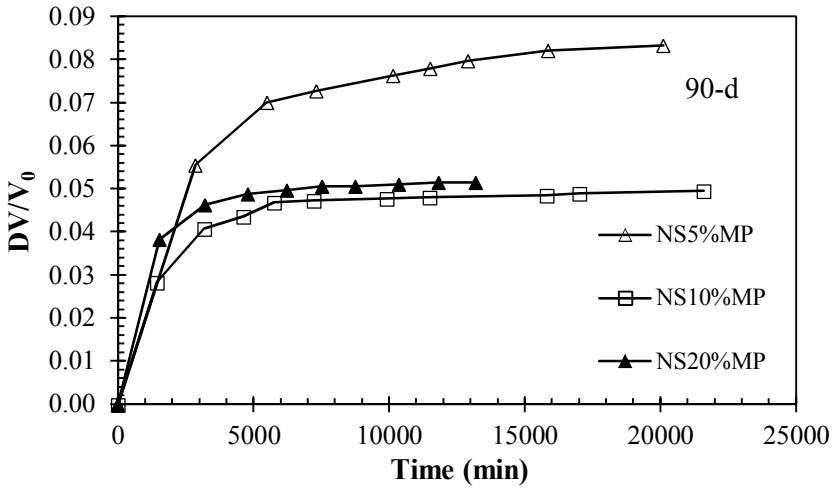

(d)

Figure 4.8. (Cont.)

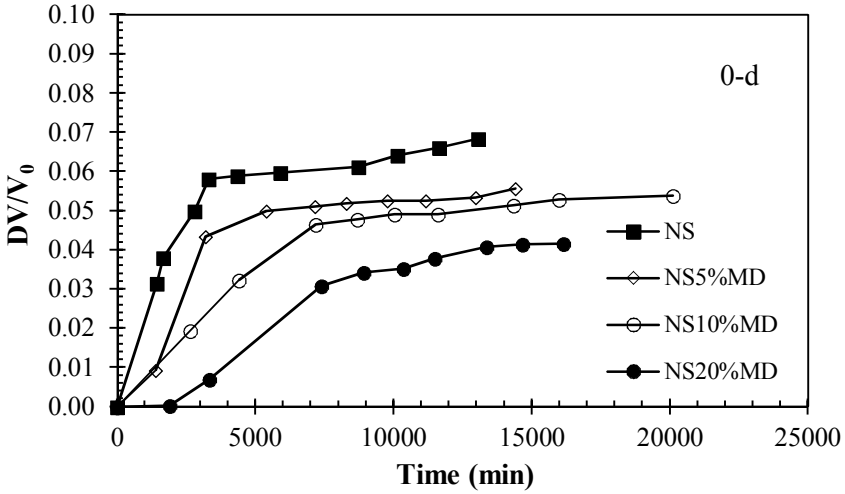

(a)

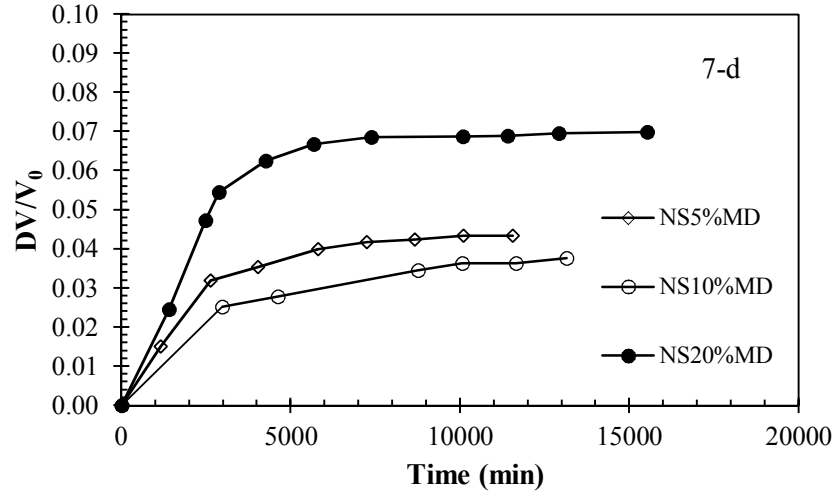

(b)

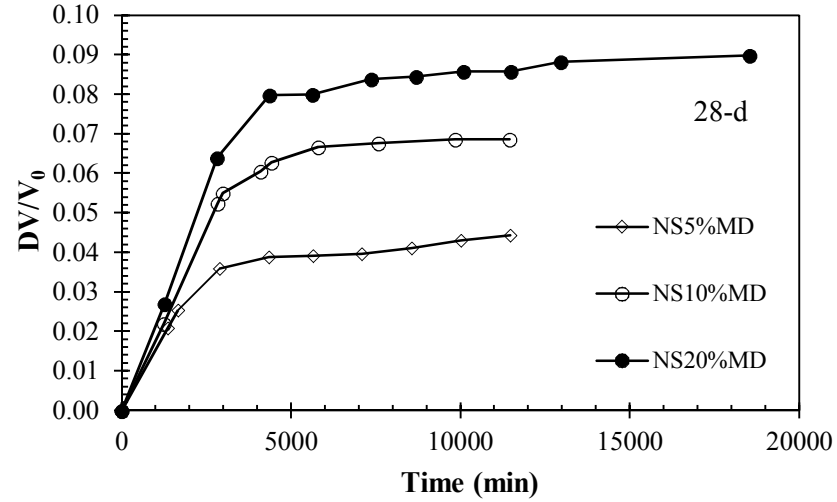

(c)

Figure 4.9. Volumetric shrinkage strain versus time of MD group for (a) 0-day, (b) 7-day, (c) 28-day and (d) 90-day curing periods.

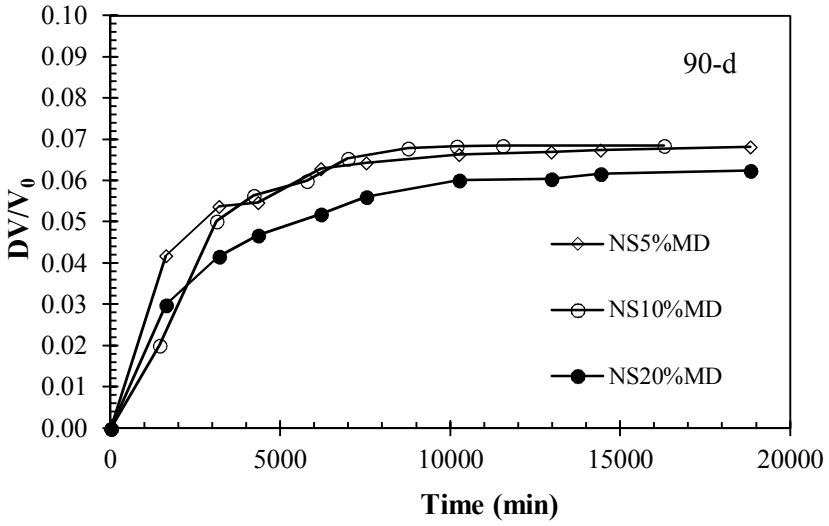

(d)
Figure 4.9. (Cont.)

Table 4.6. Volumetric shrinkage strain results.

Material	0-d	7-d	28-d	90-d
NS	0.068	-	-	-
NS5%MP	0.073	0.046	0.077	0.080
NS10%MP	0.056	0.039	0.050	0.049
NS20%MP	0.059	0.063	0.068	0.052
NS5%MD	0.056	0.043	0.044	0.067
NS10%MD	0.052	0.036	0.069	0.068
NS20%MD	0.042	0.070	0.088	0.063

Comparing the test results, it is observed that lower shrinkage values were obtained with the addition of 10% MP in all curing time periods. In MD group, however, 5% and 10% MD inclusions have given similar results, whereas 5% MD has lower results after 28 and 90-day aging periods. On the other hand, 20% MD included sample had inconsistent results with the curing time. Based on these findings, it can be deduced that 5% MD is more effective in lessening the volumetric shrinkage strain. These results are suitable for the recommendation of safe volumetric shrinkage strain value

of about 5% upon drying for soil liners (Kleppe and Olson, 1985; Daniel and Wu, 1993; Tay et al., 2001; Osinubi and Eberemu, 2010; Moses and Afolayan, 2013). A similar shrinkage strain value can be presumed for compacted road sub-base for limitation of crack formation, hence shrinkage settlements.

Shrinkage occurs due to desiccation by loss of water through evaporation and cracking starts from the soil surface to deeper soil diminishing at the end of the tensile zone (Tang et al., 2010). Excessive shrinkage causes cracking and deterioration of compacted soil structure which results in settlements and increase of hydraulic conductivity, which are undesirable attributes in road bases and landfills. Therefore, the shrinkage behavior should be examined with respect to variation of water content with time. One good parameter which can be used as a measure of affinity of mixtures to excessive shrinkage is the swell-shrinkage index, which was explained earlier in Chapter 3. In this study, 90-day cured soil specimens are selected in the investigation of evaporation graphs in order to observe the behavior in longer periods, hence to assure the sustainability of the waste marble stabilization. Table 4.7 depicts shrink-swell indices determined from the evaporation curves given in Figure 4.10.

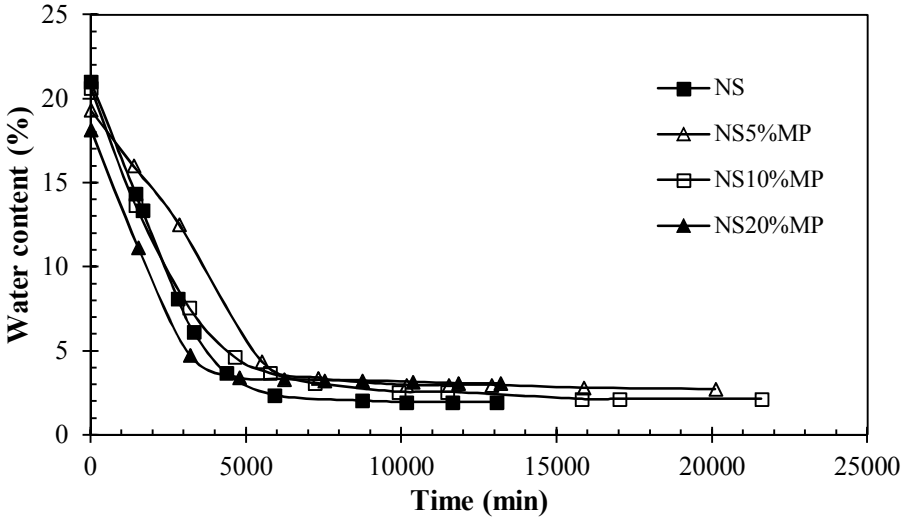

(a)

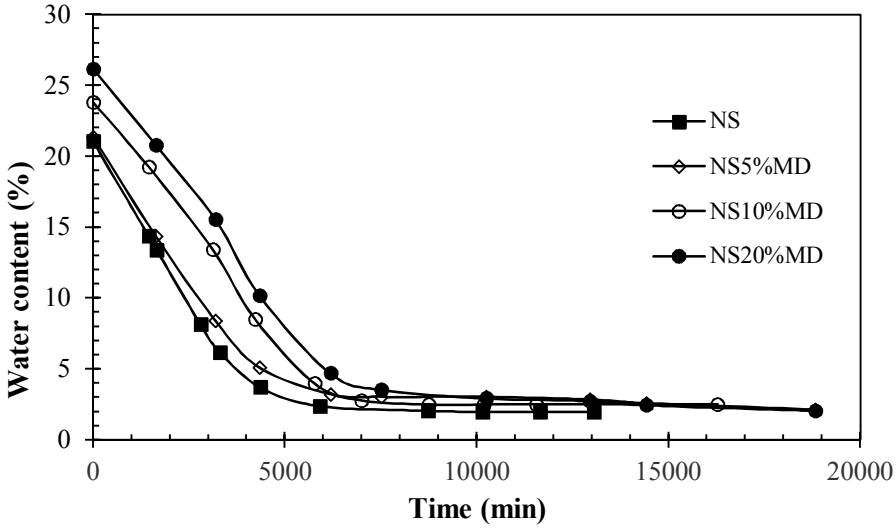

(b)

Figure 4.10. Evaporation graphs with 90-day cured (a) MP and (b) MD groups.

Studying the evaporation curves, it can be deduced that during desiccation, initially the water content of soil samples were reduced linearly, the rate of drying reducing with marble content, which is more defined in MD group. After the completion of rapid drying period, the drying continued with a reduced rate, finally reaching a constant value. The water evaporation was fast in the first approximately 5000 minutes for MP and MD groups. The required times to reach equilibrium while drying at room temperature were 7000 and 8000 minutes for MP and MD groups respectively, hence slower drying occurring in MD group which has been undergoing a more efficient

pozzolanic process.

Table 4.7. Evaporation results of 90-days cured soils.

	Initial water content (%)	Final water content (%)	Shrink-swell index (I_{ss})
NS	21.00	2.20	18.80
NS5%MP	19.35	2.74	16.61
NS10%MP	20.65	2.15	18.50
NS20%MP	18.20	3.09	15.11
NS5%MD	21.36	2.14	19.22
NS10%MD	23.80	2.50	21.30
NS20%MD	26.18	2.05	24.13

Table 4.7 gives the shrink-swell index parameter (I_{ss}), determined from the initial and final water content values, which indicate that all combinations in the MP group are less than the maximum allowed value of 20%, whereas only 5% MD included sample satisfies this recommended requirement.

Volumetric shrinkage data are also presented in the form of void ratio versus water content, and the hyperbolic model of Fredlund et al. (2002) was fitted to the experimental data. Figures 4.11-4.14 and Figures 4.15-4.18 represent the shrinkage curves of MP and MD respectively. Minimum void ratios and shrinkage limits are attained from the fitting parameters of a_{sh} and b_{sh} respectively and are summarized in Table 4.8.

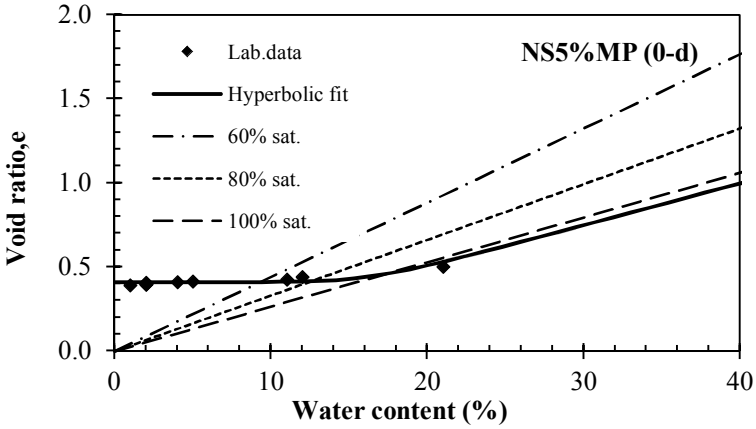

(a)

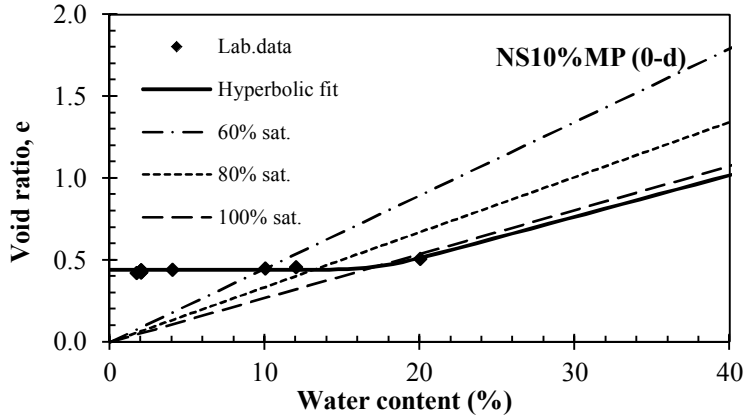

(b)

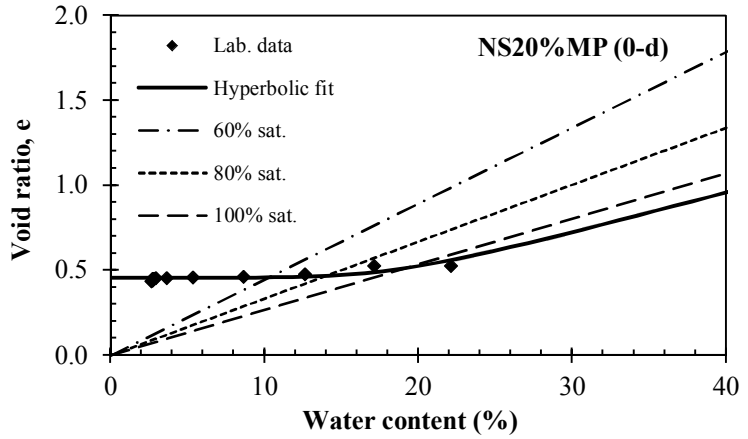

(c)

Figure 4.11. Shrinkage curves of 0-day cured (a) NS5%MP, (b) NS10%MP, (c) NS20%MP.

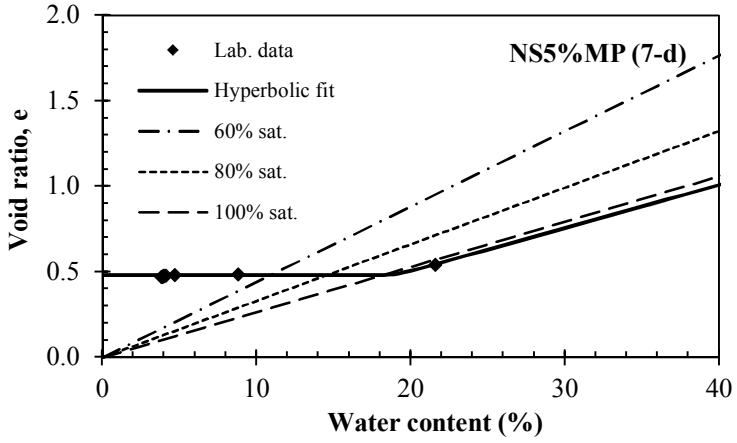

(a)

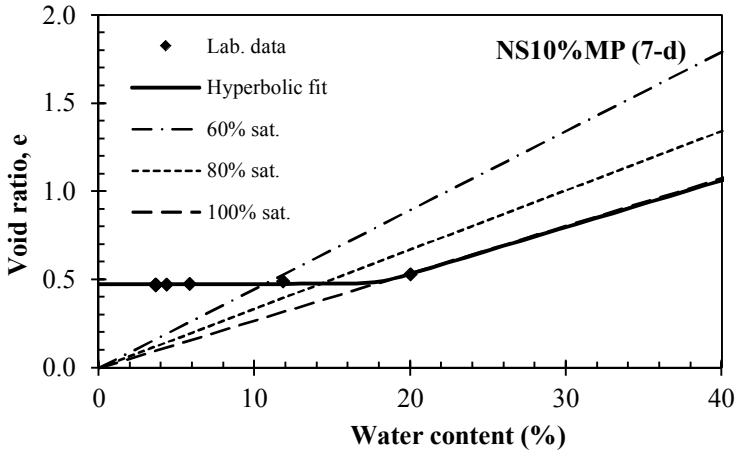

(b)

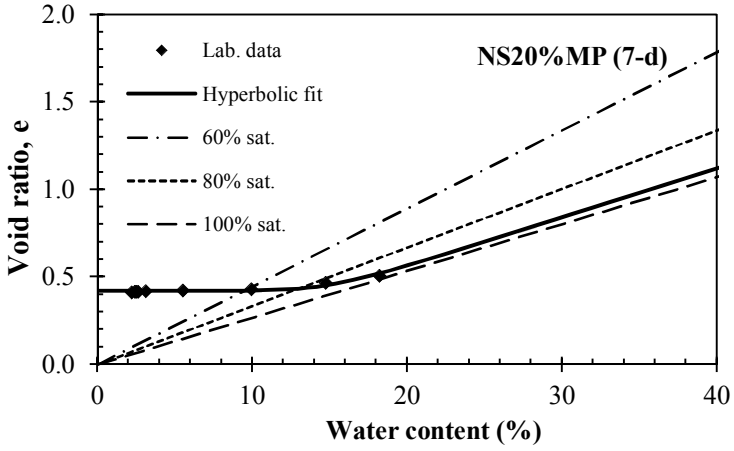

(c)

Figure 4.12. Shrinkage curves of 7-day cured (a) NS5%MP, (b) NS10%MP, (c) NS20%MP.

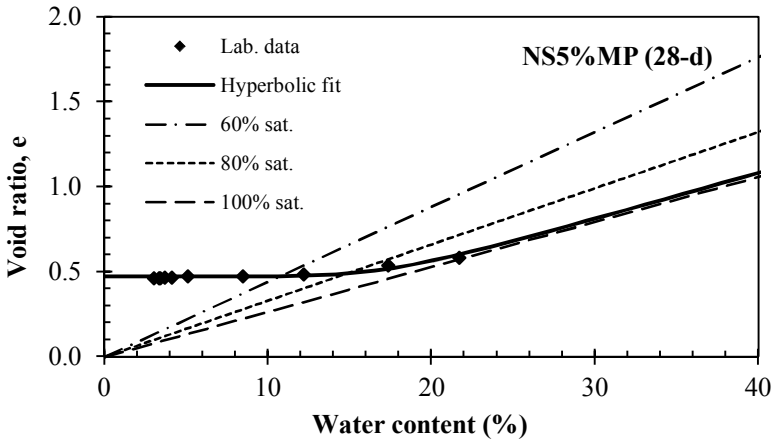

(a)

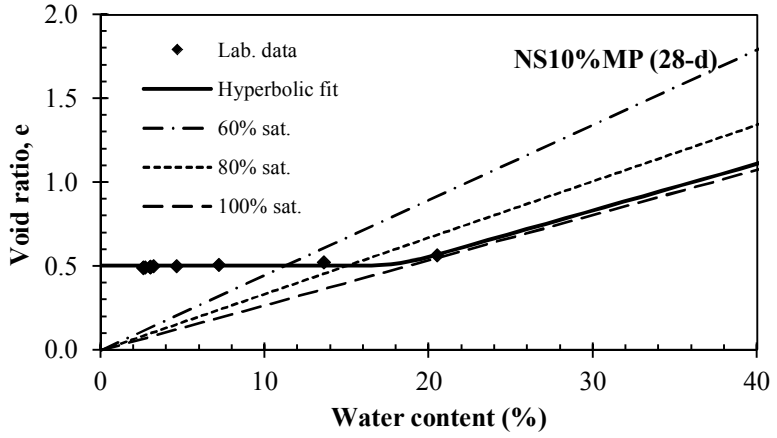

(b)

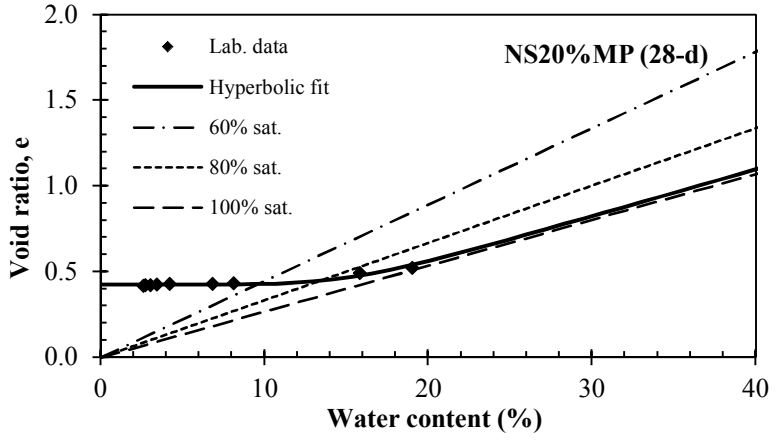

(c)

Figure 4.13. Shrinkage curves of 28-day cured (a) NS5%MP, (b) NS10%MP, (c) NS20%MP.

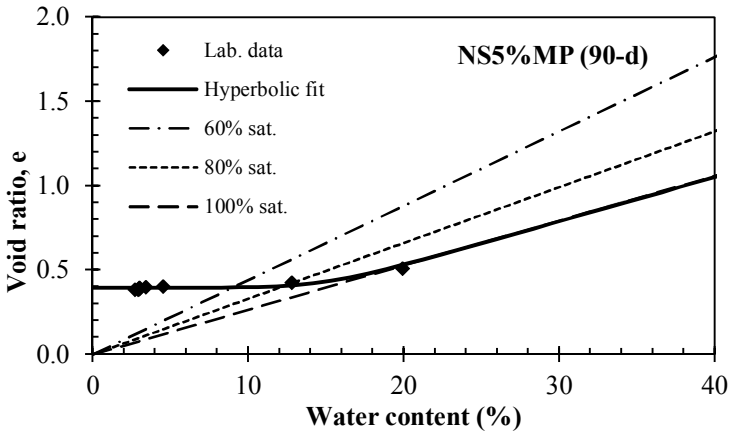

(a)

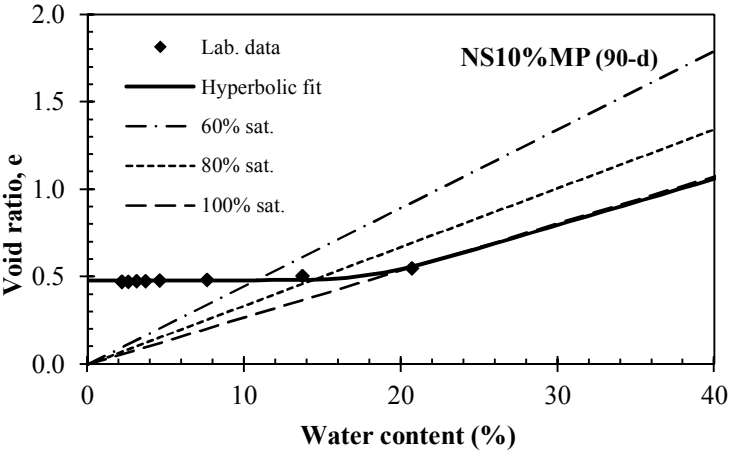

(b)

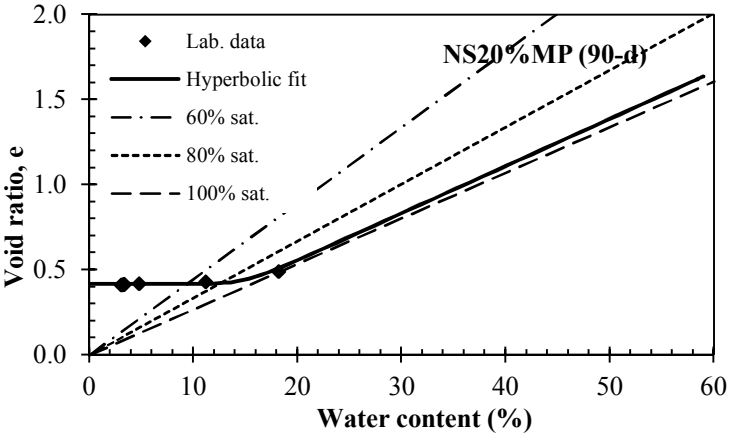

(c)

Figure 4.14. Shrinkage curves of 90-day cured (a) NS5%MP, (b) NS10%MP, (c) NS20%MP.

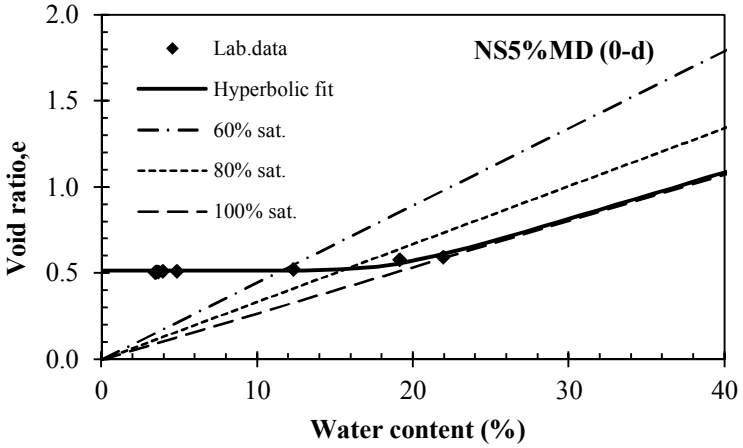

(a)

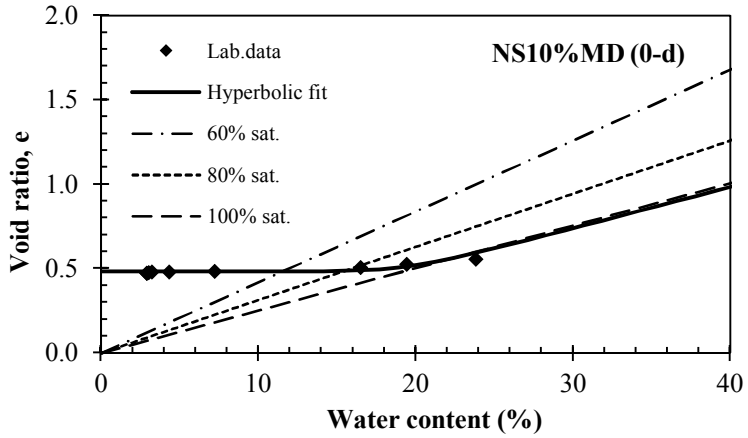

(b)

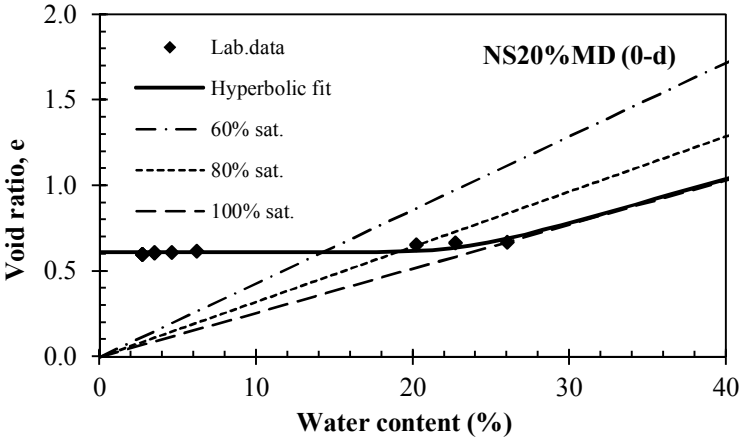

(c)

Figure 4.15. Shrinkage curves of 0-day cured (a) NS5%MD, (b) NS10%MD, (c) NS20%MD.

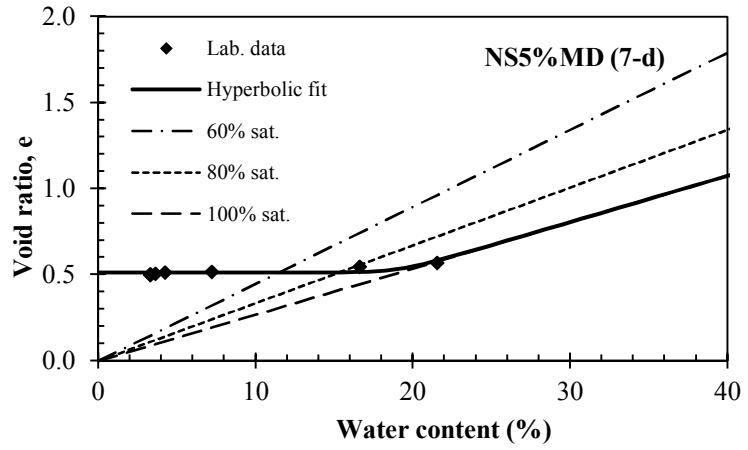

(a)

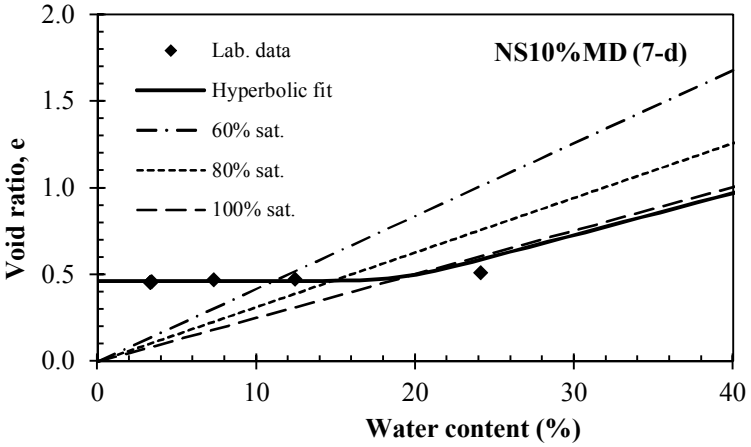

(b)

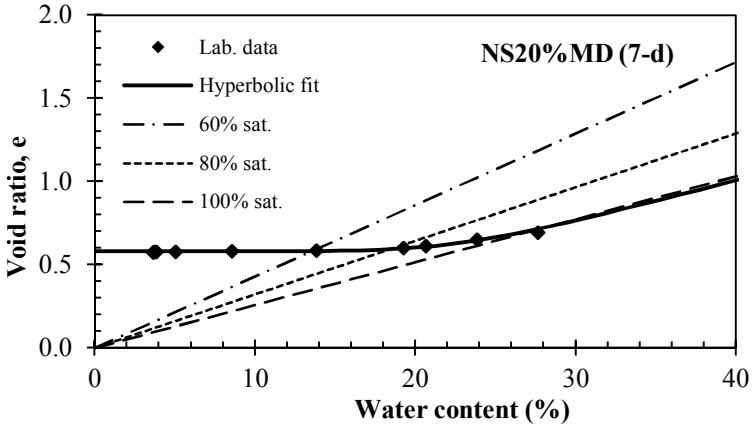

(c)

Figure 4.16. Shrinkage curves of 7-day cured (a) NS5%MD, (b) NS10%MD, (c) NS20%MD.

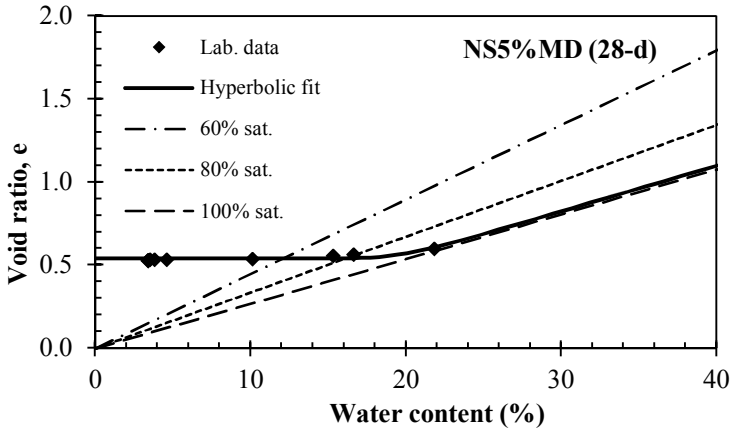

(a)

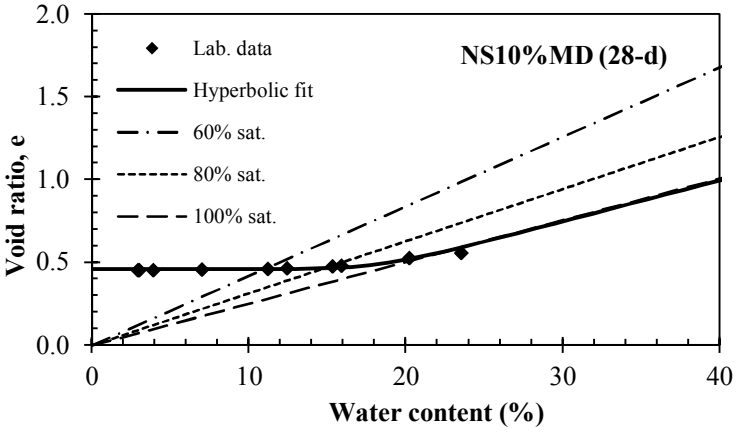

(b)

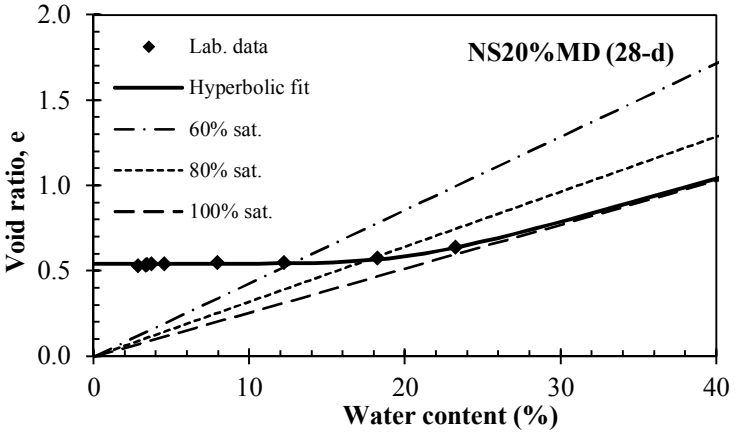

(c)

Figure 4.17. Shrinkage curves of 28-day cured (a) NS5%MD, (b) NS10%MD, (c) NS20%MD.

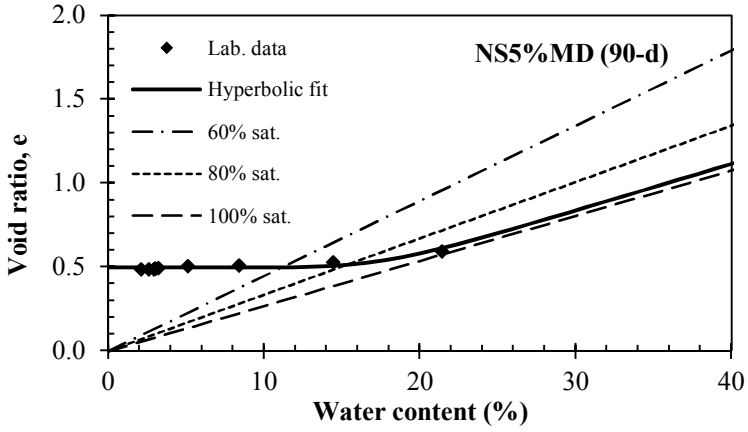

(a)

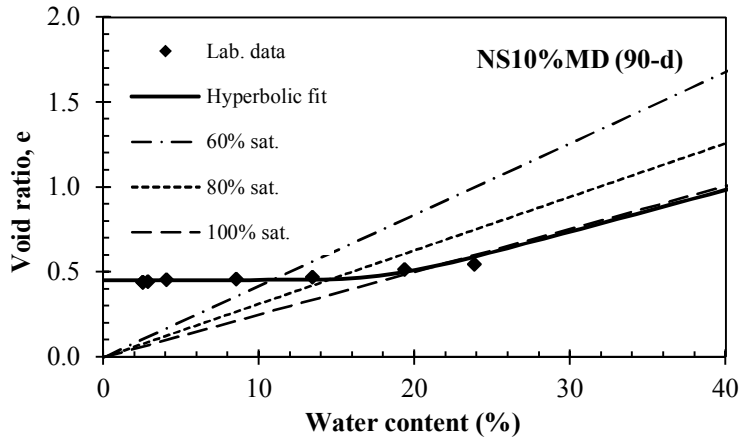

(b)

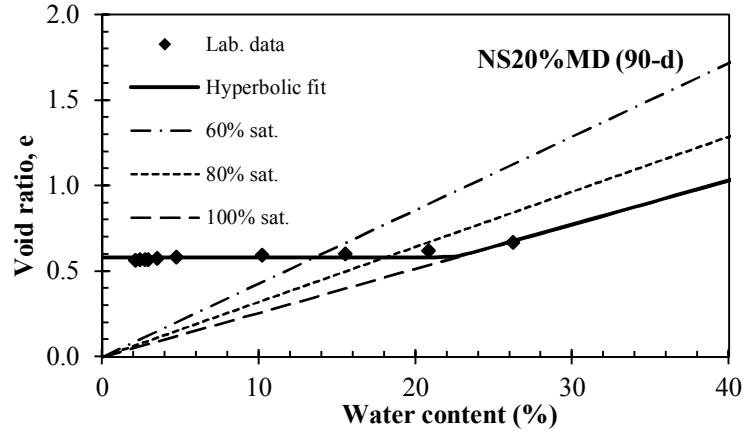

(c)

Figure 4.18. Shrinkage curves of 90-day cured (a) NS5%MD, (b) NS10%MD, (c) NS20%MD.

Table 4.8. Hyperbolic fitting parameters of the shrinkage curves.

Curing time	Fitting Parameter	NS	MP			MD		
			5%	10%	20%	5%	10%	20%
0-day	a_{sh}	0.401	0.410	0.439	0.456	0.514	0.481	0.611
	b_{sh}	0.143	0.164	0.173	0.191	0.189	0.196	0.235
	c_{sh}	9.469	8.522	14.66	6.031	9.035	10.218	12.45
7-day	a_{sh}	-	0.480	0.476	0.422	0.513	0.464	0.580
	b_{sh}	-	0.190	0.179	0.146	0.191	0.191	0.231
	c_{sh}	-	46.81	29.92	16.52	17.735	14.688	7.85
28-day	a_{sh}	-	0.472	0.503	0.425	0.538	0.46	0.543
	b_{sh}	-	0.174	0.181	0.150	0.196	0.185	0.209
	c_{sh}	-	7.380	25.50	6.740	15.085	10.098	7.24
90-day	a_{sh}	-	0.395	0.480	0.417	0.497	0.454	0.582
	b_{sh}	-	0.150	0.181	0.150	0.178	0.185	0.226
	c_{sh}	-	8.055	10.80	11.72	8.097	10.074	78.79

Shrinkage results are examined to analyze the volumetric shrinkage behavior of MP and MD included NS samples with the effect of aging. Based on the fitting parameters a_{sh}, representing the minimum void ratio at the end of drying phase and the b_{sh} parameter, representing the shrinkage limit, the best values were obtained for 10% MP and 20%MD included specimens. These are the highest values which indicate that less volume change has occurred. However, 20% MD is considered an excessive amount, whereas 5% MD usage is sufficient enough to maintain the integrity of the specimens during shrinkage.

4.3.3.3 Compressibility Results

Void ratio versus effective consolidation pressure curves of MP and MD groups at different curing periods are depicted in Figure 4.19 and Figure 4.20 respectively. Compressibility characteristics, which are compression index (C_c), rebound index (C_r) and swelling pressure (p_s') are given in Table 4.9. When the test results are compared, utilization of 10% MP and 5% MD have given the lowest results for all of the curing times. Compressibility results of NS10%MP and NS5%MD satisfied "slightly compressible" case for all of the curing periods (Coduto, 2001). Hence waste marble

usage has been very effective in reducing the compressibility through pozzolanic reactions causing cementation, hence durability against consolidation pressures.

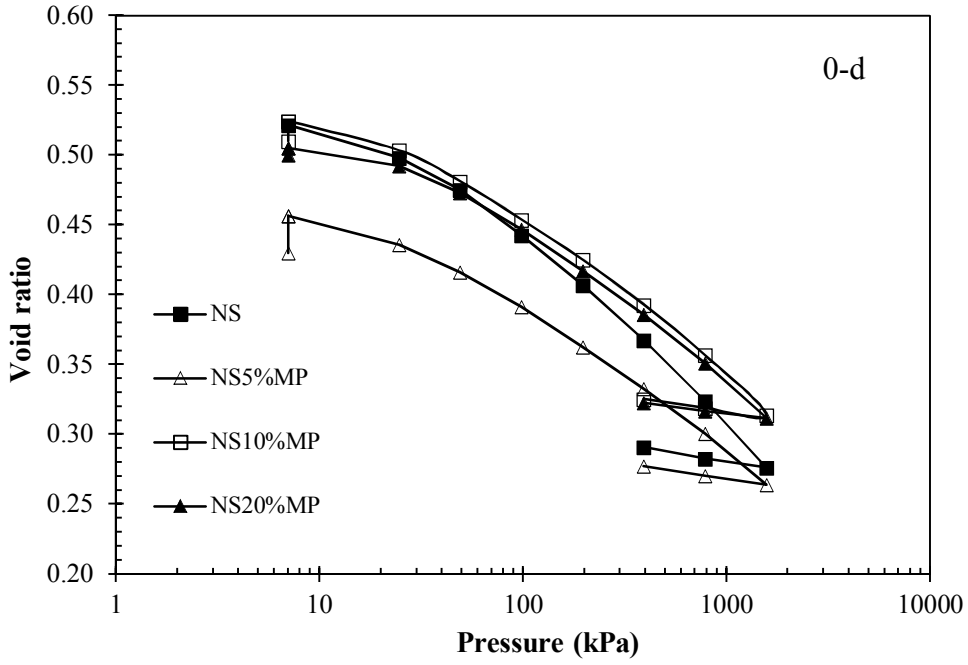

(a)

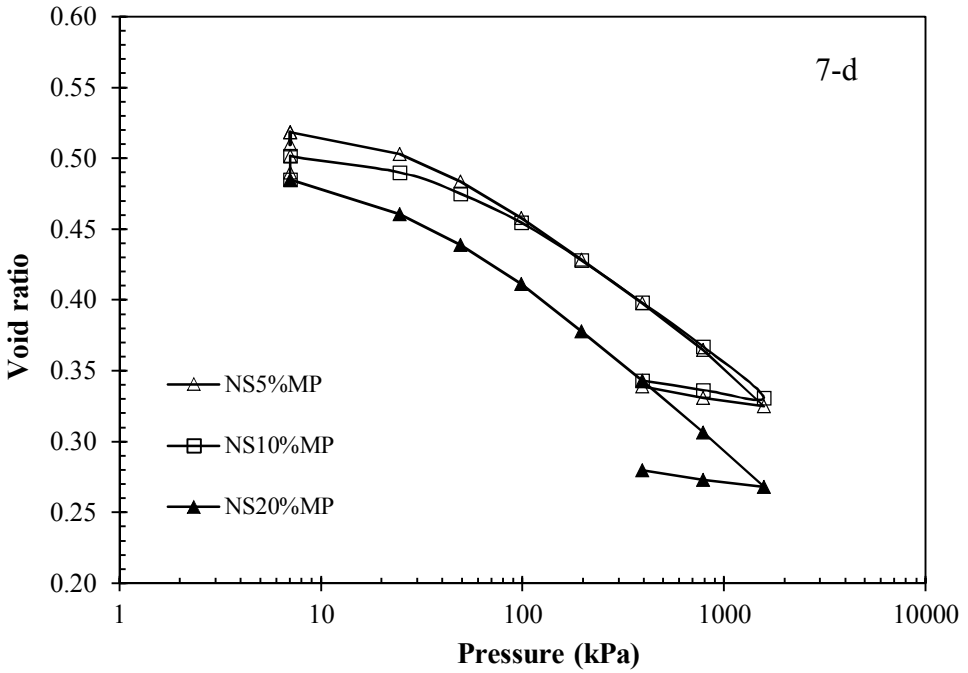

(b)

Figure 4.19. Consolidation curves of MP group due to curing period of (a) 0 day, (b) 7 days, (c) 28 days and (d) 90 days.

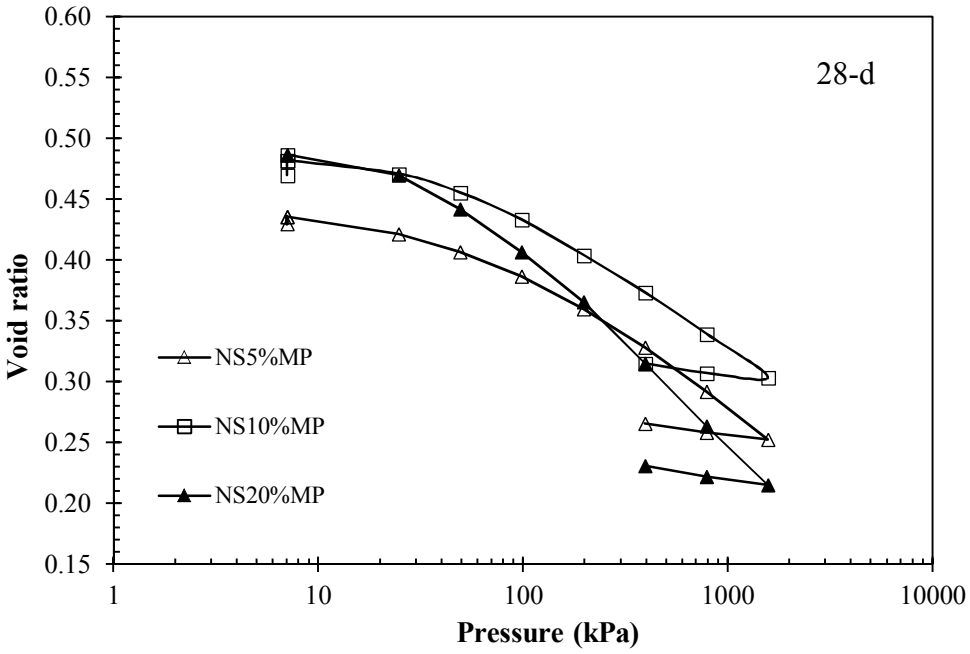

(c)

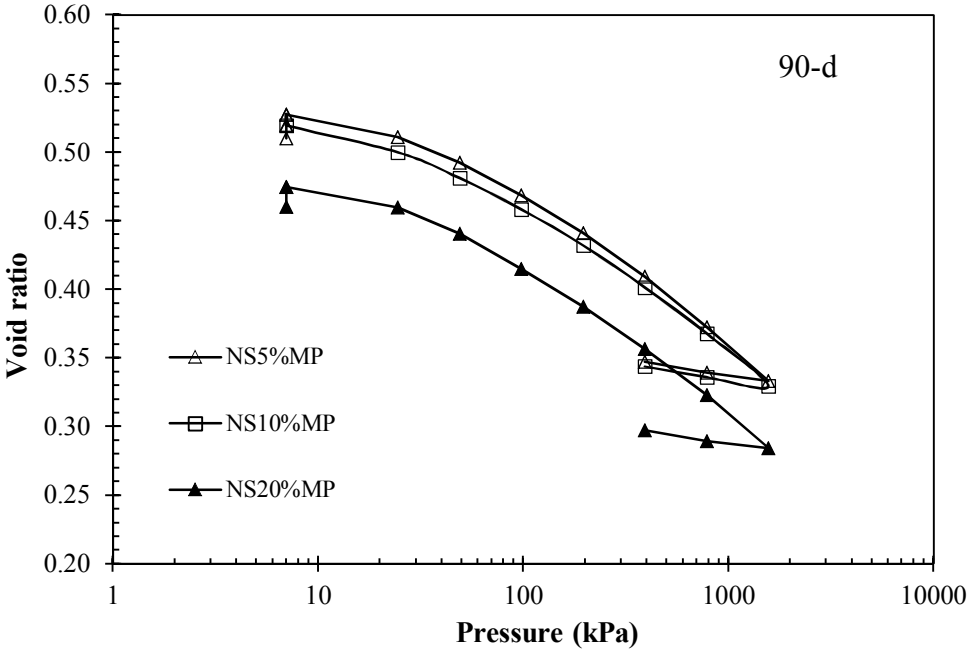

(d)

Figure 4.19. (Cont.)

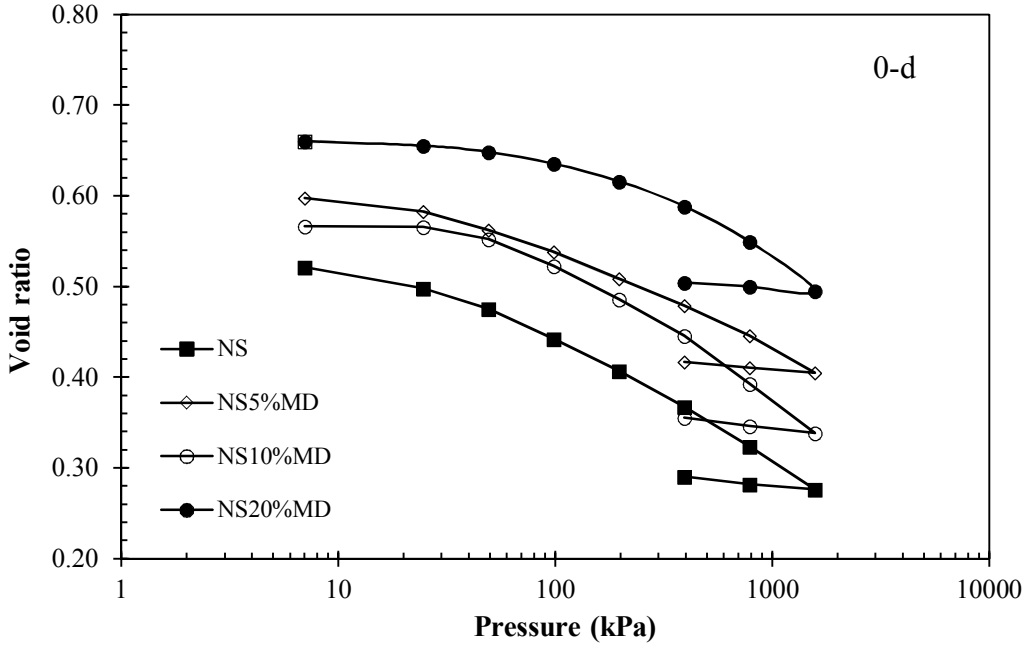

(a)

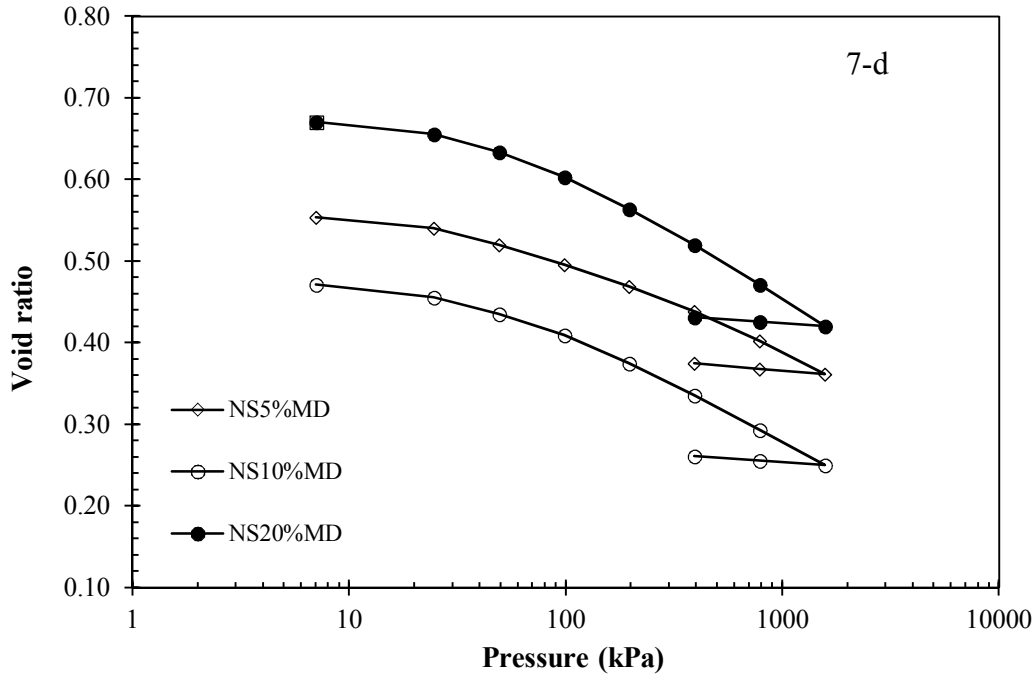

(b)

Figure 4.20. Consolidation curves of MD group due to curing period of (a) 0 day, (b) 7 days, (c) 28 days and (d) 90 days.

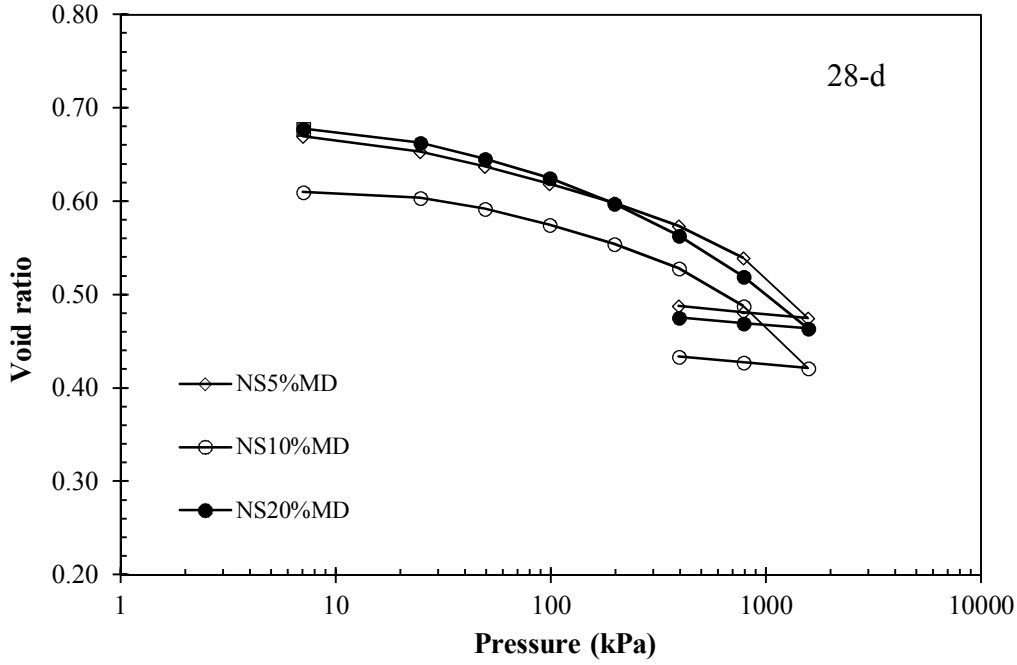

(c)

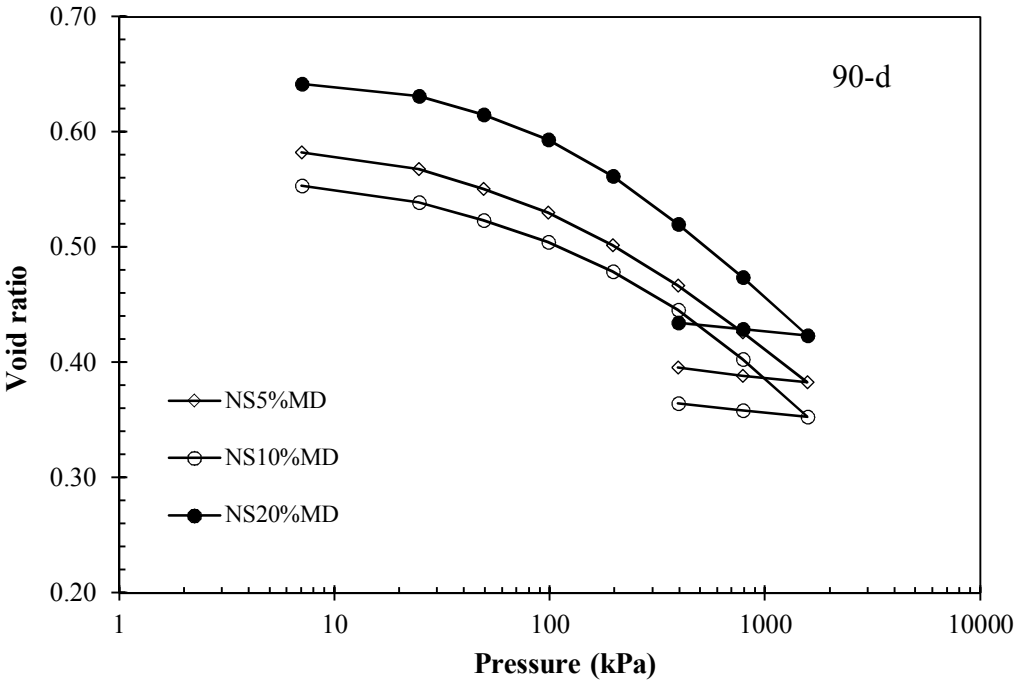

(d)

Figure 4.20. (Cont.)

Table 4.9. Compressibility parameters of the soil groups.

Curing time	Parameter	NS	MP			MD		
			5%	10%	20%	5%	10%	20%
0-day	C_c	0.133	0.104	0.122	0.110	0.110	0.133	0.136
	C_r	0.028	0.023	0.023	0.020	0.020	0.020	0.017
	p_s' (kPa)	-	32	18	14	-	-	-
7-day	C_c	-	0.112	0.107	0.122	0.114	0.134	0.158
	C_r	-	0.025	0.022	0.023	0.023	0.020	0.020
	p_s' (kPa)	-	16	25	-	-	-	-
28-day	C_c	-	0.113	0.108	0.168	0.126	0.189	0.196
	C_r	-	0.027	0.027	0.029	0.027	0.025	0.020
	p_s' (kPa)	-	14	27	-	8	-	-
90-day	C_c	-	0.114	0.100	0.110	0.129	0.150	0.147
	C_r	-	0.027	0.025	0.025	0.027	0.022	0.025
	p_s' (kPa)	-	13	15	15	8	-	-

Examining the parameters in Table 4.9, 10% MP gives the best result in compression index after 90 days of curing instigating a reduction of 25% with respect to NS. 10% MP also displays a steady reduction in the compressibility with curing time, whereas in the MD group there is an erratic behavior of the compressibility, yielding the best value for 5% MD within 90 days, which is only 3% reduced with respect to NS. The rebound index, however remained almost the same at 90-day curing period for all the specimens.

Based on the experimental findings, evidently the best combinations of marble waste with the soil mixture are NS10%MP and NS5%MD, giving the best results in the volume change characteristics. Therefore, the saturated hydraulic conductivity values were calculated for these material combinations using one-dimensional consolidation data and the results are given in Table 4.10. The saturated hydraulic conductivity values obtained are well below the regulatory limit of 1×10^{-7} cm/s for all ranges of effective confining pressures, reducing with the increasing pressures and curing times. The NS5%MD specimen has yielded lower values than the NS10%MP specimen.

Table 4.10. Saturated hydraulic conductivity results.

Curing time		k_{sat} (cm/s)			
		98-196 (kPa)	196-392 (kPa)	392-784 (kPa)	784-1568 (kPa)
0-day	**NS**	4.97×10^{-8}	2.82×10^{-8}	1.60×10^{-8}	9.01×10^{-9}
	NS10%MP	5.70×10^{-8}	5.78×10^{-8}	1.84×10^{-8}	1.13×10^{-8}
	NS5%MD	3.74×10^{-8}	2.20×10^{-8}	1.20×10^{-8}	7.05×10^{-9}
90-day	**NS10%MP**	6.30×10^{-8}	3.81×10^{-8}	2.08×10^{-8}	1.23×10^{-8}
	NS5%MD	5.03×10^{-8}	3.09×10^{-8}	1.91×10^{-8}	1.28×10^{-8}

4.3.4 Strength Properties

4.3.4.1 Unconfined Compression Test Results

Unconfined compression tests were performed for MP and MD groups at different aging periods, and the results of unconfined compressive strength versus failure strain are displayed in the form of bar charts in Figure 4.21. In MP group, it is observed that 5% and 10% MP added specimens have higher UCS than 20% MP included samples at all curing periods. UCS of NS is 245 kPa, which increased to 346 kPa and 384 kPa after inclusion of 5% and 10% MP respectively, whereas it decreased to 187 kPa with the usage of 20% MP dosage. Curing time has no significant effect on the treatment of UCS in MP mixtures, however there is a marked increment of strength in MD specimens with time, mainly with 5% and 20% marble inclusions. Strength of NS is raised with the marble powder addition of up to 10% and followed a decreasing trend with 20% MP addition. This can be attributed to reduction in the cohesion between marble powder and clay particles, as also stated by Gurbuz (2015). In MD added specimens, it appeared that 20% more fines added to the expansive silt led to improvement of the cohesive component which might be attributed to increased strength in 90-day cured specimens.

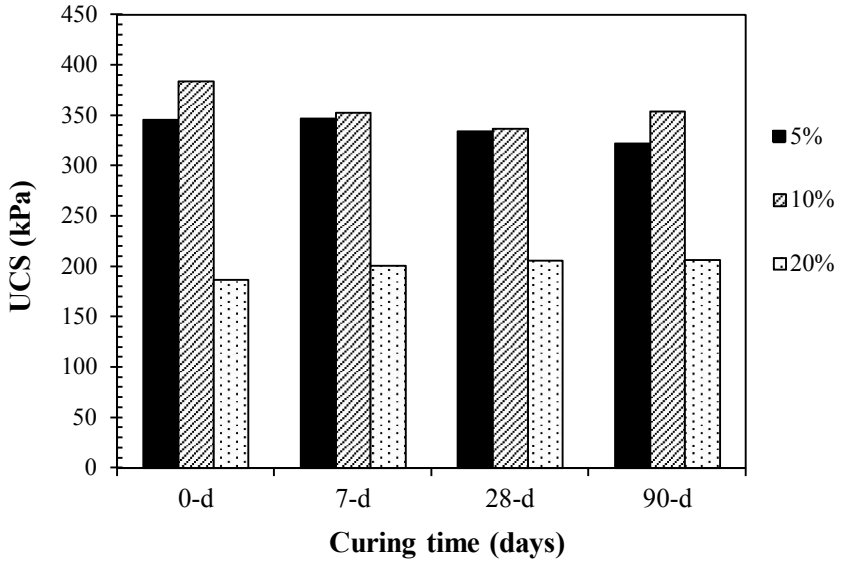

(a)

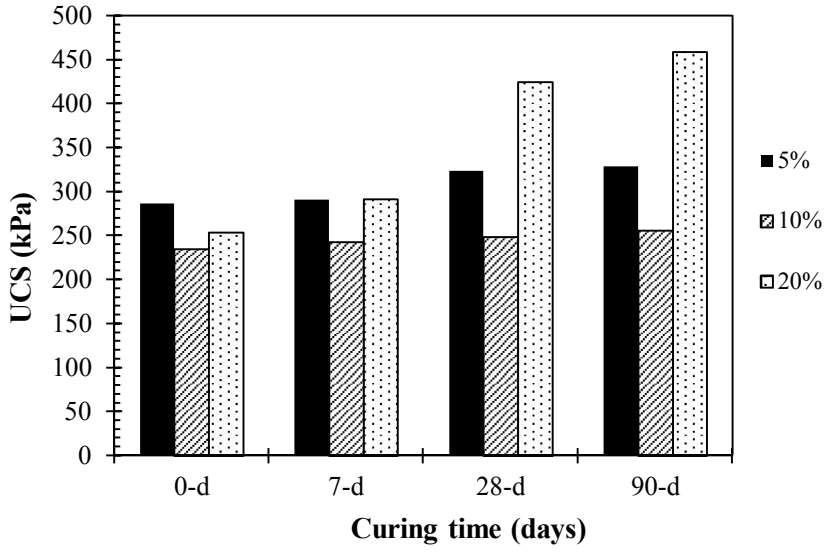

(b)

Figure 4.21. Unconfined compressive strength results of (a) MP and (b) MD groups.

Strain at failure is an important parameter in the assessment of the ductility behavior, and they are compared with respect to curing time and marble content in Figure 4.22. In MP group, 20% marble added samples have given the highest results in all curing periods although the lowest UCS values. At 5% and 10% MP dosages, a similar trend is observed whereas failure strain values reduced with the increase of aging. Unfortunately, the highest UCS and failure strain values have not been observed with

the same marble content. On the other hand, failure strain indicate a decreasing trend with the increment of marble content and curing time in MD group. It is also noted that the UCS and failure strain results of MD are more consistent than the results of MP. Addition of 5% MD reached the highest UCS and failure strain values.

The secant modulus (detailed definition is given in Section 3.3.4.1) of NS and waste marble added soil groups are presented in Table 4.11. These values are calculated for 0-day and 90-day cured samples in order to observe influence of aging on the stiffness of material. The test results showed that the stiffness of waste marble added soils increased with the increment of curing time and the material became stiffer due to the pozzolanic reaction.

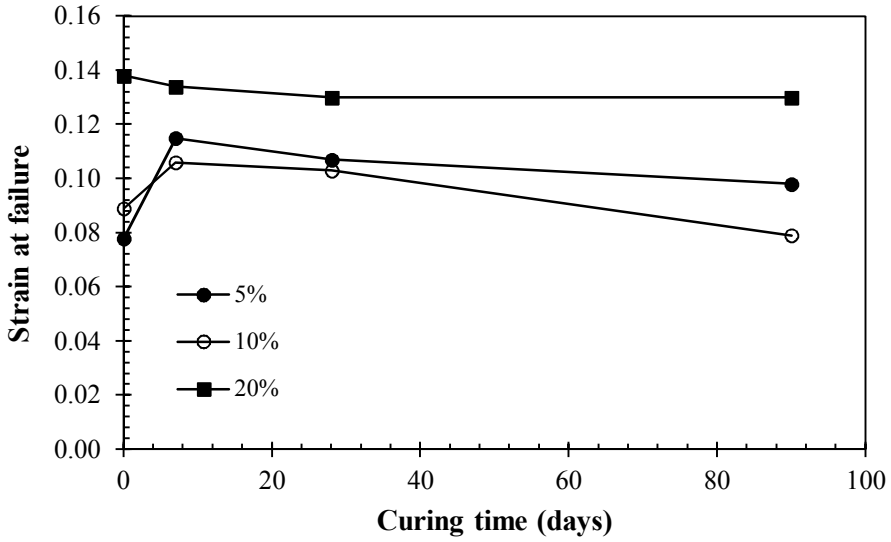

(a)

Figure 4.22. Strain at failure results of (a) MP and (b) MD groups.

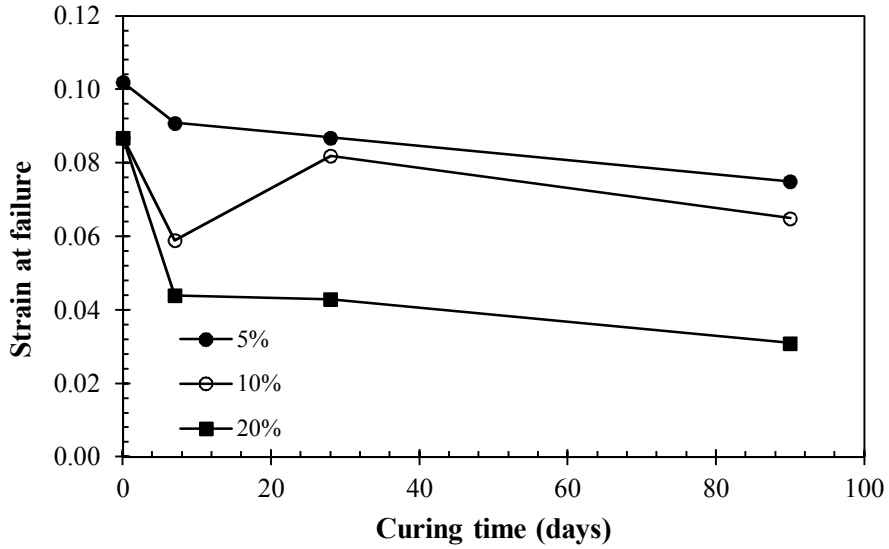

(b)

Figure 4.22. (Cont.)

Table 4.11. Secant modulus (E_{50}) results.

	E_{50} (kPa)	
Material	**0-d**	**90-d**
NS	5169	-
NS5%MP	6654	9758
NS10%MP	8000	8178
NS20%MP	1798	3044
NS5%MD	3596	11786
NS10%MD	3456	9846
NS20%MD	3850	18254

4.3.4.2 Flexural Strength Test Results

Flexural strength tests carried out for all soil groups with different curing times and load-deflection curves are presented in Figure 4.23 and Figure 4.24. Flexural strengths were calculated by inserting the flexural loads in Equation 2.1.

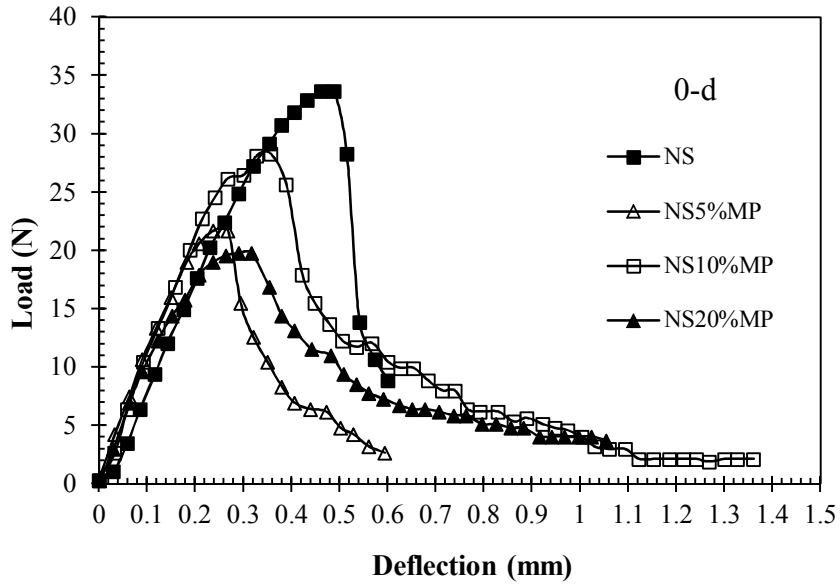

(a)

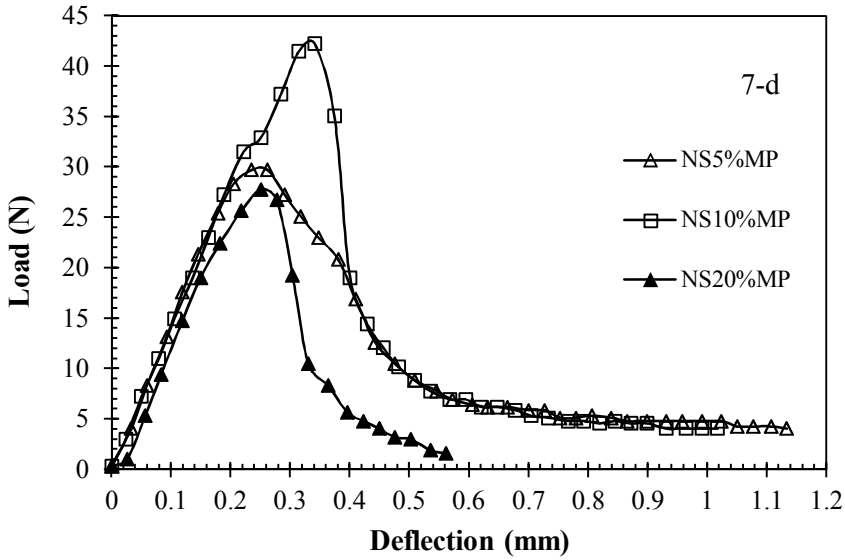

(b)

Figure 4.23. Load-deflection curves of MP for (a) 0-day, (b) 7-day, (c) 28-day and (d) 90-day samples

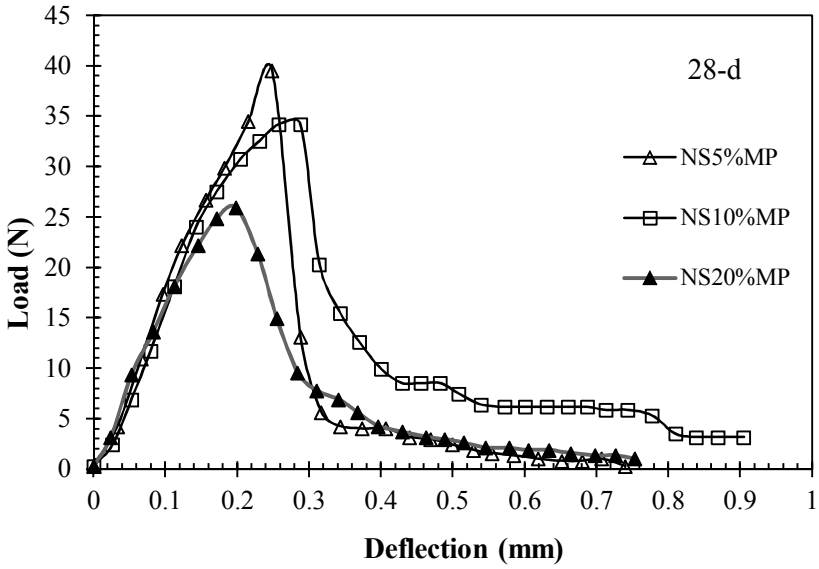

(c)

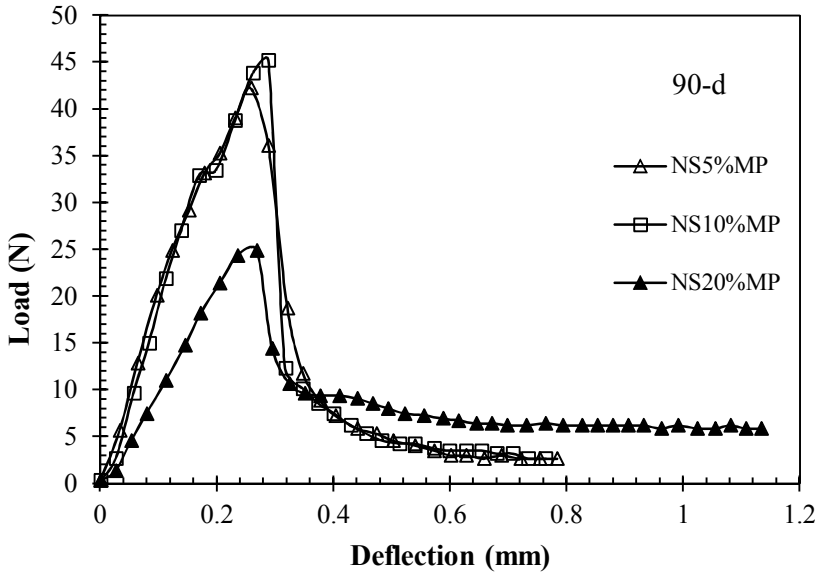

(d)

Figure 4.23. (Cont.)

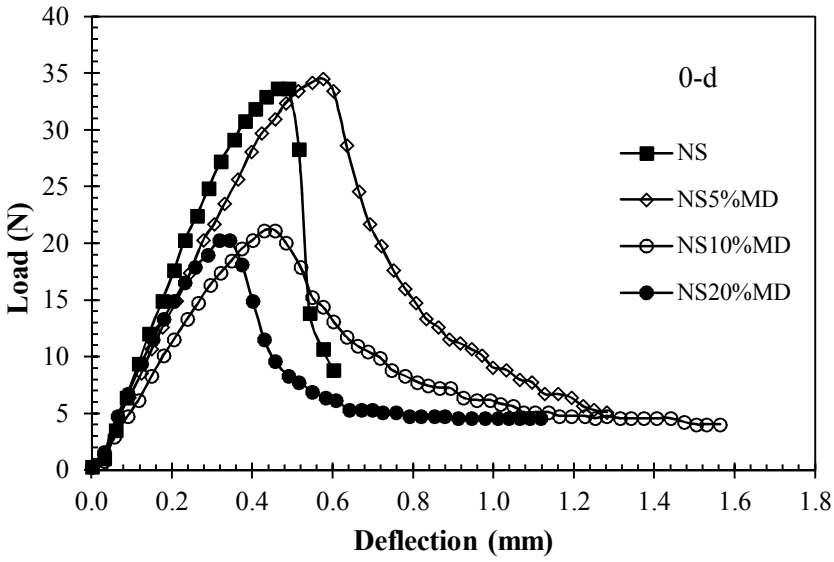

(a)

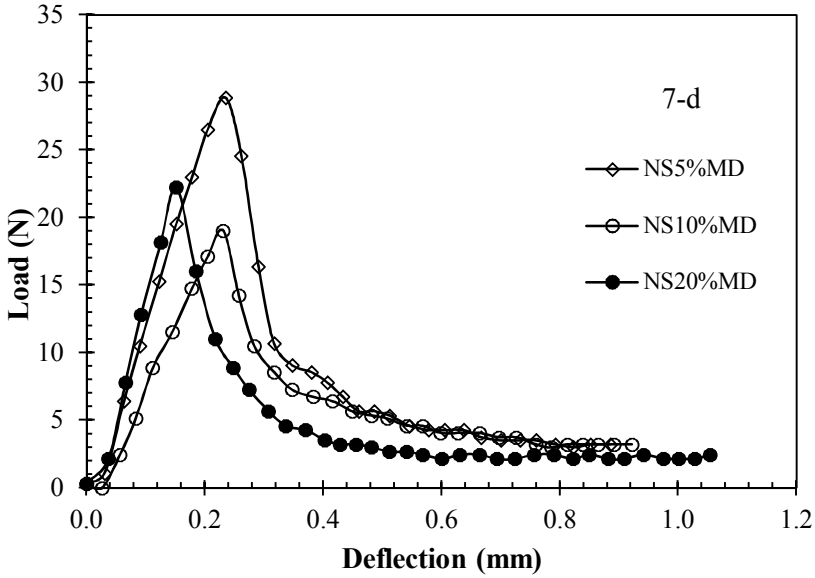

(b)

Figure 4.24. Load-deflection curves of MD for (a) 0-day, (b) 7-day, (c) 28-day and (d) 90-day samples.

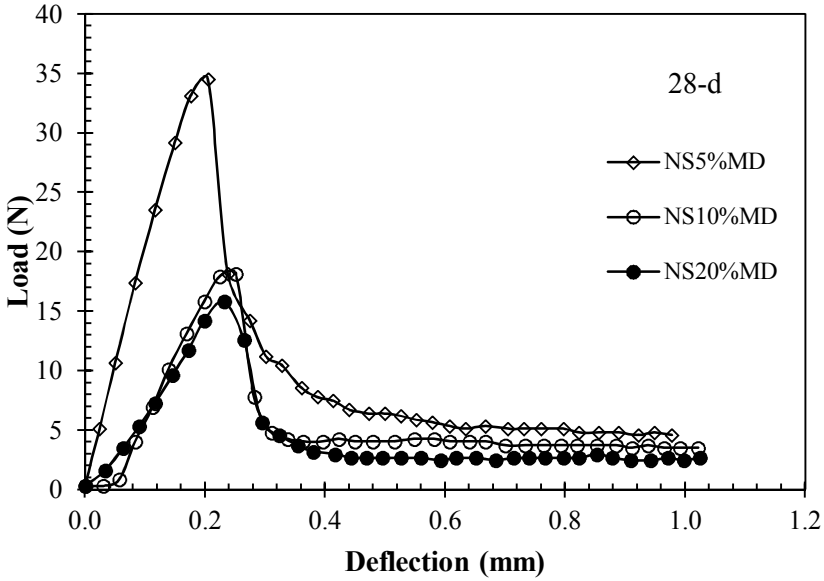

(c)

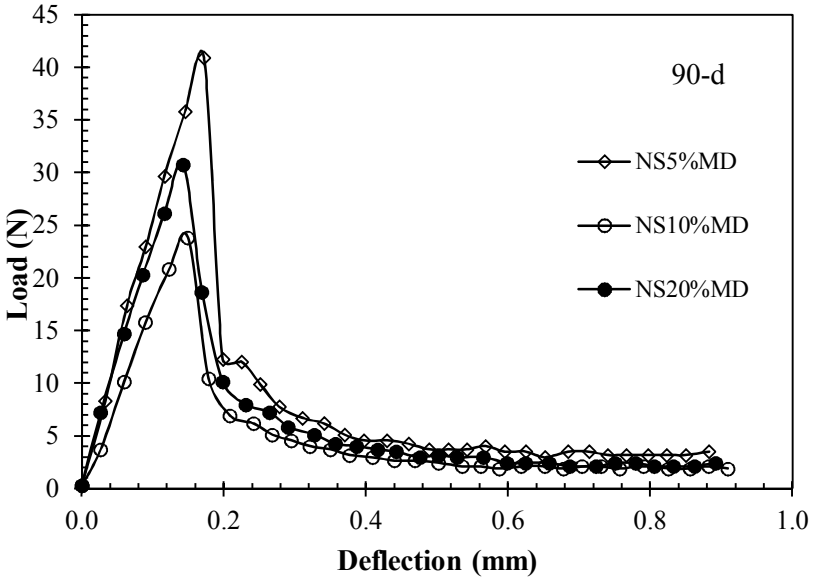

(d)

Figure 4.24. (Cont.)

Flexural strength, deflection and toughness values are summarized in Table 4.12 for NS, NSMP and NSMD soil groups.

Table 4.12. Flexural strength parameters.

Curing time	Flexural parameters	NS	MP			MD		
			5%	10%	20%	5%	10%	20%
0-day	f (kPa)	79	51	66	46	81	50	48
	ΔH (mm)	0.49	0.27	0.36	0.32	0.58	0.47	0.34
	T (Nmm)	11	6	13	8	12	8	7
7-day	f (kPa)	-	70	99	65	68	45	52
	ΔH (mm)	-	0.26	0.34	0.25	0.24	0.23	0.15
	T (Nmm)	-	10	12	7	7	5	4
28-day	f (kPa)	-	93	80	70	85	43	57
	ΔH (mm)	-	0.25	0.29	0.20	0.21	0.25	0.28
	T (Nmm)	-	7	10	7	7	4	5
90-day	f (kPa)	-	99	106	58	96	56	72
	ΔH(mm)	-	0.26	0.29	0.27	0.17	0.15	0.14
	T (Nmm)	-	9	10	7	7	4	5

f: Flexural strength, ΔH: Deflection, T: Toughness

Flexural strength showed an increasing trend while the deflection at failure decreased with the curing time in MP and MD groups. In addition, toughness reduced with aging for both MP and MD groups. In MP group, 10% inclusion has given the best results for all of the parameters, whereas in MD group 5% addition provided the highest flexural strength in all curing periods. Therefore, it was concluded that while aging has enhanced the flexural strength, ductility and toughness have decreased, displaying a brittle behavior under tension, similar to findings of Chinkulkijniwat and Horpibulsuk (2012) and Kampala and Horpibulsuk (2013). The significant increment of flexural strength was obtained within 90-day curing period for all soil combinations. The increment in flexural strength is 94%, 50% and 52% for NS5%MP, NS10%MP and NS20%MP samples respectively. In addition, the same behavior is observed in MD group for which flexural strength of NS5%MD, NS10%MD and NS20%MD is increased by 50%, 32% and 57% respectively.

Relationships between swell potential and flexural strength presented in Figure 4.25

for MP and MD groups indicate that flexural strength is indirectly proportional to swell potential. In the 10% optimum MP included mixture, 50% increment in flexural strength resulted in 55% reduction in swell potential over the 90-day curing period. Conversely, while the flexural strength of 5% optimum MD included mixture has increased by 50%, swell potential decreased by 65%. The latter reduction is appreciably larger due to higher content of finer particles in MD, with higher surface area, hence more reactive during aging period.

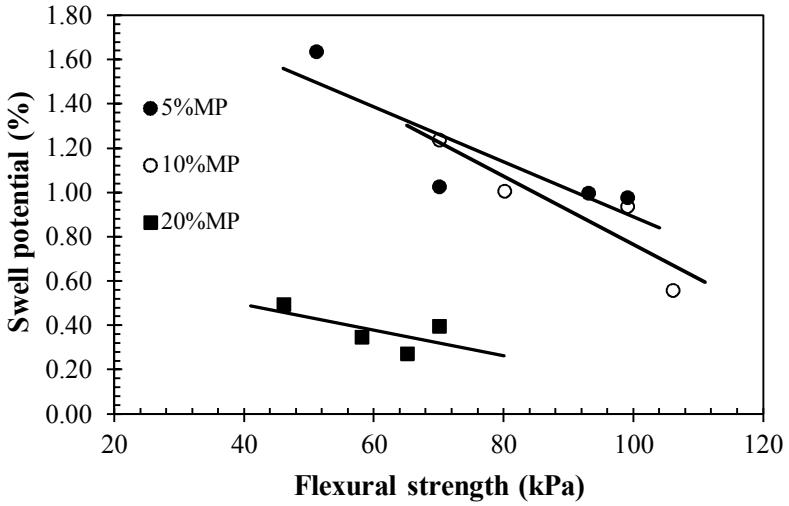

(a)

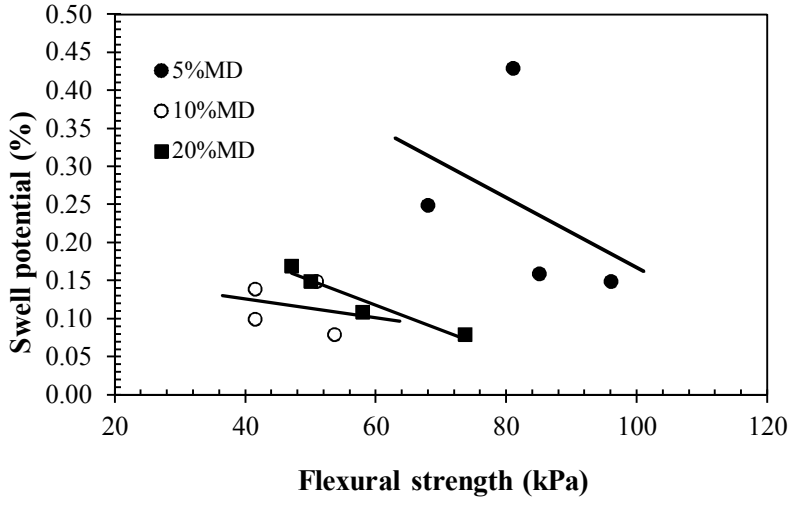

(b)

Figure 4.25. Relationship between swell potential and flexural strength of (a) MP and (b) MD groups.

4.4 Conclusions

An experimental program was undertaken to study the efficacy of two types of waste marble addition to sand stabilized expansive soil for further enhancement of the physical properties, volume change and flexural strength characteristics. Conclusions derived from the experimental findings are summarized below:

1) Utilization of 10% MP and 5% MD were observed to provide the best improvement in reducing swell percentage, by 66% and 61% respectively in 90 days. However, the swell potential of MD group is about 75% less than the MP group at 0-day which remained almost the same after 90 days curing.

2) Lower volumetric shrinkage strains were obtained with the addition of 10% MP and 5% MD within each curing period. However 5% MD displayed better results and lower shrink-swell index.

3) On the basis of compressibility results, inclusion of 10% MP and 5% MD have given the lowest results for all of the curing times, the lowest compression index being recorded for 10% MP inclusion.

4) Hydraulic conductivity values are observed to be well below the regulatory limit for both 10%MP and 5% MD specimens under different pressure ranges and within all curing time periods.

5) Addition of 10% MP and 5% MD provided the highest flexural strength values for all curing times, whereas toughness is observed to have reduced slightly with the addition of marble, the specimens becoming more brittle.

6) A linear relationship was observed between swell potential and flexural strength, over 90-day curing period, swell potential decreasing with the increasing flexural strength and aging. These correlation might be utilized for preliminary predictions of material behavior.

Chapter 5

DURABILITY ANALYSIS

5.1 Introduction

Seasonal changes cause moisture variations of soil water, increasing in the wet season and decreasing in the dry season. Evaporation of soil water during drying period causes volume shrinkage and desiccation cracks to occur. Swelling and shrinkage are the most important parameters in the investigation of volume change properties of expansive soils. Several factors affect shrinkage and cracking such as clay mineralogy, clay content, compaction conditions, temperature changes, cyclic wetting and drying, soil particle orientation, moisture and density conditions. Temperature changes have great impact on the behavior of compacted soil, mainly when landfill barrier materials are subjected to elevated temperatures due to bio-chemical reactions of the waste contained. Past research has indicated that engineering properties vary due to thermally induced changes in the micro structure. For the purpose of investigating the climatic (wetting-drying) and environmental (elevated temperatures in the landfill containment) effects on the durability and the stability of the soil mixtures, a testing program was conducted. Literature review on these effects, results and discussions of the experimental program are given in this chapter. Next section gives a brief literature information on the shrinkage component which is more detrimental than swelling, due to possible crack formations and loss of structural integrity, mainly in landfill barriers, resulting in increased hydraulic conductivity during desiccation.

5.2 Shrinkage

Fine-grained soils are more susceptible to shrinkage and crack development than coarse-grained soils (Daniel and Wu, 1993; Yeşiller et al., 2000; Mitchell and Soga, 2005; Taha and Taha, 2011). Some authors recommended the use of coarse-grained materials that would decrease swell-shrink potential and hydraulic conductivity. DeJong and Warkentin (1965), Kleppe and Olson (1985) and Daniel and Wu (1993) indicated that addition of sand to clayey soils can reduce the amount of shrinkage and cracking. DeJong and Warkentin (1965) observed that shrinkage is directly proportional to clay content, and that minor or no shrinkage occurs in specimens with less than 3% clay. Kleppe and Olson (1985) performed shrinkage tests on highly plastic clay and sand with clay contents varying between 12 to 100%, and observed that shrinkage strain is directly dependent on clay content as well as compaction water content, but was independent of the compactive effort. Daniel and Wu (1993) also reported that shrinkage decreased at low compaction water content, and higher compactive effort. Albretch and Benson (2001) stated that the volumetric shrinkage strain experienced by compacted natural clays during desiccation is directly proportional to the volume of water/volume of soil at the saturated state. Soil properties and compaction conditions are the two factors which affect the amount of water held in the soil. Soils containing higher clay fraction, hence higher plasticity index are more susceptible to large volumetric shrinkage strains during desiccation. However, specimens compacted near optimum water content and with higher compactive effort experience lower volumetric shrinkage strains due to lower water/unit volume in saturated state. Similarly, Osinubi and Eberemu (2010) observed the increase in volumetric shrinkage strain with increasing moulding water content and compactive effort in stabilization of lateritic soil using blast furnace slag. It was also observed that

on the wet side of the optimum water content, the volumetric shrinkage strain increased and vice versa towards the dry side. Consequently, increase of compaction energy caused increase of initial degree of saturation, hence the volumetric shrinkage strain, regardless of the slag content.

5.3 Cyclic Swell-Shrink

In the literature, several researchers studied the influence of the wetting and drying cycles on the swelling potential of clays. Warkentin and Bozozuk (1961), Chen (1965), Chu and Mou (1973), Chen et al. (1985), Chen and Ma (1987), Rao and Satyadas (1987), Dif and Bluemel (1991), Al-Homoud et al. (1995) deduced that clay samples showed a fatigue behavior after each wetting and drying cycle, therefore swelling ability is reduced. Dif and Bluemel (1991) indicated that the fatigue of expansive soils depends on three factors which include the clay mineral type, deterioration of clay structure due to particle reorientations and the lateral confinement loss when cracks occur. On the other hand, some researchers determined converse opinion about cyclic swelling. Nordquist and Bauman (1967), Obermier (1973), Popescu (1980), Osipov et al. (1987) and Day (1994) concluded that the swelling potential increases with the number of wetting and drying cycles, which eventually reaches an equilibrium state. According to Popescu (1980) the equilibrium state is reached after the fifth cycle. Abouleid (1985) observed the equilibrium cycle range after at least three or four cycles. Al-Homoud et al. (1995) recorded that the change of swelling completed between the fourth and fifth cycles. Bilsel and Tuncer (1998) stated that a considerable increment in swell was observed at the end of fourth cycle.

Influence of aging (7, 15, 30 and 90 days) on the swelling potential and cyclic swell-shrink of expansive soil was examined by Rao and Tripathy (2003) and deduced that

aging caused a reduction in the swelling potential. According to this study, the cyclic swell-shrink eliminated the effect of aging when subjected to higher strains. However, aging was found to be effective at lower shrinkage strains. Rao et al. (2001) studied the effect of wetting and drying cycles on the swelling character of ash-modified soils and lime-treated black cotton soils by performing four cycles. They stated that the effectiveness of lime partially disappeared after 4 cycles of wetting and drying in lime-treated black cotton soils which caused disruption of the cemented aggregates. Swelling behavior of lime-stabilized soils after wetting-drying cycles was studied by Guney et al. (2007). They tested three types of soils with untreated and treated (3% and 6% lime) conditions and concluded that the swelling potential of untreated soils reduced and the equilibrium was achieved after 4-6 cycles. Lime stabilization caused partial destruction of inter-particle cementation during wetting-drying cycles, therefore lime-stabilized soils were not recommended in the presence of climatic influences. Conversely, Akcanca and Aytekin (2012) studied sand-bentonite mixture in the form of unstabilized and lime stabilized soil groups exposed to 5 wetting-drying cycles. They found that swelling pressures of sand-bentonite mixtures were decreased with the addition of lime, and suggested utilization of lime treated sand-bentonite mixtures in the sanitary landfill liners which were prone to wetting-drying cycles. Estabragh et al. (2013) compared the effect of wetting-drying cycles on the swelling potential of untreated and stabilized soils. Lime, cement and coal ash were used as stabilizing agents and they were added to the soil with various amounts. Test results showed that the swelling potential of untreated soil, lime and cement stabilized soils were decreased with the increment of wetting and drying cycles. On the contrary, a reverse effect was observed in the coal ash stabilized soils. Equilibrium condition was achieved in five cycles.

Influence of silica fume modification on the swelling behavior during cyclic swell-shrink test was investigated by Kalkan (2011). Swelling pressure and swelling potential were reduced with the increment of wetting-drying cycles for the untreated and silica fume treated soils and the equilibrium state was obtained at the fifth cycle. The gradual destruction of clay structure caused by cyclic swelling-shrinking reduced the swelling potential which led to disorientation and reconstruction of the structural elements of the large microaggregates.

Yazdandoust and Yasrobi (2010) evaluated untreated and non-ionic polymer treated expansive soils subjected to wetting-drying cycles and concluded that all of the samples reached the equilibrium after four cycles. They stated that the efficacy of polymer stabilization was conserved during cyclic wetting-drying and also suggested polymer utilization in the treatment of expansive soils.

Effect of wetting-drying cycles on desiccation cracking of soil was examined by Yeşiller et al. (2000) and deduced that there was no remarkable change in the amount of cracking after the second cycle. Also, Tang et al. (2016) studied the desiccation cracking in five cycles. They observed that the second cycle caused an important rearrangement of soil particles and improvement of pore system during this phase "rapid clods slaking phenomenon" was observed which is caused by softening of bonds between particles, instigating differential swelling pressures and entrapped pore air. Upon rewetting the original cracks were closed, giving rise to inception of large amount of new micro cracks on soil surface, enhancing an aggregated structure and therefore increased soil heterogeneity. After the second wetting-drying cycle, the number of crack segments per unit area reached the highest amount.

Akcanca and Aytekin (2014) pointed out that addition of lime to sand-bentonite mixture causes a reduction in the hydraulic conductivity with wetting and drying cycles. They compared the hydraulic conductivity values of sand-bentonite mixtures with and without lime, and concluded that lime treated sand bentonite mixture can be more suitable in liner construction.

Various procedures were implemented for drying process of the soil samples. Desiccating soil specimens by air drying under sunshine or room temperature were studied by Day (1994), Al-Homoud et al. (1995) and Basma et al. (1996), Albretch and Benson (2001), Guney et al. (2007), Kalkan (2011), Widomski et al. (2015). Dif and Bluemel (1991) performed the desiccation process by air drying under the surcharge pressures of 2-4 kPa. Rao and Satyadas (1987) and Tripathy et al. (2002) provided the intended temperature around the oedometer cell for each drying stage. Also, cyclic swell-shrink tests were carried out by using modified fixed ring oedometer cell with 50 kPa surcharge pressure and each shrinkage cycle was done under a temperature of 40 ± 5°C (Tripathy and Rao, 2009). Drying temperature was used at 35 ± 5°C in the studies of Akcanca and Aytekin (2012) and Akcanca and Aytekin (2014).

5.3.1 Cyclic Swell-Shrink Tests

In this study, 28-day cured samples of NS and NZ were selected for performing cyclic swell-shrink test. Compacted soil samples of NS and NZ were prepared by using standard Proctor energy (ASTM D698-12e2) in their optimum water content and maximum dry densities with the dimensions of 75 mm diameter and 15 mm height. These specimens were wrapped carefully with nylon membranes and stored in a desiccator for 28 days. When 28 days curing period completed, one-dimensional swell tests (ASTM D4546-14) were started in a temperature controlled room (25°C).

Swelling tests were done under 7 kPa surcharge pressure and the dial gauge readings were taken every day. When the readings showed a constant value and observed no further tendency to swell, the soil specimens were taken out from the oedometer cell and the water was drained. The wet specimens were let to air dry in a 25°C temperature controlled room, with no surcharge (Figure 5.1 (a)). This method was in good agreement with Day (1994), Al-Homoud et al. (1995) and Basma et al. (1996), Guney et al. (2007), Kalkan (2011). The mass of soil specimens were weighed at different time intervals until constant values were achieved. Dimensions of the soil samples (diameter and height) were measured at each time interval. After completion of drying period, the same soil samples were placed in the consolidometers for the subsequent swelling cycle. This procedure was repeated 7 and 8 times for NS and NZ samples respectively, in order to observe the effect of wetting and drying cycles on the swell-shrink behavior.

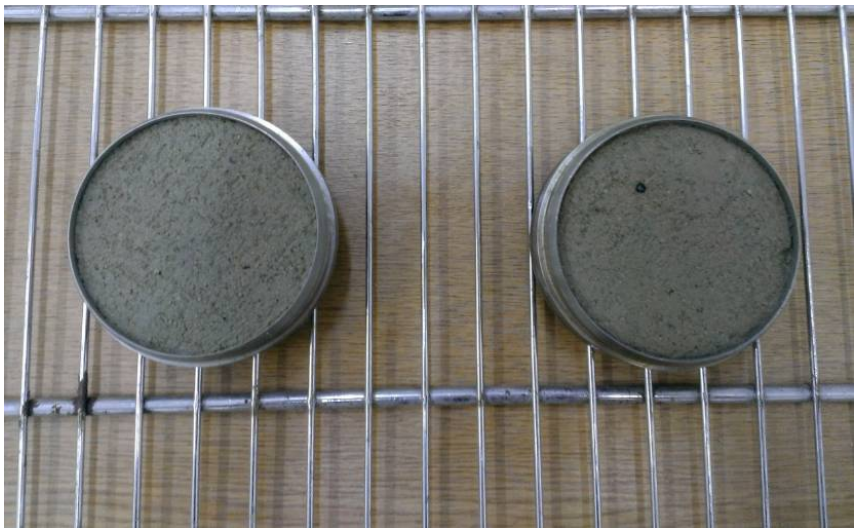

(a)

Figure 5.1. Specimen (a) at the start of drying period, (b) at the end of drying period.

(b)

Figure 5.1. (Cont.)

5.3.2 Experimental Results and Discussions

Cyclic swell-shrink test results are presented in Figure 5.2 and Figure 5.3 for NS (28-d) and NZ (28-d) samples respectively. It can be seen from Figure 5.2 that the highest swell and shrinkage values were recorded at the 2nd cycle for NS sample after which the swell strain showed a decreasing trend. Addition of sand or low-plastic materials to the expansive soil causes an interaction between particles and swelling reduces (Kalkan, 2011). The significant reduction in both swell potential and axial shrinkage were obtained after the 5th cycle, which is consistent with the findings of Al-Homoud et al. (1995). Swell potential results of 6th and 7th cycles were lower than the result of 1st cycle and are quite close to each other. From these results one can interpret that equilibrium state has been reached after the 5th cycle for NS specimens.

In NZ samples, there is a tendency for decreasing in both swell potential and axial shrinkage after the 5th cycle and 63% and 67% reduction in swelling and shrinkage respectively were obtained at the 8th cycle. Zeolite contains high amount of silica, therefore has a pozzolanic character which was explained in Chapter 3. Pozzolanic

reaction takes place between expansive soil and zeolite and this reaction leads to binding of particles, and the texture of soil mixture becoming more granular. The binding particles form cementation in the soil and this process causes the reduction in the swelling ability (Estabragh et al., 2013). This behavior was observed after the 5th cycle in NZ mixture and it can be stated that NZ samples reached the equilibrium at the 5th cycle.

As a result, swelling potential and axial shrinkage decreased with the increment of wetting-drying cycles in both NS and NZ samples. The biggest change in axial strain (both swell and shrinkage) occurred at the 7th cycle for NS (28-d) and the 8th cycle for NZ (28-d).

The surface deformation of soil specimens due to wetting-drying cycles were presented in Figure 5.4 and 5.5 for NS and NZ groups respectively. Images of first cycle (at the beginning), 5th cycle (equilibrium) and last cycle were given in order to show the impact of wetting-drying cycles on the soil samples. More cracks and deformation were observed in the NZ samples.

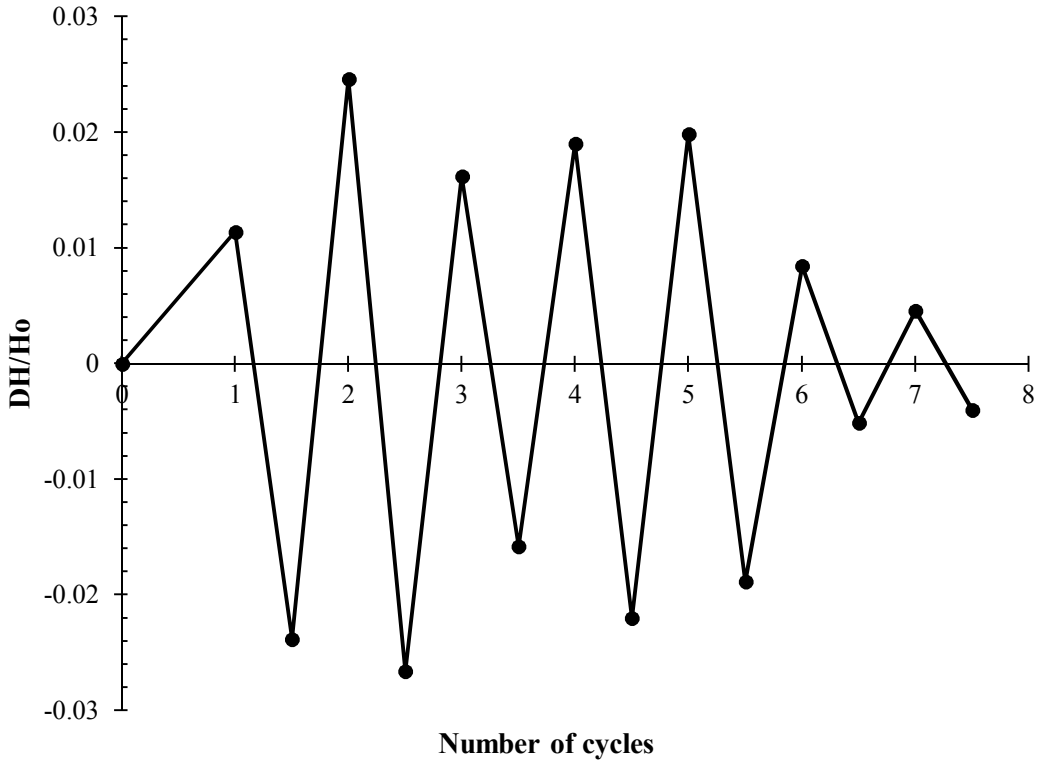

Figure 5.2. Variation of axial strain due to wetting-drying cycles of NS (28-d).

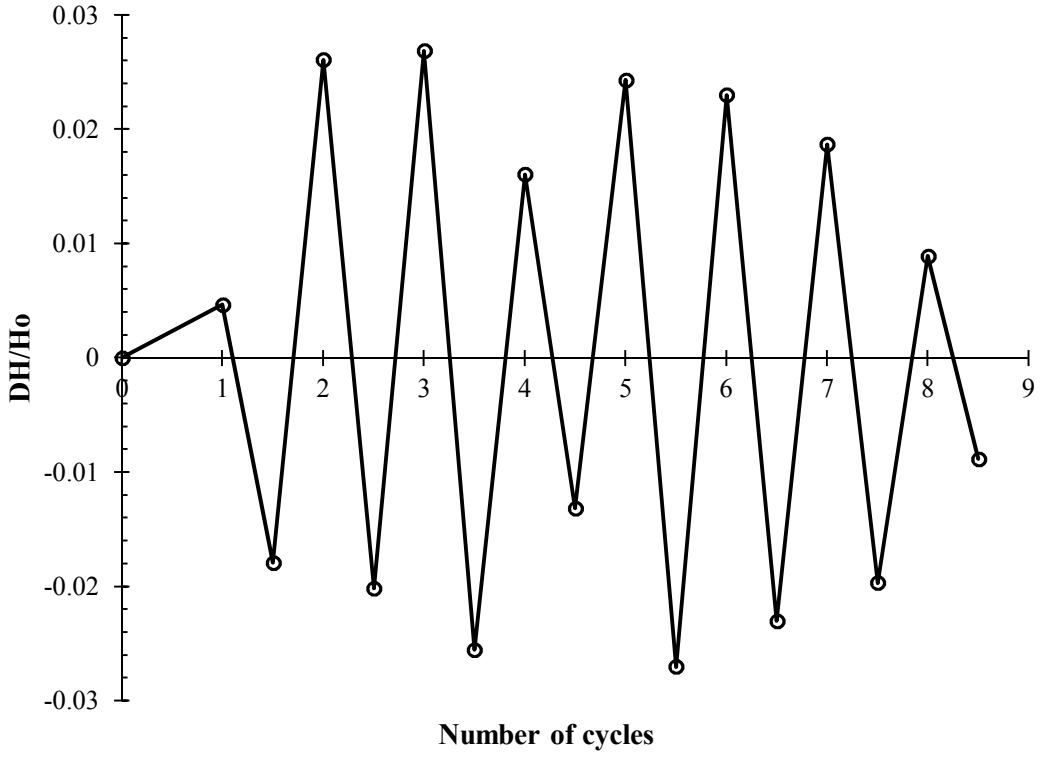

Figure 5.3. Variation of axial strain due to wetting-drying cycles of NZ (28-d).

(a)

(b)

(c)

Figure 5.4. NS sample (a) after 1st cycle drying, (b) after 5th cycle drying and (c) after 7th cycle drying.

(a)

(b)

(c)

Figure 5.5. NZ sample (a) after 1st cycle drying, (b) after 5th cycle drying and (c) after 8th cycle drying.

5.4 Influence of Temperature on Swell and Consolidation

Lloret and Villar (2007) stated that the swelling capacity of compacted bentonite

reduced with temperature from 30°C to 80°C, which could be explained with the effect of temperature on water affinity. Hence decrease of swelling pressure was observed as a function of temperature. Romero et al. (2005) investigated the swelling strain of bentonite with a temperature range of 30°C to 80°C and observed that first heating caused an irreversible change in the clay macrostructure due to aggregate volume changes. This could be explained by the aggregate thermal expansion as well as the structural disturbance of the interlayer water lattice in smectitic clays, causing aggregate contraction due to grouping of packs of flakes, and favoring the transition from adsorbed water to free water. Furthermore they have concluded that with elevated temperatures, two reverse mechanisms occur at aggregate scale which are volume increase caused by thermal expansion of mineral particles and adsorbed water, and reduction in volume due to water losses in intra-aggregate.

Estabragh et al. (2016) deduced that swell parameters, which include swell potential and swell pressure are functions of temperature as well as the duration it prevails. Increment of the temperature and duration of heating is efficient for the decrease of the swelling behavior. Villar et al. (2010) studied the change of swelling pressure, swelling capacity and hydraulic conductivity at the temperature interval of 30°C to 90°C. They reported that the reduction of swelling capacity of bentonite is indistinctly with the increasing temperature while there is a marked decrease observed in swelling pressure. On the other hand, the saturated hydraulic conductivity increases with the temperature.

Shirazi et al. (2010) tested the swelling pressure by applying 20°C to 80°C and determined that swelling pressure increased with the temperature increment. A linear

relationship is observed between swelling pressure and temperature. Cho et al. (2012) evaluated the suitability of Ca-bentonite as a sealing material at elevated temperature. The swelling pressure of bentonite at different dry densities with the temperature interval of 20°C to 80°C and the test results showed that as the temperature increases swelling pressure also increases but this increment is insignificant if the maximum temperature is kept below 80°C. This can be explained by alterations of hydration, osmotic and pore water pressures with temperature elevations. In addition, hydraulic conductivity tests were carried out between 20°C and 150°C and an increasing trend is obtained with the increase of temperature.

Shariatmadari and Saeidijam (2011) performed swell test with three temperatures (25°C, 55°C and 90°C) and found that swelling reduces with the increasing temperature. Swelling decreased by 20% from 25°C to 90°C. Compressibility increased at higher temperatures. Lloret and Villar (2007) performed the compression test by applying 25°C, 40°C and 60°C temperature and found that the compressibility of bentonite increases as the temperature increases. Sultan et al. (2002) proposed an exponential expression between the temperature and the variation of preconsolidation pressure. Delage et al. (2010) observed that the compressibility of clays are independent with the variations of temperature. Kholghifard et al. (2014) performed the consolidation test on residual granitic soil with the temperatures of 27°C, 40°C and 60°C and concluded that the compression index does not depend on the temperature.

Cho et al. (1999) examined the influence of temperature on the hydraulic conductivity of compacted bentonite. They made the tests at different temperatures (20°C, 40°C, 60°C and 80°C) and found that the hydraulic conductivity increases as the temperature

increases. Hydraulic conductivity at 80°C raised up to three times of the value at 20°C. Villar and Lloret (2004) indicated that the swelling capacity of clay decreases at high temperatures yet this behavior is less evident under high vertical stresses. Similarly, a decrease in swelling pressure was also observed in relation to temperature. Conversely, the effect of temperature on permeability is small and slightly lower than what would be expected contrary to the thermal changes in water kinematic viscosity.

Abuel-Naga et al. (2005) investigated the effect of temperature on the consolidation up to 90°C and stated that the change of the preconsolidation pressure is nonlinear under thermal effect and the hydraulic conductivity of saturated soils increases with the increasing temperature. This increment is mostly occurred by the reduction of the soil viscosity with temperature. Tsutsumi and Tanaka (2012) applied 10°C and 50°C temperatures in their experiments and specified that the hydraulic conductivity of clays was vigorously dependent on temperature because the water viscosity increases as the temperature reduces. Consequently, the excess pore water pressure generated at the lower temperature was much higher than that at the higher one.

5.4.1 Temperature-Controlled Swelling and Consolidation

Variations of temperature affect the volume change behavior of swelling-shrinking soils. Therefore, three different temperatures (25°C, 40°C and 60°C) were applied to selected soil samples which are NS (28-day) and NZ (28-day). Two of one-dimensional consolidometers were modified to accomplish tests under elevated temperatures. Two fiber consolidation cells, were designed and produced in the workshop (Figure 5.6). The reason of choosing this material is due to being a light and refractory material, resistant to high temperatures, hence more suitable than metallic cells.

Figure 5.6. Fiber cell.

General view of temperature controlled oedometer system is depicted in Figure 5.7. The connection between constant temperature water bath and fiber consolidation cell provides water circulation by a small pump placed in the tank. Temperature of water in the water bath is adjusted by a thermostat to maintain a constant temperature during experiment. One-dimensional swell and consolidation tests were repeated with this system at 40°C and 60°C.

Figure 5.7. General view of temperature controlled oedometer system.

5.4.2 Test Results and Discussions

Swell potential (%) versus time (min) graphs were obtained from one-dimensional swell tests conducted at 25°C, 40°C and 60°C on 28-day cured NS and NZ soil groups, and the results are shown in Figure 5.8 and Figure 5.9. Test results are summarized in Table 5.1.

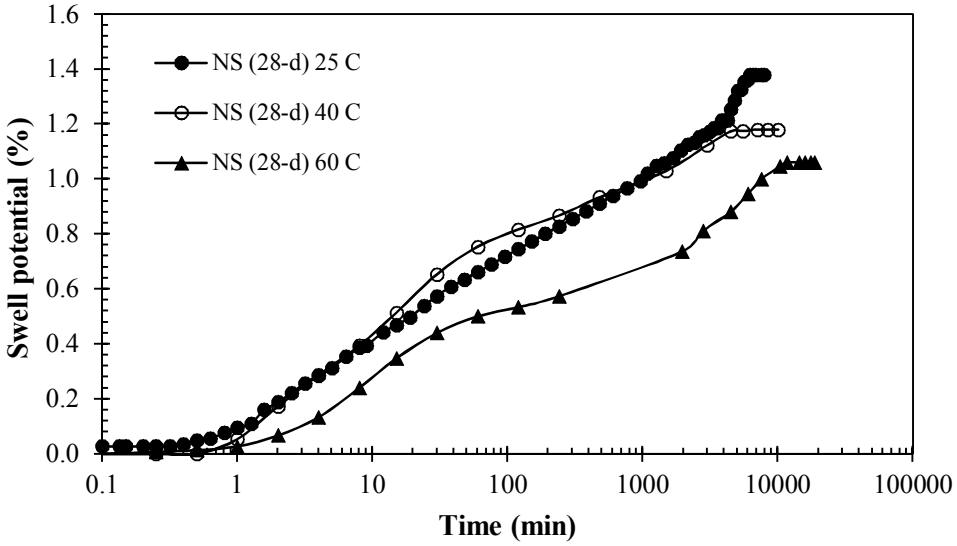

Figure 5.8. Swell curves for different temperatures of NS (28-d) soil group.

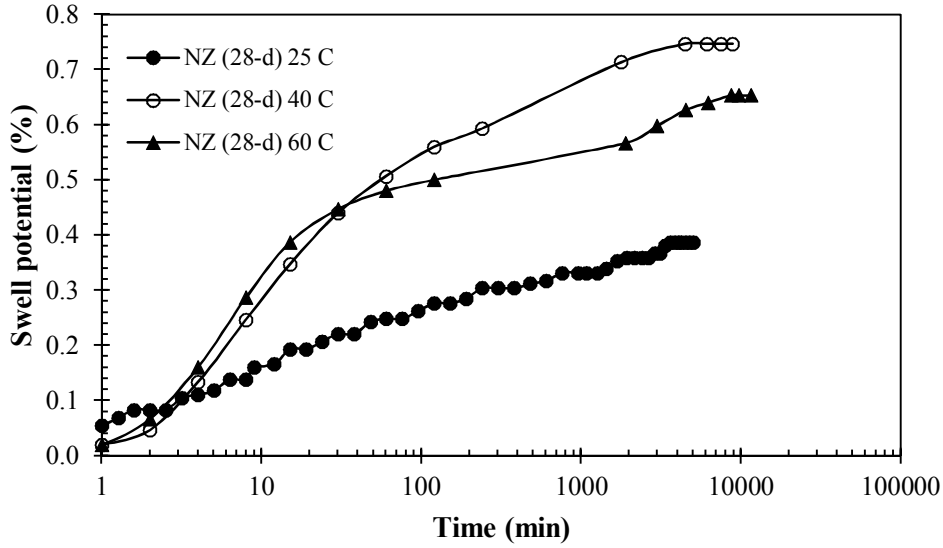

Figure 5.9. Swell curves for different temperatures of NZ (28-d) soil group.

Table 5.1. Swell test results.

	Primary swell potential (%)	Time (min)
NS (25°C)	1.20	4000
NS (40°C)	0.76	60
NS (60°C)	0.44	30
NZ (25°C)	0.38	3500
NZ (40°C)	0.48	35
NZ (60°C)	0.46	22

Swell test results showed that primary swell reduced with the increase of temperature in NS group which is also stated by Villar et al. (2004), Lloret and Villar (2007), Shariatmadari and Saeidijam (2011), Estabragh et al. (2016) however, observed a reverse behavior in NZ group. Swelling potential of NZ group increased at elevated temperatures and this behavior can be attributed to the increment of repulsion between clay platelets at micro level due to temperature increase, which can be explained by diffuse double layer (DDL) theory, hence causing increase in swelling capacity (Ye et al., 2013). Increasing temperature caused a salient decrease in the completion of primary swell time for both NS and NZ groups. The largest reduction has occurred between the temperatures of 25°C and 40°C and which continued to reduce gradually until 60°C.

Consolidation curves which are obtained from one-dimensional compressibility tests were shown in Figure 5.10 and 5.11 and the compressibility characteristics were listed in Table 5.2.

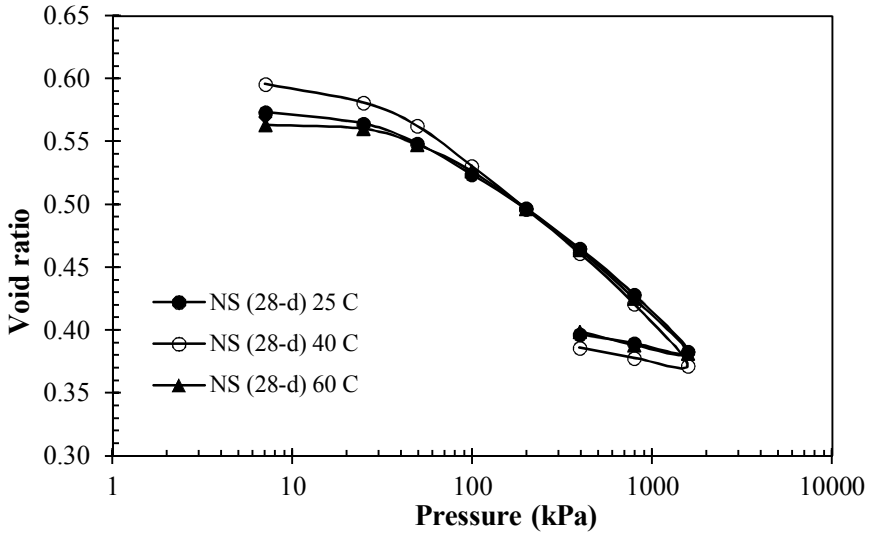

Figure 5.10. Consolidation curves at different temperatures for NS (28-d) soil group.

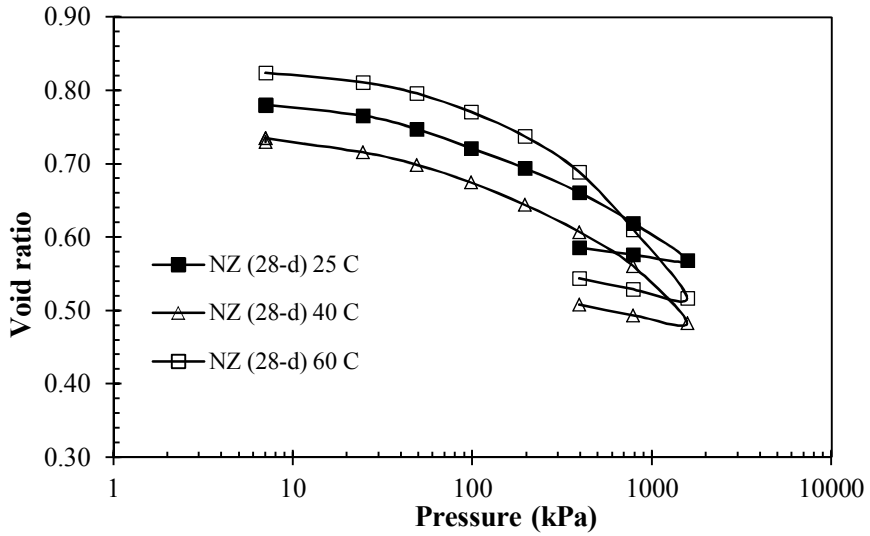

Figure 5.11. Consolidation curves at different temperatures for NZ (28-d) soil group.

Table 5.2. Compressibility characteristics of all soil groups.

Material	C_c	C_r
NS (25°C)	0.124	0.023
NS (40°C)	0.112	0.030
NS (60°C)	0.112	0.030
NZ (25°C)	0.145	0.030
NZ (40°C)	0.148	0.054
NZ (60°C)	0.128	0.025

There is no significant variation of the compression index and rebound index values with the increase of temperature and this conclusion is consistent with the findings of previous researchers (Delage et al., 2010; Kholghifard et al., 2014).

Saturated hydraulic conductivity values were calculated for different confining pressure ranges as given in Table 5.3. Hydraulic conductivity of NZ group showed an increasing trend with the increment of temperature due to the reduction of water viscosity which is agreeing with the findings of Cho et al. (1999), Abuel-Naga et al. (2005), Villar et al. (2010), Tsutsumi and Tanaka (2012) and Ye et al. (2013). However, hydraulic conductivity of NS group raised when temperature increased from 25°C to 40°C, then decreased with the application of 60°C. Therefore, a consistent behavior was not observed in NS group. However, hydraulic conductivity of NS at all temperature ranges and pressure ranges remained below the regulatory limit, whereas NZ does not satisfy this requirement at any temperature for confining pressures less than 196 kPa.

Table 5.3. Saturated hydraulic conductivity results.

	k_{sat} (cm/s)			
Soil group	**98-196 (kPa)**	**196-392 (kPa)**	**392-784 (kPa)**	**784-1568 (kPa)**
NS (25°C)	4.27×10^{-8}	2.33×10^{-8}	1.34×10^{-8}	8.77×10^{-9}
NS (40°C)	7.18×10^{-8}	4.67×10^{-8}	2.78×10^{-8}	1.45×10^{-8}
NS (60°C)	3.90×10^{-8}	2.18×10^{-8}	1.29×10^{-8}	7.67×10^{-9}
NZ (25°C)	1.44×10^{-7}	6.35×10^{-8}	4.02×10^{-8}	2.61×10^{-8}
NZ (40°C)	1.13×10^{-7}	6.89×10^{-8}	4.37×10^{-8}	3.82×10^{-8}
NZ (60°C)	1.14×10^{-7}	8.63×10^{-8}	7.07×10^{-8}	4.46×10^{-8}

5.5 Conclusions

The effect of wetting-drying cycles on swelling potential and axial shrinkage of NS

and NZ were investigated. In addition, influence of temperature on the swelling, compressibility characteristics and hydraulic conductivity of 28 days cured samples of NS and NZ were studied. Based on these test results, the following conclusions were derived.

Swelling potential and axial shrinkage were reduced with the increasing of wetting-drying cycles of both NS and NZ samples. The biggest variation of swell potential and axial shrinkage occurred at 7^{th} cycle for NS (28-d) soil specimen and 8^{th} cycle for NZ (28-d) soil sample. More cracks and deformation were observed in the NZ samples.

Primary percent swell decreased with the increase of temperature in NS group however, a reverse behavior was observed in NZ group. A marked decrease was observed in the completion of primary swell time in both NS and NZ groups. The biggest reduction has occurred between the temperatures of 25°C and 40°C. There was no significant change in the compression index and rebound index values with the increment of temperature. Hydraulic conductivity of NZ group showed an increasing trend with the increasing temperature due to the reduction of water viscosity. However, a remarkable change was not observed with the temperature increment in NS group.

Chapter 6

CONCLUSION

6.1 Conclusions

This thesis is aimed to use local soil resources together with two waste materials from construction industry and form the best combination to be utilized in the compacted form as a landfill liner. The uncovered landfill deposition and the accumulation of industrial waste are the two concerns which prompted this study. There is a major environmental degradation due to unmanaged hazardous waste storage and toxic waste piles of the abandoned copper mine in the western part of the island. The study is mainly based on selecting proportions of locally available expansive soil and beach sand, with additions of industrial waste for enhancing the mechanical properties and/or for recycling purpose. The waste additives selected are a synthetic one, pipe scrap collected from the pipe processing plant, denoted as polymeric fiber, and a non-synthetic one, marble waste from marble processing plant. A totally different material is also selected which is abundantly produced in Turkey, the zeolite (clinoptilolite). The choice of this material is aimed to investigate it as a possible barrier material with filtering capacity for its possible utilization to contain toxic wastes, such as mine waste rock or tailings.

The experimental program was undertaken in four phases. The first phase investigated the mixtures of expansive soil-sand (NS) and expansive soil-zeolite (NZ) for comparison reasons with addition of polymeric fiber (PF). The experimental results

showed that addition of an optimum amount of PF, as a reinforcing material, has been more effective in reducing swell-shrinkage potential and compressibility of NS. Saturated hydraulic conductivity values were determined to be below the regulatory limit except in NZ. Inclusion of PF has improved tensile strength significantly, by changing the brittle tensile failure to ductile behavior, and in addition a residual tensile load being maintained after failure. However, no significant improvement was recorded in the unconfined compressive strength values. Therefore, stabilization in areas of expansive soils as landfill liner or sub-base can be efficiently done using an available sand resource mixed and compacted with expansive soil, forming a stable structure, which can further be reinforced using a plastic waste locally produced. Incorporation of such materials in soil mitigation is a favorable technique, also offering an opportunity to recycling non-biodegradable wastes.

The pozzolanic activity of zeolite was not considered in phase one, for comparison reasons with sand amendment, which was not aged as well. Therefore, phase two of the experimental program studies the pozzolanic effect of zeolite on mechanical properties of the NZ mixtures. Effect of different curing periods on expansive soil-zeolite mixtures were investigated, to further understand the suitability of this material for the solution of local geo-environmental problems. The swell-shrinkage potential and compressibility were substantially reduced within the selected curing periods. The hydraulic conductivity, which is the most important parameter in landfill barrier design, remained below the regulatory limit after the curing periods. As far as strength properties are concerned, zeolite improvement enhanced the flexural strength, while had no substantial effect on unconfined compressive strength.

Third phase of this study includes the experimental work investigating the efficacy of two types of waste marble (MP and MD) addition to expansive soil-sand mixtures at different curing times. The waste marble has been effective in reducing the swell-shrinkage potential in 10% MP and 5% MD proportions. The same percentages have been effective in reducing compressibility, and hydraulic conductivity, while increasing flexural strength, with no appreciable improvement in unconfined compressive strength. However, it was also noted that the samples have become more brittle when treated with marble waste. Therefore, this treatment can only be recommended to be used under light loading, such as road sub-base material for light traffic.

In the fourth phase of the study, durability of NS and NZ mixtures was studied to investigate the climatic and environmental effects on the sustainability of the proposed materials. The climatic effect is studied in terms of cyclic swell-shrinking and the environmental effect, mainly due to temperature elevations in the landfills, is studied in swell-compressibility tests. The results of this phase revealed that cyclic swell-shrink values reduced after the fifth cycle, and that no major cracks appeared on the drying samples disrupting the integrity of the compacted specimens. The fine crack pattern appearing on NZ specimens could have been prevented had the drying tests were done under a surcharge load.

6.2 Recommendations

The recommendations and plans for future research include the following:

1. It is worthwhile to do further research on zeolite, investigating the unsaturated soil parameters, water retention capacity, shrinkage studies under different surcharges, hydraulic conductivity and diffusivity functions in the unsaturated

state.

2. Since marble waste is in abundance on the island, it is recommended to do more research on its evaluation in expansive soil stabilization, and would be better if a stronger pozzolan is also mixed with it, possibly ash of a locally available industrial waste. Its effectiveness was not very significant in this study, mainly because of its use in the presence of sand.

3. Leaching tests could be carried out mainly to compare the effectiveness of using zeolite instead of sand in containing toxic wastes, such as mine tailings.

REFERENCES

Abdi, M. R., Parsapajouh, A., & Arjomand, M. A. (2008). Effects of random fiber inclusion on consolidation, hydraulic conductivity, swelling, shrinkage limit and desiccation cracking of clays. *International Journal of Civil Engineering*, 6(4), 284-292.

Abdulla, R. S., & Majeed, N. N. (2014). Some physical properties treatment of expansive soil using marble waste powder. *International Journal of Engineering Research & Technology*. 3(1), 591-600.

Abdullah, W. S., & Alsharqi, A. S. (2011) Rehabilitation of medium expansive soil using cement treatment. *Jordan Journal of Civil Engineering*, 5(3), 343-356.

Abouleid, A. F. (1985). Foundation on swelling soils. *Proceedings of Seminar on Foundation Problems in Egypt and Northern Germany*, Cairo, Egypt, pp. 4-43.

Abuel-Naga, H. M., Bergado, D. T., Soralump, S., & Rujivipat, P. (2005). Thermal consolidation of soft Bangkok clay. *Lowland Technology International,* 7(1), 13-21.

Agrawal, V., & Gupta, M. (2011). Expansive soil stabilization using marble dust. *International Journal of Earth Sciences and Engineering*, 4 (6), 59-62.

Akbulut, S., Arasan, S., & Kalkan, E. (2007). Modification of clayey soils using scrap

tire rubber and synthetic fibers. *Applied Clay Science*, 38, 23-32.

Akcanca, F., & Aytekin, M. (2012). Effect of wetting–drying cycles on swelling behavior of lime stabilized sand–bentonite mixtures. *Environmental Earth Sciences*, 66, 67–74.

Akcanca, F., & Aytekin, M. (2014). Impact of wetting–drying cycles on the hydraulic conductivity of liners made of lime-stabilized sand–bentonite mixtures for sanitary landfills. *Environmental Earth Sciences*, 72, 59-66.

Akgün, H., Koçkar, M. K., & Aktürk, Ö. (2006). Evaluation of a compacted bentonite/sand seal for underground waste repository isolation. *Environmental Geology*, 50, 331-337.

Akinwumi, I. I., & Booth, C. A. (2015). Experimental insights of using waste marble fines to modify the geotechnical properties of a lateritic soil. *Journal of Environmental Engineering and Landscape Management,* 23(2), 121-128.

Albrecht, B. A., & Benson, C. H. (2001). Effect of desiccation on compacted natural clays. *Journal of Geotechnical and Geoenvironmental Engineering*, 127(1), 67-75.

Aldaood, A., Bouasker, M., & Al-Mukhtar, M. (2014). Soil–water characteristic curve of gypseous soil. *Geotechnical and Geological Engineering,* doi: 10.1007/s10706-014-9829-5.

Al-Homoud, A. S., Basma, A. A., Husein Malkawi, A. I., & Al-Bashabsheh, M. A. (1995). Cyclic swelling behavior of clays. *Journal of Geotechnical Engineering, ASCE,* 121(7), 562–565.

Amit, V., & Singh, R. R. (2013). Utilization of marble slurry to enhance soil properties and protect environment. *Journal of Environmental Research and Development,* 7(4A), 1479-1483.

Anggraini, V., Huat, B. B. K, Asadi, A. & Nahazanan, H. (2015). Effect of coir fibers on the tensile and flexural strength of soft marine clay. *Journal of Natural Fibers*, 12:185-200.

Arasan, S., & Yetimoğlu, T. (2008). Effect of inorganic salt solutions on the consistency limits of two clays. *Turkish Journal of Engineering Environment Science,* 32, 107 – 115.

ASTM D4318-10e1 (2010). Standard test methods for liquid limit, plastic limit and plasticity index of soils. *Annual book of ASTM Standards*.

ASTM D854-14 (2014). Standard test methods for specific gravity of soil solids by water pycnometer. *Annual book of ASTM Standards*.

ASTM D422-63e2 (2007). Standard test methods for particle size analysis of soils. *Annual book of ASTM Standards*.

ASTM D2487-11 (2011). Standard practice for classification of soils for engineering purposes. *Annual book of ASTM Standards*.

ASTM D698-12e2 (2012). Standard test methods for laboratory compaction characteristics of soil using standard effort (12 400 ft-lbf/ft3 (600 kN-m/m3)). *Annual book of ASTM Standards*.

ASTM D4546-14 (2014). Standard test methods for one-dimensional swell or collapse of soils. *Annual book of ASTM Standards*.

ASTM D2435-11 (2011). Standard test methods for one-dimensional consolidation properties of soils using incremental loading. *Annual book of ASTM Standards*.

ASTM D2166-06 (2006). Standard test method for unconfined compressive strength of cohesive soil. *Annual book of ASTM Standards*.

ASTM C1609-10 (2010). Standard test method for flexural performance of fiber-reinforced concrete (using beam with third-point loading). *Annual book of ASTM Standards*.

ASTM C348-14 (2014) Standard test method for flexural strength of hydraulic-cement mortars. *Annual book of ASTM Standards*.

ASTM C618-15 (2015). Standard specification for coal fly ash and raw or calcined natural pozzolan for use in concrete. *Annual book of ASTM Standards*.

Basma, A. A., Al-Homoud, A. S., Husein Malkawi, A. I. & Al-Bashabsheh, M. A. (1996). Swelling-shrinkage behavior of natural expansive clays. *Applied Clay Science*, 11 (2–4), 211– 227.

Başer, O. (2009). Stabilization of expansive soils using waste marble dust. *MSc Thesis*, Middle East Technical University, Turkey.

Başer, O., & Çokça, E. (2010). Stabilization of expansive soils using waste marble dust. *13th National Conference on Soil Mechanics and Foundation Engineering*, September 30- October 1, Vol. 1, (in Turkish), pp. 143-152, Istanbul, Turkey.

Benson, C. H. (1999). Final covers for waste containment systems: a North American perspective. *XVII Conference of Geotechnics of Torino*, November 23-25, 1-32, Torino, Italy.

Bilsel, H. & Tuncer, E. R. (1998). Cyclic swell-shrink behavior of Cyprus clay. *Proceedings of International Conference on Problematic soils,* Yanagisaiva, Moroto, and Mitachin, Eds., pp.337–340.

Bish, F., & Guthrie, G. D. (1994). Clays and zeolites. In: Guthrie, G.D., Mossmann, B.T. (Eds.), Health effects of mineral dusts: *Reviews in Mineralogy*, 28, 168–184.

Bhattacharja, S., Bhatty, J. I., & Todres, H. A. (2003). Stabilization of clay soils by

portland cement or lime-a critical review of literature. *Portland Cement Association*, PCA R&D Serial No. 2066.

Briaud, J.-L., Zhang, X., & Moon, S. (2003). Shrink test-water content method for shrink and swell predictions. *Journal of Geotechnical and Geoenvironmental Engineering*, 129(7), 590-600.

BS 1377-2:90 (1990). Soils for civil engineering purposes. *British Standards*.

Cai, Y., Shi, B., Ng, C. W. W., & Tang, C-S. (2006). Effect of polypropylene fibre and lime admixture on engineering properties of clayey soil. *Engineering Geology*, 87:230-240.

Cambridge University Engineering Department (2003). Materials Data Book. http:// www-mdp.eng.cam.ac.uk/web/library/enginfo/cueddatabooks/materials.pdf. (Accessed on 15 November 2016).

Caputo, D., Liguori, B., & Colella, C. (2008). Some advances in understanding the pozzolanic activity of zeolites: The effect of zeolite structure. *Cement & Concrete Composites,* 30, 455-462.

Cincotti, A., Lai, N., Orru, R., & Cao, G. (2001). Sardinian natural clinoptilolites for heavy metals and ammonium removal: experimental and modelling. *Chemical Engineering Journal*, 88, 275-282.

Chauhan, M. S., Mittal, S., & Mohanty, B. (2008). Performance evaluation of silty sand subgrade reinforced with fly ash and fibre. *Geotextiles and Geomembranes,* 26, 429–435.

Chinkulkijniwat, A., & Horpibulsuk, S. (2012). Field strength development of repaired pavement using the recycling technique. *Quarterly Journal of Engineering Geology and Hydrogeology*, 45(2), 221–229.

Chen, F. H. (1965). The use of piers to prevent the uplifting of lightly loaded structures founded on expansive soils. *Proceedings of Engineering Effects of Moisture Changes in Soils. International Research and Engineering Conference on Expansive Clay Soils*, Texas, A & M Press.

Chen, X. Q., Lu, Z. W., & He, X. F. (1985). Moisture movement and deformation of expansive soils. *Proceedings of 11th International Conference on Soil Mechanics and Foundation Engineering,* Vol. 4, San Francisco, pp. 2389-2392.

Chen, F. H. & Ma, G. S. (1987). Swelling and shrinkage behavior of expansive clays. *Proceedings of 6th International Conference on Expansive Soils:* 127-129. New Delhi.

Cho, W-J., Lee, J-O., & Chun, K. S. (1999). The temperature effects on hydraulic conductivity of compacted bentonite. *Applied Clay Science*, 14, 47-58.

Chu, T. Y. & Mou, C. H. (1973). Volume change characteristics of expansive soils determined by controlled suction tests. *Proceedings of 3rd International Conference on Expansive Soils*, Haifa, Vol. 2, pp. 177-185.

Coduto, D. P. (2001). *Foundation Design: Principles and Practices*, 2nd edition. Prentice Hall Inc.

Consoli, N. C., Lopes, L. S., & Heineck, K. S. (2009). Key parameters for the strength control of lime stabilized soils. *Journal of Materials in Civil Engineering*, 21(5), 210–216.

Consoli, N. C, Bassani, M. A. A., & Festugato, L. (2010). Effect of fiber-reinforcement on the strength of cemented soils. *Geotextiles and Geomembranes*, 28, 344-351.

Cömert, T., Fırat, S., Yımaz, G., & Sümer, M. (2010). Reuse of fly ash, marble dust and disposal sand for road subbase fill. *Proceedings of 13th National Conference on Soil Mechanics and Foundation Engineering*, Vol. 1, pp. 153-162 (in Turkish), Istanbul, Turkey.

Çimen, Ö., Keskin, S. N., Seven, S., Erişkin, E., & Güllü, D. (2011). The effect of waste marble pieces on swelling pressure at compacted clay. *Proceedings of Fourth Geotechnical Symposium*, (in Turkish), Çukurova University, December 1-2, pp. 206-211, Adana, Turkey.

Daniel, D. E., & Wu, Y. K. (1993). Compacted clay liners and covers for arid sites. *Journal of Geotechnical Engineering*, 119(2), 223-237.

Day, R. W. (1994). Swell-shrink behavior of compacted clay, *Journal of Geotechnical Engineering*, 120(3), 618-623.

DeJong, E., & Warkentin, B. P. (1965). Shrinkage of soils samples with varying clay content. *Canadian Geotechnical Journal*, 2(1), 16-22.

Delage, P., Cui, Y. J., & Tang, A. M. (2010). Clays in radioactive waste disposal. *Journal of Rock Mechanics and Geotechnical Engineering*, 2(2), 111–123.

Demirbaş, G. (2009). Stabilization of expansive soils using Bigadic zeolite (Boron by-product). *MSc Thesis*, Middle East Technical University, Turkey.

Dif, A. F., & Bluemel, W. F. (1991). Expansive soils under cyclic drying and wetting. *Geotechnical Testing Journal,* 14(1), 96–102.

Disfani, M. M., Arulrajah, A., Haghihi, H., Mohammadinia. A., & Horpibulsuk, S. (2014). Flexural beam fatigue strength evaluation of crushed brick as a supplementary material in cement stabilized recycled concrete aggregates. *Construction and Building Materials*, 68, 667–676.

Du, Y. J., Fan, R. D., Liu, S. Y., Reddy, K. R., & Jin, F. (2015). Workability, compressibility and hydraulic conductivity of zeolite-amended clayey

soil/calcium-bentonite backfills for slurry-trench cutoff walls. *Engineering Geology*, 195, 258-268.

Eades, J. L., & Grim, R. E. (1960). Reaction of hydrated lime with pure clay minerals in soil stabilization. *Highway Research Board Bulletin*, 262, 51-63.

Eades, J. L., Nichols, F. P. Jr., & Grim, R. E. (1962). Formation of new minerals with lime stabilization as proven by field experiments in Virginia. *Highway Research Board Bulletin,* 335, 31-39.

Erdem, E., Karapinar, N., & Donat, R. (2004). The removal of heavy metal cations by natural zeolites. *Journal of Colloid and Interface Science*, 280, 309-314.

Estabragh, A. R., Pereshkafti, M. R. S., Parsaei, B., & Javadi, A. A. (2013). Stabilised expansive soil behaviour during wetting and drying. *International Journal of Pavement Engineering*, 14(4), 418-427.

Estabragh, A. R., Khosravi, F., & Javadi, A. A. (2016). Effect of thermal history on the properties of bentonite. *Environmental Earth Sciences*, 75, 657.

EPA (2000). Landfill Manuals of the Environmental Protection Agency, Landfill Manuals: Landfill Site Design, ISBN: 1 84095 026 9.

Farooq, S. M., Rouf, M. A., Hoque, S. M. A., & Ashad S. M. A. (2011). Effect of lime and curing period on unconfined compressive strength of Gazipur soil,

Bangladesh. *4th Annual Paper Meet and 1st Civil Engineering Congress*, Dhaka, Bangladesh.

Fırat, S., Yılmaz, G., Cömert, A. T., & Sümer, M. (2012). Utilization of marble dust, fly ash and waste sand (silt-quartz) in road subbase filling materials. *KSCE Journal of Civil Engineering,* 16(7), 1143-1151.

Fredlund, D. G. & Rahardjo, H. (1993). *Soil mechanics for unsaturated soils*. John Wiley & Sons, New York.

Fredlund, D. G., & Xing, A. (1994). Equations for the soil-water characteristic curve. *Canadian Geotechnical Journal*, 31(4), 521–532.

Fredlund, D. G. (2000). The 1999 R.M. Hardy Lecture: The implementation of unsaturated soil mechanics into geotechnical engineering. *Canadian Geotechnical Journal*, 37, 963–986.

Fredlund, M. D., Wilson, G. W., & Fredlund, D. G. (2002). Representation and estimation of the shrinkage curve. *Proceedings of the Third International Conference on Unsaturated Soils*, UNSAT 2002, Recife, Brazil, 145-149.

Galvão, T. C. B., Kaya, A., Ören, A. H., & Yükselen, Y. (2008). Geomechanics of landfills-Innovative technology for liners. *Soil and Sediment Contamination*, 17(4), 411-424.

Gandhi, K. S. (2013). Stabilization of expansive soil of Surat region using rice husk ash and marble dust. *International Journal of Current Engineering and Technology*, 3(4), 1516-1521.

Gueddouda, M. K., Goual, I., Lamara, M., Smaida, A., & Mekarta, B. (2011). Chemical stabilization of expansive clays from Algeria. *Global Journal of Researches in Engineering*, 11(5), 1-8.

Guney, Y., Sari, D., Cetin, M., & Tuncan, M. (2007). Impact of cyclic wetting–drying on swelling behavior of lime-stabilized soil. *Building and Environment*, 42, 681–688.

Gupta, C., & Sharma, R. K. (2014). Influence of marble dust, fly ash and beas sand on sub grade characteristics of expansive soil. *Journal of Mechanical and Civil Engineering*, 13-18.

Gurbuz, A. (2015). Marble powder to stabilise clayey soils in subbases for road construction. *Road Materials and Pavement Design,* 16(2), 481-492.

Hannawi, K., Prince, W., & Bernard, S. K. (2013). Strain capacity and cracking resistance improvement in mortars by adding plastic fines. *Journal of Materials in Civil Engineering*, 25(11):1602-1610.

Harianto, T., Hayashi, S., Du, Y-J., & Suetsugu, D. (2008). Effects of fiber additives on the desiccation crack behavior of the compacted akaboku soil as a material

for landfill cover barrier. *Water Air Soil Pollution*, 194, 141-149.

Jacobs, P. H., & Förstner, U. (1999). Concept of subaqueous capping of contaminated sediments with active barrier systems (ABS) using natural and modified zeolites. *Water Research*, 33 (9), 2083-2087.

Jamsawang, P., Voottipruex, P., & Horpibulsuk, S. (2014). Flexural strength characteristics of compacted cement-polypropylene fiber sand. *Journal of Materials in Civil Engineering*, 04014243:1-9.

Jayasree, P. K, Balan, K., Peter, L., & Nisha, K. K. (2014). Volume change behavior of expansive soil stabilized with coir waste. *Journal of Materials in Civil Engineering,* 04014195:1-8.

Jha, A. K., & Sivapullaiah, P. V. (2015). Mechanism of improvement in the strength and volume change behavior of lime stabilized soil. *Engineering Geology*, 198, 53-64.

Jiang, H., Cai, Y., & Liu, J. (2010). Engineering properties of soils reinforced by short discrete polypropylene fiber. *Journal of Materials in Civil Engineering,* 22:1315-1322.

Kalkan, E. (2011). Impact of wetting-drying cycles on swelling behavior of clayey soils modified by silica fume. *Applied Clay Science*, 52, 345–352.

Kampala, A., & Horpibulsuk, S. (2013). Engineering properties of calcium carbide residue stabilized silty clay. *Journal of Materials in Civil Engineering*, 25(5), 632-644.

Kaya, A., & Durukan, S. (2004). Utilization of bentonite-embedded zeolite as clay liner. *Applied Clay Science*, 25, 83-91.

Kaya, A., Durukan, S., Ören, A. H., & Yükselen, Y. (2006). Determining the engineering properties of bentonite-zeolite mixtures. *Teknik Dergi*, 17(3), 3879-3892.

Kayabalı, K. (1997). Engineering aspects of a novel landfill liner material: bentonite-amended natural zeolite. *Engineering Geology*, 46, 105-114.

Kayabalı, K., & Kezer, H. (1998). Testing the ability of bentonite-amended natural zeolite (clinoptinolite) to remove heavy metals from liquid waste. *Environmental Geology*, 34, 95-102.

Khattab, S. A., Al-Mukhtzr, M., & Fleureau, J. M., (2007). Long-term stability characteristics of a lime-treated plastic soil. *Journal of Materials in Civil Engineering*, 19(4), 358–366.

Kholghifard, M., Ahmad, K., Ali, N., Kassim, A., Kalatehjari, R., & Babakanpour, F. (2014). Temperature effect on compression and collapsibility of residual granitic soil. *Journal of the Croatian Association of Civil Engineers*, 66(3),

191-196.

Kiliç, R., Küçükali, Ö., & Ulamiş, K. (2015). Stabilization of high plasticity clay with lime and gypsum (Ankara, Turkey). *Bulletin of Engineering Geology and the Environment*, DOI 10.1007/s10064-015-0757-2.

Kleppe, J. H., & Olson, R. E. (1985). Desiccation cracking of soil barriers. In: Johnson A. J., Frobel R. K., Cavallis N. J., and Patterson C.B. (eds) Hydraulic barrier in soil and rock. ASTM S.T.P. 874, *Journal of ASTM International*, 263-275.

Kumar, D. & Alappat, B. J. (2005). Evaluating leachate contamination potential of landfill sites using leachate pollution index. *Clean Technology Environment Policy,* 7, 190-197.

Kumar, A., Walia, B. S., & Mohan, J. (2006). Compressive strength of fiber reinforced highly compressible clay. *Construction and Building Materials*, 20:1063-1068.

Kumar, A., Walia, B. S, & Bajaj, A. (2007). Influence of fly ash, lime, and polyester fibers on compaction and strength properties of expansive soil. *Journal of Materials in Civil Engineering*, 19:242-248.

Langella, A., Pansini, M., Cappelletti, P., Gennaro, B., Gennaro, M., & Colella, C. (2000). NH^{+4} , Cu^{2+}, Zn^{2+}, Cd^{2+} and Pb^{2+} exchange for Na^{+} in a sedimentary clinoptilolite, North Sardinia, Italy. *Microporous and Mesoporous Materials*, 37, 337-343.

Lin, B. & Cerato, A. B. (2012). Investigation on soil–water characteristic curves of untreated and stabilized highly clayey expansive soils. *Geotechnical and Geological Engineering,* 30, 803-812.

Little, D. L. (1999). Evaluation of structural properties of lime stabilized soils and aggregates. *National Lime Association*, 1.

Lloret, A., & Villar, M. V. (2007). Advances on the knowledge of the thermo-hydro-mechanical behaviour of heavily compacted ‘‘FEBEX’’ bentonite. *Physics and Chemistry of the Earth*, 32, 701-715.

Maher, M. H., & Ho, Y. C. (1994). Mechanical properties of kaolinite/fiber soil composite, *Journal of Geotechnical Engineering*, 120:1381-1393.

Meer, S. R. & Benson, C. H. (2007). Hydraulic conductivity of geosynthetic clay liners exhumed from landfill final covers. *Journal of Geotechnical and Geoenvironmental Engineering*, 133, 550-563.

Mertens, G., Snellings, R., Balen, K. V., Bicer-Simsir, B., Verlooy, P., & Elsen, J. (2009). Pozzolanic reactions of common natural zeolites with lime and parameters affecting their reactivity. *Cement and Concrete Research*, 39, 233-240.

Mier, M. V., Callejas, R. L., Gehr, R., Cisneros, B. E. J., & Alvarez, P. J. J. (2001). Heavy metal removal with Mexican clinoptilolite: Multi-component ionic

exchange. *Water Research*, 35(2), 373-378.

Miller, C. J., & Rifai, S. (2004). Fiber reinforcement for waste containment soil liners. *Journal of Environmental Engineering*, 130(8), 891-895.

Misaelides, P. (2011). Application of natural zeolites in environmental remediation: A short review. *Microporous and Mesoporous Materials*, 144, 15-18.

Mitchell, J. K., & El Jack, S. A. (1966). The fabric of soil-cement and its formation. *Clays and Clay Minerals*, 14, 297-305.

Mitchell, J. K., & Soga, K. (2005). *Fundamentals of soil behavior*. John Wiley & Sons, USA.

Moses, G. & Afolayan, J. O. (2013). Desiccation-induced volumetric shrinkage of compacted foundry sand treated with cement kiln dust. *Geotechnical and Geological Engineering*, 31, 163–172.

Motsi, T., Rowson, N. A., & Simmons, M. J. H. (2009). Adsorption of heavy metals from acid mine drainage by natural zeolite. *International Journal of Mineral Processing*, 92, 42-48.

Muntohar, A. S. (2011). Engineering characteristics of the compressed-stabilized earth brick. *Construction and Building Materials*, 25, 4215–4220.

Muntohar, A. S, Widianti, A., Hartono, E., & Diana, W. (2013). Engineering properties of silty soil stabilized with lime and rice husk ash and reinforced with waste plastic fiber. *Journal of Materials in Civil Engineering*, 25(9):1260-1270.

Nalbantoglu, Z., & Gucbilmez, E. (2001). Improvement of calcareous expansive soils in semi-arid environments. *Journal of Arid Environment*, 47: 453-463.

Nelson, J. D., & Miller, D. J. (1992). *Problems and practice in foundation and pavement engineering*. John Wiley & Sons, USA.

Nordquist, E. C., & Bauman R. D. (1967). Stabilization of expansive Mancos shale. *Proceedings of 3rd Asian Regional Conference in Soil Mechanics and Foundation Engineering*, Israel, Vol. 1, pp.107-110.

Obermeier, S. F. (1973). Evaluation of laboratory techniques for measurement of swell potential of clays and shales. *Proceedings of Workshop on Expansive Clays and Shales,* Denver, Colorado, pp. 214-217.

Olofsson, B., Jernberg, H., & Rosenqvist, A. (2006). Tracing leachates at waste sites using geophysical and geochemical modelling. *Environmental Geology*, 49, 720-732.

Onyejekwe, S., & Ghataora, G. S. (2014). Effect of fiber inclusions on flexural strength of soils treated with nontraditional additives. *Journal of Materials in Civil Engineering*, 04014039:1-9.

Osinubi, K. J., & Eberemu, A. O. (2010). Desiccation induced shrinkage of compacted lateritic soil treated with blast furnace slag. *Geotechnical and Geological Engineering*, 28, 537-547.

Osipov, V. I., Nguen, N. B. & Rumjantseva, N. A. (1987). Cyclic swelling of clays. *Applied Clay Science*, 2, 363–374.

Önal, O. (2015). Lime stabilization of soils underlying a salt evaporation pond: a laboratory study. *Marine Georesources & Geotechnology,* 33(5), 391-402.

Ören, A. H., & Kaya, A. (2006). Factors affecting adsorption characteristics of Zn^{2+} on two natural zeolites. *Journal of Hazardous Materials*, B131, 59-65.

Ören, A. H., & Özdamar, T. (2013). Hydraulic conductivity of compacted zeolites. *Waste Management & Research*, 31(6), 634-640.

Özen, S. (2013). Pozzolanic activity of natural zeolites: Mineralogical, chemical and physical characterization and examination of hydration products. *PhD Thesis*, Middle East Technical University, Turkey.

Phanikumar, B. R. (2009). Effect of lime and fly ash on swell, consolidation and shear strength characteristics of expansive clays: a comparative study. *Geomechanics and Geoengineering Journal,* 4(2), 175-181.

Popescu, M. (1980). Behavior of expansive soils with crumb structures. *Proceedings,*

4th International Conference on Expansive Soils, Vol. 1, Denver, CO, pp. 158–171.

Punthutaecha, K., Puppala, A. J., Vanapalli, S. K., & Inyang, H. (2006). Volume change behaviors of expansive soils stabilized with recycled ashes and fibers. *Journal of Materials in Civil Engineering*, 18:295-306.

Puppala, A. J., Punthutaecha, K., & Vanapalli, S. K. (2006). Soil-water characteristic curves of stabilized expansive soils. *Journal of Geotechnical and Geoenvironmental Engineering,* 132(6), 736-751.

Rajasekaran, G., Rao, N. S. (2002). Compressibility behaviour of lime-treated marine clay. *Ocean Engineering*, 29(5), 545-559.

Rao, K. S. S. & Satyadas, G. C. (1987). Swelling potential with cycles of swelling and partial shrinkage. *Proceedings of 6th International Conference on Expansive Soils,* Vol. 1, New Delhi, India, pp. 137–142.

Rao, S. M., Reddy, B. V. V., & Muttharam, M. (2001). The impact of cyclic wetting and drying on the swelling behaviour of stabilized expansive soils. *Engineering Geology*, 60, 223-233.

Rao, K. S. S., & Tripathy, S. (2003). Effect of aging on swelling and swell-shrink behavior of a compacted expansive soil. *Geotechnical Testing Journal,* 26 (1), 36-46.

Romero, E., Villar, M., & Lloret, A. (2005). Thermo-hydro-mechanical behaviour of two heavily overconsolidated clays. *Engineering Geology*, 81, 255–268.

Sabat, A. K., & Nanda, R. P. (2011). Effect of marble dust on strength and durability of rice husk ash stabilised expansive soil. *International Journal of Civil and Structural Enginering*, 1(4), 939-948.

Sahoo, J. P. & Prahdan, P. K. (2010). Effect of lime stabilized soil cushion on strength behaviour of expansive soil. *Geotechnical and Geological Engineering*, 28, 889–897.

Şenol, A. (2012). Effect of fly ash and polypropylene fibres content of on the soft soils. *Bulletin of Engineering Geology and Environment*, 71, 379-387.

Shahjahan, A. B. M. (2001). Long term strength development of lime stabilized soils. *MSc Thesis*, Bangladesh University of Engineering and Technology, Dhaka.

Shariatmadari, N. & Saeidijam, S. (2011). The effect of elevated temperature on compressibility and swelling of bentonite-sand mixtures. *Electronic Journal of Geotechnical Engineering*, 16, 137-146.

Shirazi, S. M., Kazama, H., Kuwano, J., & Rashid, M. M. (2010). The influence of temperature on swelling characteristics of compacted bentonite for waste disposal. *Environment Asia*, 3(1), 60-64.

Shrivastava, D., Singhai, A. K, & Yadav, R. K. (2014). Effect of lime and rice husk ash on index properties of black cotton soil. *International Journal of Engineering Sciences & Research Technology,* 3(4), 4030-4033.

Sivrikaya, O., Kıyıldı, K. R., & Karaca, Z. (2014). Recycling waste from natural stone processing plants to stabilise clayey soil. *Environmental Earth Sciences*, 71, 4397-4407.

Snethen, D. R, Johnson, L. D., & Patrick, D. M. (1977). An evaluation of expedient methodology for identification of potentially expansive soils. Soils and Pavements Laboratory, U.S. Army Engineers Waterway Experiment Station, Vicksburg, MS, Report No. FHWA-RE-77-94: 1-43.

Sultan, N., Delage, P., & Cui, Y. J. (2002). Temperature effects on the volume change behaviour of Boom clay. *Engineering Geology*, 64, 135–145.

Suneel, M., Kwon, J., Im, J-C., & Jeon, C. W. (2010). Long-term consolidation and strength behavior of marine clay ımproved with fly ash. *Marine Georesources and Geotechnology*, 28, 105–114.

Sunil, B. M., Shrihari, S., & Nayak, S. (2008). Soil-leachate interaction and their effects on hydraulic conductivity and compaction characteristics. *12th International Conference of International Association for Computer Methods and Advances in Geomechanics* (IACMAG) Goa, India.

Sukontasukkul, P., & Jamsawang, P. (2012). Use of steel and polypropylene fibers to improve flexural performance of deep soil–cement column. *Construction and Building Materials*, 29, 201-205.

Taha, O. M. E., & Taha, M. R. (2011). Cracks in soils related to desiccation and treatment. *Australian Journal of Basic and Applied Sciences*, 5(8), 1080-1089.

Tang, C., Shi, B., Gao, W., Chen, F., & Cai, Y. (2007). Strength and mechanical behaviour of short polypropylene fiber reinforced and cement stabilized clayey soil. *Geotextiles and Geomembranes*, 25(3):194–202.

Tang, C-S., Cui, Y-J., Tang, A-M., & Shi, B. (2010). Experiment evidence on the temperature dependence of desiccation cracking behavior of clayey soils. *Engineering Geology*, 114, 261-266.

Tang, C-S., Shi, B., & Zhao, L-Z. (2010). Interfacial shear strength of fiber reinforced soil. *Geotextiles and Geomembranes*, 28:54-62.

Tang, A., Vu, M., & Cui, Y., (2011). Effects of the maximum grain size and cyclic wetting/drying on the stiffness of a lime-treated clayey soil. *Géotechnique*, 61, 421–429.

Tang, C-S., Cui, Y-J., 2, Shi, B., Tang, A-M., & An, N. (2016). Effect of wetting-drying cycles on soil desiccation cracking behaviour. *Proceedings of 3rd European Conference on Unsaturated Soils*, Paris, France, DOI:

10.1051/e3sconf /20160912003.

Tay, Y. Y., Stewart, D. I., & Cousens, T. W. (2001). Shrinkage and desiccation cracking in bentonite-sand landfill liners. *Engineering Geology*, 60, 263-274.

Tej, P. R., & Singh, D. N. (2013). Estimation of tensile strength of soils from penetration resistance. *International Journal of Geomechanics*, 13(5), 496-501.

Tuncan, A., Tuncan, M., & Koyuncu, H. (2000). Use of petroleum-contaminated drilling wastes as sub-base material for road construction. *Waste Management and Research*, 18, 489-505.

Tuncan, A., Tuncan, M., Koyuncu, H., & Guney, Y. (2003). Use of natural zeolites as a landfill liner. *Waste Management & Research*, 21, 54-61.

Tripathy, S., Rao, K. S. S, & Fredlund, D. G. (2002). Water content-void ratio swell–shrink paths of compacted expansive soils. *Canadian Geotechnical Journal*, 39, 938–959.

Tripathy, S., & Rao, K. S. S. (2009). Cyclic swell–shrink behaviour of a compacted expansive soil. *Geotechnical and Geological Engineering*, 27, 89-103.

Tsutsumi, A., & Tanaka, H. (2012). Combined effects of strain rate and temperature on consolidation behavior of clayey soils. *Soils and Foundations*, 52(2), 207–

215.

Uzal, B., Turanlı, L., Yücel, H., Göncüoğlu, M. C., & Çulfaz, A. (2010). Pozzolanic activity of clinoptilolite: A comparative study with silica fume, fly ash and a non-zeolitic natural pozzolan. *Cement and Concrete Research*, 40, 398-404.

van Genuchten, M. Th. (1980). A closed-form equation for predicting the hydraulic conductivity of unsaturated soils. *Soil Science of America Journal*, 44, 892-898.

Vaníček, I. (2013). The importance of tensile strength in geotechnical engineering. *Acta Geotechnica Slovenica*, 1, 5-17.

Villar, M. V., & Lloret, A. (2004). Influence of temperature on the hydro-mechanical behaviour of a compacted bentonite. *Applied Clay Science*, 26, 337-350.

Villar, M. V., Gómez-Espina, R., & Lloret, A. (2010). Experimental investigation into temperature effect on hydro-mechanical behaviours of bentonite. *Journal of Rock Mechanics and Geotechnical Engineering*, 2(1), 71–78.

Viswanadham, B. V. S., Phanikumar, B. R., & Mukherjee, R. V. (2009). Swelling behaviour of a geofiber-reinforced expansive soil. *Journal of Geotextiles and Geomembranes*, 27, 73-76.

Wang, Y. (1999). Utilization of recycled carpet waste fibers for reinforcement of

concrete and soil. *Polymer-Plastics Technology and Engineering*, 38(3):533-546.

Wang, Y., Duc, M., Cui, Y-J., Tang, A. M., Benahmed, N., Sun, W. J., & Ye, W. M. (2017). Aggregate size effect on the development of cementitious compounds in a lime-treated soil during curing. *Applied Clay Science*, 136, 58–66.

Warkentin, B. P. & Bozozuk, M. (1961). Shrinking and swelling properties of two Canadian clays. *Proceedings of 5th International Conference on Soil Mechanics and Foundation Engineering*, Dunod, Paris, Vol. 1, pp. 851-855.

Widomski, M. K., Stępniewski1, W., Horn, R., Bieganowski, A., Gazda, L., Franus, M., & and Pawłowska, M. (2015). Shrink-swell potential, hydraulic conductivity and geotechnical properties of clay materials for landfill liner construction. *International Agrophysics*, 29, 365-375.

Yazdandoust, F., & S. Shahaboddin Yasrobi, S. S. (2010). Effect of cyclic wetting and drying on swelling behavior of polymer-stabilized expansive clays. *Applied Clay Science*, 50, 461–468.

Yılmaz, Y., & Sevencan, Ü. (2010). Investigation of some geotechnical properties of polypropylene fiber and fly ash amended Ankara clay. *Proceedings of the 13th National Conference on Soil Mechanics and Foundation Engineering*, Vol. 1, (in Turkish), Istanbul; pp. 133-142.

Ye, W. M., Wan, M., Chen, B., Chen, Y. G., Cui, Y. J., & Wang, J. (2013). Temperature effects on the swelling pressure and saturated hydraulic conductivity of the compacted GMZ01 bentonite. *Environmental Earth Sciences*, 68, 281-288.

Yesiller, N., Miller, C. J., Inci, G., & Yaldo, K. (2000). Desiccation and cracking behavior of three compacted landfill liner soils. *Engineering Geology,* 57, 105-121.

Yükselen-Aksoy, Y. (2010). Characterization of two natural zeolites for geotechnical and geoenvironmental applications. *Applied Clay Science*, 50, 130-136.

Ziegler, S., Leshchinsky, D., Ling, H. I., & Perry, E. B. (1998). Effect of short polymeric fibers on crack development in clays. *Soils and Foundations*, 38(1), 247-253.

Zorluer, I., & Usta, M. (2003). Stabilization of soils by waste marble dust. *Fourth National Marble Symposium*, pp. 305-311 (in Turkish), Afyon, Turkey.